COMBATING HIGH TEMPERATURE CORROSION BY NEW MATERIALS, TESTING PROCEDURES AND IMPROVED MATERIAL SELECTION

- CORROSION EXPOSURES IN THE WASTE FIRED CFB BOILER P15 AT HÄNDELÖ
- THE EFFECT OF INCREASED FRACTIONS OF WASTE WOOD ON WATER WALL- AND SUPERHEATER CORROSION

KME-711 & KME-720

KME
CONSORTIUM MATERIALS TECHNOLOGY
for thermal energy processes

KME-711

Combating high temperature corrosion by new materials and testing procedures

Corrosion exposures in the waste fired CFB boiler P15 at Händelö

KME-720

The effect of increased fractions of waste wood on water wall- and superheater corrosion

Combating corrosion by new materials and improved material selection

L.PAZ, A.OLIVAS, T.JONSSON, A. PETTERSSON, F. MORADIAN, A.JONASSON, J. ASPEN, P. SCHNEIDER, J. MAHANEN, K. VÄNSKÄ, V. BARIŠIĆ, B.JÖNSSON, J. HERNBLOM, M. HUHTAKANGAS, J. LISKE

ISBN 978-91-7673-092-8 | © 2018 ENERGIFORSK

Energiforsk AB | Phone: 08-677 25 30 | E-mail: kontakt@energiforsk.se | www.energiforsk.se

Preface

The project has been performed within the framework of the materials technology research programme KME, Consortium materials technology for thermal energy processes, period 2014-2018. The consortium is at the forefront of developing material technology to create maximum efficiency for energy conversion of renewable fuels and waste. KME has its sights firmly set on continuing to raise the efficiency of long-term sustainable energy as well as ensuring international industrial competitiveness.

KME was established 1997 and is a multi-cliental group of companies over the entire value chain, including stakeholders from the material producers, manufacturers of systems and components for energy conversion and energy industry (utilities), that are interested in materials technology research. In the current programme stage, eight industrial companies and 14 energy companies participate in the consortium. The consortium is managed by Energiforsk.

The programme shall contribute to increasing knowledge within materials technology and process technology development to forward the development of thermal energy processes for efficient utilisation of renewable fuels and waste in power and heat production. The KME goals are to bring about cost-effective materials solutions for improved fuel flexibility, improved operating flexibility, increased availability and power production with low environmental impact.

KME's activities are characterised by long term industry and demand driven research and constitutes an important part of the effort to promote the development of new energy technology with the aim to create value and an economic, environmentally friendly and long term sustainable energy society.

The industry has participated in the project through own investment (60 %) and the Swedish Energy Agency has financed the academic partners (40 %).

Bertil Wahlund, Energiforsk

Abstract

This study has been investigating several factors that is expected to have an influence on the overall plant economy for biomass and waste fired boilers. This has been performed in two CFB boilers built by Sumitomo SHI FW and in two parallel projects. The data obtained within this study may be used by the industry in order to optimize material selection and corrosion testing methods. The main scientific aim of this study is to generate new knowledge about various corrosion exposures within boilers with a wide range of materials, both commercially available and newly developed, in a horizontally designed superheater region. Some of the results in short:

- In general, the corrosion load of the superheater region in the waste fired boiler was rather low (for many samples below 0.1 mm/year and for some samples about 0.2 mm/year), including both low alloyed and stainless steels.
- In the biomass fired boiler, the material wastages were higher for the low alloyed steels showing corrosion rates of about 0.3-0.5 mm/year with 40% waste wood and 0.4-0.7 mm/year with 45% waste wood.
- The newly developed FeCrAl model alloy showed promising results, i.e. no corrosion, of the one year test performed in the SH region of the waste fired Händelö boiler.
- Both HVAF and HVOF CorEr coatings perform better compared to low alloyed steels and comparably or better results compared to stainless steels. Especially the HVAF CorEr coating showed very little corrosion attack and a good adherence to the substrate.
- The clamp testing technique is suitable for investigating the corrosion rate of large sample matrixes in multiple positions in the superheater bundles and for long periods of time with the possibility to investigate the corrosion rate in a time resolved manner.

Sammanfattning

För att globalt öka andelen förnyelsebara bränslen i värme- och kraftproduktion behöver den ekonomiska konkurrenskraften jämfört med fossila kraftverk växa. Detta kan göras genom att antingen öka intäkterna (tex genom att öka värme- och elutbytet) eller minska kostnaderna (tex genom att elda billigare bränslen, uppnå lägre underhållskostnader, etc.). Materialets prestanda och livslängd hos olika värmeväxlare i pannan är vanligtvis en kritisk faktor för kostnaden för totalekonomin hos kraftvärmeverk.

Denna rapport baseras på två projekt som har genomförts av E.ON Värme Sverige AB, Sumitomo SHI FW Energia Oy, Sandvik Materials Technology AB, Kanthal AB, MH Engineering AB, Stockholm Exergi AB, Söderenergi AB, Göteborg Energi AB, Mälarenergi AB samt Kraftringen AB inom ramen för KME, finansierat av Energimyndigheten och deltagande industri. Chalmers/HTC (Jesper Liske) har varit projektledare. Denna studie har undersökt flera faktorer som förväntas påverka totalekonomin hos kraftvärmeverk som eldar biobränslen och avfall. Studien har genomförts i två CFB-pannor byggda av Sumitomo SHI FW. Korrosionsdatan och erfarenheterna som erhålls inom detta projekt kan användas av industrin för att förbättra sina ekonomiska modeller. Denna studie innehåller emellertid inga sådana ekonomiska överväganden. De faktorer som undersöktes i denna studie har varit:

Långtidskorrosionstestning av ett stort antal material i två pannor, eldad med avfall respektive biobränsle, har genomförts inom två parallella projekt. Detta har genomförts med en nyutvecklad ”clamp testing technique”. Studien har även inkluderat en undersökning av effekten av ökad andel returträ i pannan som eldade biobränsle.

- Undersökning av korrosionen på överhettare monterade i horisontellt överhettardrag.
- Korrosionsundersökning av nyutvecklade material.
- Korrosionsundersökning av flertalet positioner och temperaturer i de två pannorna.
- Korttidskorrosionsundersökning med inriktning på klorets roll och uppstartssekvensen för sondexponeringar
- Utvärderingen av tekniker som används för att mäta/förutsäga korrosion/korrosiva miljöer

Det huvudsakliga vetenskapliga målet med denna studie är att generera ny kunskap kring korrosionsangrepp som sker i pannor med horisontellt utformade överhettarregioner. Genom att erhålla ny korrosionskunskap och materialprestanda är målet också att detta projekt kommer att underlätta för optimerade materialval i dessa typer av pannor, både vid nybyggnation och vid reparation. Detta leder därigenom också till att underlätta för en bättre totalekonomi för dessa anläggningar.

Flertalet aktiviteter inom denna studie har framgångsrikt lett till ett antal slutsatser, nya insikter och värdefulla korrosionsdata. De viktigaste resultaten inom studien anges nedan:

- Ett stort urval av material, allt från låglegerade stål till rostfritt stål och FeCrAl-modellegeringar, har undersökts i upp till tre år i två olika pannor med ett horisontellt utformade överhettarregioner på ett flertal positioner. Denna stora matris av korrosionsprovning kan användas för pannproducenter och pannägare för att optimera materialvalet.

- Korrosionsutvärderingen av överhettarregionen i den avfallsledade pannan visade på generellt låga korrosionshastigheter, de flesta utvärderade proverna uppvisade korrosionshastigheter på under 0,1 mm/år, vilket är att betrakta som lågt. Högsta korrosionshastigheten var något över 0,2 mm/år. Dessa låga korrosionshastigheter uppmättes för både låglegerade och rostfria stål. Den låga korrosionshastigheten föreslås huvudsakligen vara en effekt av en låg materialtemperatur på överhettarna samt närvaron av ett tomdrag. I tomdraget minskas rökgastemperaturen och korrosiva ämnen kondenserar ut och skiljas av innan rökgasen går in i det horisontellt utformade överhettningspasset.

- Korrosionsutvärderingen av överhettarregionen i den biomasseldade pannan visade på högre materialavverkning, korrosionshastigheter på ca 0,3-0,5 mm/år med 40 % returträ-inblandning och 0,4-0,7 mm/år med 45 % returträ-inblandning. Orsaken till de högre korrosionshastigheterna i Örtoftaverket-pannan jämfört med den avfallsbehandlade P15 Händelöpannan föreslås primärt bero på högre materialtemperatur och avsaknaden av ett tomdrag i Örtoftapannan.

- Den nyutvecklade FeCrAl-modelllegeringen visade lovande resultat, dvs. ingen mätbar korrosion, av det ettåriga testet som gjordes i överhettarregionen i den avfallseldade Händelö-pannan.

- Både HVAF- och HVOF-sprutade CorEr-beläggningar fungerar bättre jämfört med låglegerade stål och jämförbara eller bättre resultat jämfört med rostfritt stål. Särskilt HVAF CorEr-beläggningen visade mycket litet korrosionsangrepp. Beläggningen hade även god vidhäftning till substratet.

- Den nyutvecklad ”clamp testing technique” visade sig lämplig för att undersöka korrosionshastigheten hos stora provmatriser på flertalet positioner i överhettarregionen och under långa tidsperioder med möjlighet att undersöka korrosionshastigheten tidsupplöst. Enligt resultaten uppvisade clamp-proverna liknande korrosionshastighet som motsvarande tubprover. Clamp-prover förväntas sålunda vara ett billigt och icke-invasivt alternativ till tubprover och som uppvisar relevanta korrosionshastigheter.

- Online korrosionssonden följde samma trender med hänsyn till korrosionsangrepp som clamp-prover och prov exponerade på "traditionella" korrosionssonder. Online korrosionsprovningen visade på inget eller mycket litet korrosionsangrepp i överhettarregionen, i likhet med clamp-proverna och tub-proverna. Online korrosionsprovningen visade på betydligt högre korrosionsangrepp då den exponerades i tomdraget, vilket var i överensstämmelse med de ”traditionella” korrosionssonderna som exponerades under 24 respektive 144 timmar i denna position. Den allmänna trenden för exponeringarna i tomdraget var att korrosionen inleddes mycket aggressivt men att den avtog med exponeringstiden.

- Både den termodynamiska modellen och IACM syftar till att veta mängden gasformiga alkaliklorider i rökgasen. Denna information kan ge viktig information om den förväntade korrosionshastigheten. Den nyutvecklade termodynamiska modellen visade sig vara ett tillförlitligt beräkningsverktyg för att uppskatta koncentrationen av alkalikloriderna i rökgasen i CFB-pannan. Beräkningarna baserade sig på den kemiska sammansättningen av bränslet (+ ev tillsatser) samt förbränningstemperaturer i pannan. Modellen kan implementeras som en första indikation för att bedöma koncentrationen av alkaliklorider i CFB-pannor. Båda dessa tekniker är utifrån komplexitet, kostnad och risk för påverkan på anläggningstillgängligheten intressanta för att förutspå korrosionsrisken. Mer forskningsarbete krävs dock innan dessa tekniker kan användas för att skapa renodlade korrosionsprognosmodeller.

Måluppfyllelse

Det övergripande målet med denna studie har varit att förbättra anläggningsekonomin hos biobränsle- och avfallseldade kraftvärmeverk genom att erhålla ny korrosionskunskap och materialprestanda och därigenom möjliggöra ökad grön elproduktion och optimerade materialval i dessa anläggningar. Nedan presenteras de olika målen och graden av måluppfyllelse. En mer genomgripande måluppfyllelse presenteras senare i rapporten.

- *Att korrelera korrosiviteten hos rökgasen med rökgasens temperatur i förhållande till materialtemperaturen.*
- *Att verifiera och kvantifiera korrosionshastigheterna för flertalet material i en överhettarregion med horisontell design.*
- *Att verifiera och jämföra korrosionen i en biomasseldad panna (Örtoftaverket) och med en avfallseldad panna (Händelöverket).*
  Med denna stora exponeringsmatris av clamp- och tubprover, vid flertalet positioner i två olika pannor, kopplat även till korrosionssondexponeringar som ytterligare utökat temperatur- och materialmatrisen, anses dessa tre mål vara uppfyllda.

- *Att verifiera och jämföra korrosionsegenskaperna hos kommersiella överhettarmaterial samt nyutvecklade rostfria stål samt FeCrAl-legeringar.*
  Denna studie har generat nya insikter kring korrosionsprestandan hos nyutvecklade legeringar samt jämfört dessa mot korrosionsegenskaperna hos idag tillgängliga kommersiella överhettarmaterial. Detta mål anses vara uppfyllt.

- *Att verifiera och jämföra korrosionsegenskaperna hos beläggningar utförda med den nya generationen beläggningsteknologi "HVAF".*
  Prover belagda med CorER (en nickelbasbeläggning), både med HVOF och HVAF-tekniken, har undersökts och uppvisade övergripande bra korrosionsegenskaper. De HVAF-belagda proverna visade emellertid alltid lägre korrosionshastigheter jämfört med HVOF-proverna och andra rostfria stål, även om korrosionshastigheterna var låga i allmänhet. Detta mål anses vara uppfyllt.

- *Att jämföra olika korrosionsprovningsmetoder (exempelvis sondförsök, tubförsök och clamp-försök) med hänsyn till deras komplexitet, kostnad och risk för att minska anläggningstillgängligheten.*
  I denna studie har sex olika metoder för att uppskatta den potentiella korrosionen/korrosionsrisken för överhettare testats, nämligen tubförsök, clamp-försök, korrosionssondförsök, online korrosionssondsförsök, IACM och en termodynamisk modell. Dessa metoders komplexitet, kostnad och risk för att minska anläggningstillgängligheten har diskuterats i rapporten. Detta mål anses vara uppfyllt.

- *Att undersöka hur korrosionen av vattenväggar påverkas av en stegvis ökning av mängden returträ i bränslet.*
  Detta mål anses endast delvis uppfyllt. På grund av säkerhetsproblem kunde inte alla planerade aktiviteter utföras. Följaktligen har korrosionsegenskaperna hos vattenväggarna inte undersökts i detalj med sonder. Det har dock skett en stegvis ökning av mängden returträ i bränslet och enligt Kraftringens undersökningar under revisioner har de permanent installerade vattenväggarna inte uppvisat några alarmerande tecken på en accelererad korrosionshastighet.

Nyckelord: Korrosion i pannor eldade med biobränsle och avfall, Material för pannor eldade med förnyelsebara bränslen, Högtemperaturekorrosion

Summary

In order to globally increase the share of renewable fuels in heat and power production, the economical competitiveness compared to fossil fuelled power plants needs to be improved. This can be done in either increasing the reveue of plant (e.g. by increasing the heat and power output) or decreasing the costs (e.g. cheaper fuels, lower maintanece costs, etc). The material performance and life time of various heat exchangers inside the plant is usually a critical factor for the costs of the boiler operation.

This report is based on two projects that have been performed by E.ON Värme Sverige AB, Sumitomo SHI FW Energia Oy, Sandvik Materials Technology AB, Kanthal A, MH Engineering AB, Stockholm Exergi AB, Söderenergi AB, Göteborg Energi AB, Mälarenergi AB samt Kraftringen AB within the KME program, financed by the Swedish Energy Agency and participating industry. Chalmers/HTC (Jesper Liske) has been acting as project manager. This study has been investigating several factors that is expected to have an influence on the overall plant economy for biomass and waste fired boilers. This has been performed in two CFB boilers built by Sumitomo SHI FW. The data obtained within this project may be used by the industry in order to improve their economical model. This study includes however no such economical considerations.

The factors investigated in this study have been:

- Long term corrosion testing of several materials by the novel clamp testing technique in both a waste fired boiler and in a biomass (including increasing fraction of waste wood) boiler
- Investigation of horizontal pass superheaters
- Corrosion investigation of novel materials
- Corrosion investigation of several position and temperatures in the two boilers
- Short term corrosion investigation focussing on the role of chlorine and of the startup sequence of probe exposures
- The evaluation of three techniques used for predicting the corrosion/corrosive environment

The main scientific aim of this study is to generate new knowledge about various corrosion exposures within boilers with a horizontally designed superheater region. By obtaining new knowledge and material performance data the aim is also that this project will provide improved material selection in boilers and thereby also facilitate better input for the economical business model of these plants.

The activities within this study has successfully led to a number of conclusions, new insights and valuable corrosion data. The most important results achieved within the study are listed below:

- A wide range of materials, ranging from low alloyed steels to stainless steels and FeCrAl model alloys, has been investigated for up to three years in two different boilers with a horizontally designed superheater pass at several positions. This large matrix of corrosion results can be used for boiler manufactures and boiler owners in order to optimize material selection.

- In general, the corrosion load of the superheater region in the waste fired boiler was rather low (for many samples below 0.1 mm/year and for some samples about 0.2 mm/year), including both low alloyed and stainless steels. This is suggested to primarily be an effect of a rather low material temperature and the presence of an empty pass, which decreases the temperature and corrosive particle load of the flue gas before entering the horizontally designed superheater pass.
- In the biomass fired boiler, the material wastages were higher for the low alloyed steels showing corrosion rates of about 0.3-0.5 mm/year with 40% waste wood and 0.4-0.7 mm/year with 45% waste wood. The reason(s) for the higher material wastage in the Örtoftaverket boiler compared to the waste fired P15 Händelöboiler is suggested to be caused by the higher material temperature and lack of an empty pass.
- The newly developed FeCrAl model alloy showed promising results of the one year test performed in the SH region of the waste fired Händelö boiler.
- Both HVAF and HVOF CorEr coatings perform better compared to low alloyed steels and comparably or better results compared to stainless steels. Especially the HVAF CorEr coating showed very little corrosion attack and a good adherence to the substrate.
- The clamp testing technique is suitable for investigating the corrosion rate of large sample matrixes in multiple positions in the superheater bundles and for long peeriods of time with the possibility to investigate the corrosion rate in a time resolved manner. According to the results, the clamp samples exhibited similar corrosion rate as the corresponding tube samples. Thus, clamp samples are expected to be a low cost and non-invasive alternative to tube samples, still showing relevant corrosion rates.
- The online corrosion probe followed the same trends with respect towards the corrosion attack as the clamps samples and as the "traditional" corrosion probes. The online corrosion detected no or very little corrosion attack in the superheater pass, consisted with the clamps samples. When compared to the corrosion observed on the corrosion probes, exposed in the empty pass, the general trend was also the same; the initiation of the corrosion was very fast and aggressive and levelled off after some time. This was in agreement with the corrosion probes exposed for 24 and 144 hours respectively.
- The thermodynamical model and the IACM both aim at revealing the amount of gaseous alkali chlorides in the flue gas. Knowing the fraction of alkali chlorides in the flue gas may provide important information about the expected corrosion rate. The developed model proved to be a reliable calculation tool to estimate the concentration of the alkali chlorides in the flue gas of the CFB boiler, based on the chemical composition of the fuel mix and additives, as well as combustion temperature in the boiler. The model can be implemented as a first indication to assess the concentration of alkali chlorides in the CFB boiler. From a complexity, cost and plant availability point of view, both these methods show potential, e.g. the risk

of operation by deploying these two methods is low (for the IACM) or non-existing (for the modelling method). However, there is still work to be performed in order to couple this to corrosion prediction models.

Goal fulfillment

The overall goal of this study was to improve plant economy by enabling an increased green electricity production and optimum material selection. Below the different goals and it fulfilment is presented. A more thorough goal fulfilment is presented in the report.

- *To correlate the corrosivity of the flue gas with the flue gas temperature in respect to the material temperature.*
- *To verify and quantify the corrosion rates for different superheater materials in superheaters with a horizontal design.*
- *Verify and compare the corrosion properties of a biomass fired boiler (Örtoftaverket) and waste fired boiler (Händelöverket)*
  With this large exposure matrix, at several positions in two different boilers, coupled also to probe exposures which widens the temperature and material matrix even further, these three goals are considered as fulfilled.

- *Verify and compare the corrosion properties of commercial superheater materials as well as state-of-the-art stainless steels and FeCrAl alloys.*
  This study has brought new insights to the corrosion performance of newly developed alloys as well as compared these towards corrosion properties of commercial superheater materials that are available today. This goal is considered as fulfilled.

- *Verify and compare the corrosion properties of coatings performed with the new generation coating technology HVAF (High Velocity Air Fuel).*
  Samples coated with CorER (a nickel base coating), both with the HVOF and the HVAF technique, have been evaluated and performed overall well. The HVAF coated samples were however always showing lower corrosion rates compared to the HVOF samples and other stainless steels, even though the corrosion rates were low in general. This goal is considered as fulfilled.

- *Compare different corrosion testing methods (i.e. probes, coils/tubes and clamping) with respect towards their complexity, cost and plant availability risk.*
  Within this study six different methods in order to estimate the potential corrosion/corrosion risk of superheaters has been tested, namely tube samples, clamp samples, corrosion probe samples, online corrosion probe samples, IACM and a thermodynamical model. The complexity, cost and plant availability risk of these thecniques have been discussed in the report. This goal is considered as fulfilled.

- *Investigate how the corrosion performance of water walls is affected by a stepwise increase of the waste wood fraction in the fuel mix.*
  This goal is considered as only partially fulfilled. However, due to safety issues not all planned activities could be performed. Consequently, the corrosion performance of the water walls has not been investigated in detail with probes. However, there has been an stepwise increase of the waste wood fraction and according to Kraftringens investigations during revision the permanently installed water walls have not been showing any alarming signs of an accelerated corrosion rate.

Keywords: Corrosion in biomass and waste fired boilers, Materials for boilers using renewable fuels, High temperature corrosion

List of content

1 Introduction

1.1 BACKGROUND

In order to globally increase the share of renewable fuels in heat and power production, the economical competitiveness compared to fossil fuelled power plants needs to be improved. This can be done in either increasing the reveue of plant (e.g. by increasing the heat and power output) or decreasing the costs (e.g. cheaper fuels, lower maintanece costs, etc). However, there is often a delicate balance by decreasisng the costs by having cheaper (and usually more corrosive) fuels and by maintaining/decreasing the maintance costs. The material performance and life time of various heat exchangers inside the plant is usually a critical factor in what level the maintaince cost will be. By optimizing the material selection with respect towards the corrosive environment the maintance costs can be kept as low as possible. This study has been investigating several factors that is expected to have an influence on the overall plant economy. This has been performed in two CFB boilers built by Sumitomo SHI FW. The data obtained within this project may be used by the industry in order to improve their economical model. This study includes no such economical considerations.

The factors investigated in this study has been:

- Long term corrosion testing of several materials by the novel clamp testing technique in both a waste fired boiler and in a biomass (including increasing fraction of waste wood) boiler
- Investigation of horizontal pass superheaters
- Corrosion investigation of novel materials
- Corrosion investigation of several position and temperatures in the two boilers
- Short term corrosion investigation focussing on the role of chlorine and of the startup sequence of probe exposures
- The evaluation of three techniques used for predicting the corrosion/corrosive environment

Traditional CFB boilers burning difficult fuels are usually designed with vertical superheater banks after a radiation pass/empty shaft. With this design, the superheater bundle is usually subject towards flue gases with high velocity and thus, the risk of erosion damages. Furthermore, due to the geometry of the tubes, ash removal from the tubes is usually performed by steam generated soot blowers. This may further enhance the risk of erosion. In this study, we are investigating two boilers built by Sumitomo SHI FW. Both boilers are designed with a horizontal pass. Hence, the superheaters in the flue gas are arranged hanging in a horizontal path. With this design, the flue gas velocity is much lower and cleaning by hammers instead of steam soot blowers can be deployed. Furthermore, the horizontal design enables a relatively fast and easy exchange of the superheaters. However, so far no corrosion tests have been performed, showing how fast the corrosion rate is of the superheaters in a horizontal pass design. In addition to investigate the horizontal pass design, the radiation pass or empty shaft is also of interest since it is expected to affect the corrosion of the downstream superheaters. Today, boilers designed for waste fired fuels utilise a radiation pass after the separation of bed material where the flue gas is cooled by radiation to a metallic water wall down to temperatures to 600 °C before entering the superheaters.

This study also includes the investigation of increasing the fraction of waste wood on superheater corrosion. There is a constant strive for the use of cheaper fuels in commercial CHP plants. Waste wood is, compared to virgin biomass, such a cheaper fuel. However, the corrosion rate in these plants are usually increased when cheaper (and usually more corrosive) fuels are being burnt. The biomass plant in this study, the newly built boiler at Örtoftaverket, is burning a fuel mix containing about 30% waste wood (the rest being 55% wood chips and 15% peat). In this study, the fraction of waste wood has been increased to 40% and 50% on a yearly basis. By this increase of waste wood, the fuel economy is greatly improved.

This study also includes the investigation of the corrosion performance of new materials and coatings, based on alumina forming alloys, in relation to more conventional materials. The ability of an alloy to resist high temperature corrosion is due to its capacity to form a protective oxide scale and corrosion properties depend on the growth rate, adhesion, chemical reactivity and mechanical properties of that scale. Only few oxides form protective scales, e.g., SiO_2, Fe_2O_3, Cr_2O_3 and their solid solutions, spinel oxides and α-Al_2O_3. However, in practice the number of oxides responsible for corrosion protection in biomass and waste fired boilers are far less and iron and chromium oxides are dominating. In the most corrosive parts of the boiler (i.e. the hottest part of the steam superheater) different classes of Cr_2O_3-forming alloys (i.e. stainless steels) are used. This is because chromia scales are far more protective than the iron oxide scales formed on, e.g. low alloy steels. Unfortunately, most chromia forming alloys behave relatively poorly in alkali chloride rich environments, which commonly is the case in biomass and waste fired boilers. Hence, when a chromia-forming alloy is exposed to alkali chlorides in the presence of water vapour and oxygen, the protective oxide reacts to form alkali chromate. Because this process depletes the protective scale in chromium, the chromia scale tends to be replaced by an iron-rich scale, causing a sudden acceleration of oxidation. The resulting "breakaway scale" is providing a much poorer corrosion protection compared to a chromia rich scale and is susceptible towards chlorine induced corrosion.

Alumina (α-Al_2O_3) scales are expected to be superior to chromia scales in biomass and waste combustion. However, alloys forming alumina scales are not widely used in combustion of biomass and waste. Also, commercial alumina formers are designed for higher temperatures and are known to be affected by internal oxidation and nitridation in the temperature range of interest (<700 °C). However, recent (unpublished) research implies that the corrosion behaviour of commercial FeCrAl alloys may be superior to the best NiCr-base alloys in biomass and waste combustion environments. In this study, we have been investigating the corrosion performance of newly developed FeCrAl model alloys.

The coating technology has also recently made advances and this study includes the investigation of coatings performed with a new generation of coating technology, HVAF (High Velocity Air Fuel). This coating is benchmarked against the more common coating technology HVOF (High Velocity Oxy Fuel). Both coatings has been the material CorEr which is a nickelbase chromia forming alloy.

There has always been a strive towards improving the prediction of expected corrosion rates. One way of improve this may be by utilising some type of measurement technique or by deploy a prediction model. We have within this study investigated three different techniques in order to predict the risk of corrosion or the corrosive environment. These three tehniques are IACM (Insitu Alkali Chloride Monitor), Thermodynamical modelling of the corrosive environment and online corrosion probe.

1.2 RESEARCH TASK

The main scientific aim of this study is to generate new knowledge about various corrosion exposures within boilers with a horizontally designed superheater region. Furthermore, new knowledge about a wide range of materials, both commercially available today and future materials, is also one of the main scientific aims. By obtaining new knowledge and material performance data the aim is that this project will provide improved material selection in boilers and thereby also facilitate better input for the economical business model of these plants.

1.3 GOAL

The overall goal of this study is to improve plant economy by enabling an increased green electricity production and optimum material selection. The material matrix includes commercial steels available today as well as future materials developed for this type of environment. This will be achieved by generating new knowledge about the following topics:

- To correlate the corrosivity of the flue gas with the flue gas temperature in respect to the material temperature.
- To verify and quantify the corrosion rates for different superheater materials in superheaters with a horizontal design.
- Verify and compare the corrosion properties of a biomass fired boiler (Örtoftaverket) and waste fired boiler (Händelöverket)
- Verify and compare the corrosion properties of commercial superheater materials as well as state-of-the-art stainless steels and FeCrAl alloys.
- Verify and compare the corrosion properties of coatings performed with the new generation coating technology HVAF (High Velocity Air Fuel).
- Compare different corrosion testing methods (i.e. probes, coils/tubes and clamping) with respect towards their complexity, cost and plant availability risk.
- Investigate how the corrosion performance of water walls is affected by a stepwise increase of the waste wood fraction in the fuel mix.

Project goals in relation to KME goals

This project proposal contributes to the following KME goals:

- Verifying novel solutions in boiler design with respect towards corrosivity.
- Increased steam parameters and thereby higher electrical efficiency.
- Test improved material solutions – including alumina forming alloys and coatings.

Due to technical difficulties and safety issues one of the goals in this study has not been fully met. We aimed earlier to investigate the effect of an increased waste wood fraction on water wall corrosion. Since these tests was stopped due to a violation of safety environment at the boiler, the goal has not been fully met.

1.4 PROJECT ORGANISATION

1.4.1 KME711

The project is jointly performed by E.ON Värme Sverige AB, Sumitomo SHI FW Energia Oy, Sandvik Materials Technology AB, Kanthal AB, MH Engineering AB, Stockholm Exergi AB, Söderenergi AB, Göteborg Energi AB, Mälarenergi AB and HTC at Chalmers University of Technology within the framework of KME. The distribution of work was:

Part	**Participants role in the project**	**Total financial contribution**
E.ON Värme Sverige AB	Responsible for boiler operation, gas analysis and fuel analysis. Participating in the project group.	2 263 kSEK
Sumitomo SHI FW Energia Oy	Providing clamps and sample materials for probes and tubes. Responsible for clamp and tube mantling and dismantling. Responsible for online corrosion probe exposures and evaluation. Participating in the project group.	1 725 kSEK
Sandvik Materials Technology AB	Providing test material to the boiler exposures. Participating in the project group.	344 kSEK
Kanthal AB	Developing new model alloys for boiler applications. Providing test material to the boiler exposures. Participating in the project group.	2 000 kSEK
MH Engineering AB	Providing coated test material to the boiler exposures. Participating in the project group.	125 kSEK
Stockholm Exergi AB	Participating in the project group.	300 kSEK
Söderenergi AB	Participating in the project group.	248 kSEK
Göteborg Energi AB	Contributed financially to the project.	23 kSEK

Mälarenergi AB	Participating in the project group.	448 kSEK
Chalmers/HTC	Project management. Responsible for corrosion evaluation of exposed samples. Responsible for short term probe exposures.	

Table 1. Participating partners in the KME711 project

Within the project the following reseachers has been active: L.Paz (Post doc), A.Olivas (Ph. D. Student), T.Jonsson (Assoc. Prof), A. Pettersson (Assoc. Prof), F. Moradian (Ph. D. Student) and J.Liske (Assoc. Prof).

The members of the reference group were, besides members of the project;

Annika Stålenheim	Vattenfall Research & Development
Pamela Henderson	Vattenfall Research & Development
Tomas Norman	Babcock & Wilcox Völund
Rikard Norling	Swerea-KIMAB
Christoph Gruber	Andritz

The project was financed by the Swedish Energy Agency together with cash and in-kind contributions from the company members of the project. The total project budget was 12 460 kSEK and the project time was 2014-2017.

1.4.2 KME720

The project is jointly performed by Kraftringen AB, Sumitomo SHI FW Energia Oy, Sandvik Materials Technology AB, Kanthal AB, MH Engineering AB and HTC at Chalmers University of Technology within the framework of KME. The distribution of work was:

Part	**Participants role in the project**	**Total financial contribution**
Kraftringen AB	Responsible for boiler operation, gas analysis and fuel analysis. Participating in the project group.	2 122 kSEK
Sumitomo SHI FW Energia Oy	Providing water wall probes and sample materials for clamps and probes. Responsible for clamp and probe mantling and dismantling. Participating in the project group.	436 kSEK
Sandvik Materials Technology AB	Providing test material to the boiler exposures. Participating in the project group.	180 kSEK

Kanthal AB	Providing test material to the boiler exposures. Participating in the project group.	260 kSEK
MH Engineering AB	Providing coated test material to the boiler exposures. Participating in the project group.	125 kSEK
Chalmers/HTC	Project management. Responsible for corrosion evaluation and service life assessment.	

Table 2. Participating partners in the KME720 project

Within the project the following reseachers has been active: L.Paz (Post doc), A.Olivas (Ph. D. Student), T.Jonsson (Assoc. Prof) and J.Liske (Assoc. Prof).

The members of the reference group were, besides members of the project;

Anna Jonasson	E.ON Värme Sverige
Annika Stålenheim	Vattenfall Research & Development
Pamela Henderson	Vattenfall Research & Development
Tomas Norman	Babcock & Wilcox Völund
Sören Aakjaer Jensen	Ørsted
Rikard Norling	Swerea-KIMAB
Christoph Gruber	Andritz
Dag Wiklund	Jämtkraft

The project was financed by the Swedish Energy Agency together with cash and in-kind contributions from the company members of the project. The total project budget was 5 205 kSEK and the project time was 2015-2018.

2 Description of the plants

2.1 P15 HÄNDELÖVERKET

Figure 1. Overview of the Händelö plant, Norrköping

The waste fired plant P15 at Händelö has a capacity of 250 000 metric tonnes/year and is shown in Figure 1 and Figure 2. The plant is a modern Energy-from-Waste plant with great fuel flexibility. The fuel is mainly household waste and industrial waste. The plant consists of a fuel preparation, boiler, steam turbine and a flue gas cleaning.

Figure 2. The waste incinerator plant P15 at Händelöverket

2.1.1 The boiler

The boiler, Figure 3, is a Circulating Fluidised Bed (CFB) boiler with a thermal capacity of 85 MW supplied by former Foster Wheeler (today: Sumitomo SHI FW Energia). The boiler produces steam, primarily used for production of electricity, industrial process steam and district heating. Some boiler data are shown in Table 3.

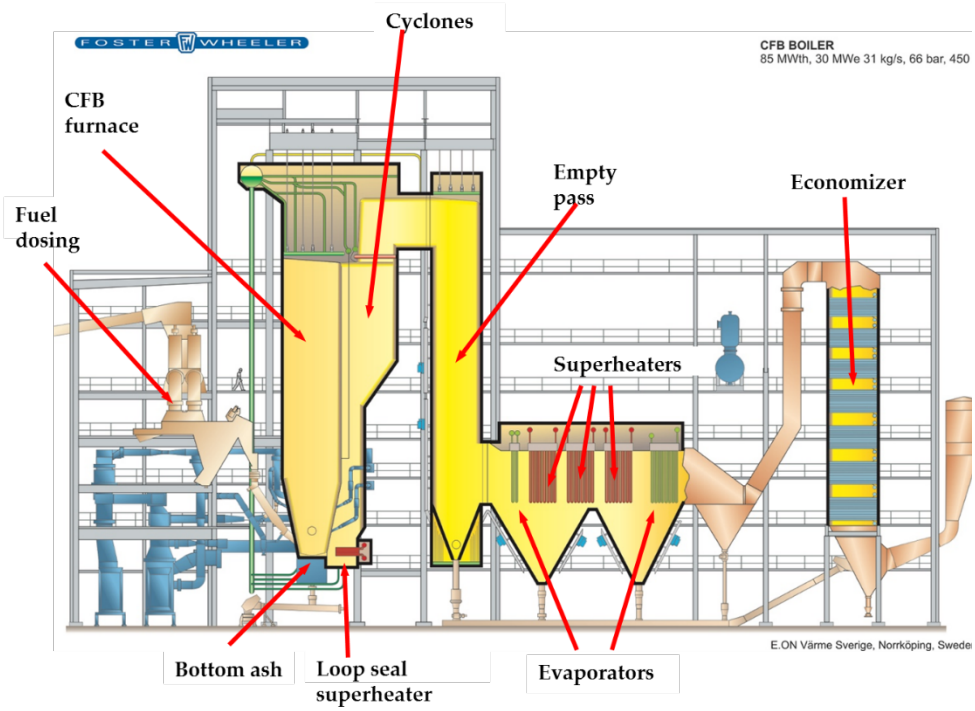

Figure 3. Schematic overview of the P15 boiler in Händelö

The design of the Sumitomo SHI FW CFB boiler used for combustion of MSW/RDF (Municipal Solid Waste, Refused Devised Fuels) fuels comprises some characteristic features to be outlined in the following text. The main parts in the boiler system are a water-cooled furnace with two integrated water cooled cyclones and loop seals, containing the final superheaters, Figure 3. The cyclones are followed by a single pass radiation cavity (empty pass) and a horizontal convection pass with superheater banks and boiler banks. The flue gas meets the economizer banks before entering the flue gas treatment system.

The boiler is top supported and designed for circulation by means of an circulating pump, characterised by the steam separating system including the steam overflow headers, in combination with the downcomers, which run from the top to the bottom of the boiler. Saturated water from the drum is distributed through a number of downcomers to the bottom part of the boiler, the wall tubes in the furnace, the cyclone loop seal and the radiation cavity/back pass enclosure. The water/steam mixture is transferred back to the steam drum by a number of steam separating connecting pipes. The circulating system is integrated between all components.

All four walls of the furnace are refractory lined, for erosion protection and to sustain furnace temperature above 850 °C during 2 seconds after the last injection of air. The latter is a European requirement when firing waste. It is also required to install auxiliary burners in the furnace to secure the furnace temperature 850 °C before adding the RDF during start up and in case of a sudden drop in the furnace temperature during boiler operation.

Coarse fuel ash entering the furnace is transported through the bottom bed, by means of the directed primary air nozzles, to discharge openings in the bottom plate, from which the ash is transported to a first sieve of the ash. Small bed particles are separated from the coarse ash particles. The coarse ash is sent to containers and the finer particles proceed to a further screening. Here again, the coarser share is sent to the containers, while the finer ash is either sent back to the furnace again, if needed, or sent to a silo for fine-bottom ash. The screws under the furnace are water-cooled to withstand incoming ash temperatures. The ash is cooled through the passage in the screws.

The boiler features two hot gas cyclones for separation of the bed material entrained by the flue gas and leaving the furnace at the furnace top. The separated material is returned to the lower part of the furnace via a smaller loop seal, called wall seal, and a conventional loop seal. The loop seal contains a bubbling fluidized bed and is equipped with a number of air nozzles to ensure material transport. Moreover, it is designed to prevent flue gas from the furnace entering the cyclones through the bed material return leg.

The loop seal, which is a feature of the CFB process, offers a location of the final superheater (SH) for two reasons;

1. The heat transfer coefficient in the bubbling bed is 5 to 10 times higher than in the back pass. Hence, the SH area required is reduced by 80 to 90%.
2. The gaseous atmosphere in the loop seal contains less of chlorine and water vapor since the chlorine and water released during the combustion of the RDF is in a gaseous form in the cyclone and therefore follows the flue gas to the back pass. Only the particles separated by the cyclone reach the loop seal.

The cyclones are constructed from water-cooled membrane walls, which form part of the water circulation system. The feature of this design is that the cyclones are part of the natural water circulation circuit and therefore expand in the same way as the furnace and back pass enclosure. This feature allows the cyclones to be gas-tight welded to the furnace and the back pass, thus avoiding all expansion bellows of huge dimensions always causing a lot of maintenance problems and costs. The cyclone interior is fully refractory lined with a thin layer for erosion protection, which minimizes the amount/thickness of refractory and further reduces the maintenance costs and shortens the start-up time. An SNCR-system is installed, with ammonia injection in both cyclones

The cyclones are followed by an empty pass for lowering the flue gas temperature to a temperature, which makes the ash ”dry” and non-sticky to the back pass tube banks. This will minimize deposit formation and corrosion attacks. The bottom of the empty pass and the horizontal pass are equipped with an ash extraction conveyor system.

Water/steam		
Feed water temp	°C	135
Steam flow	kg/s	31
Steam pressure	bar	65
Steam temperature	°C	450
Miscellaneous		
Boiler efficiency	%	90
Exit flue gas temperature	°C	165-170
Unburned in bottom ash	%	<0,1
Unburned in fly ash	%	< 0,5

Table 3. Operating data at MCR (Maximum Continues Rate).

The P15 boiler is integrated with the other boilers at the plant. The water treatment, district heating system, steam turbine and the condenser are commonly used, by two or more boilers. The plant is supervised from one control room.

2.1.2 The fuel preparation

The fuel preparation plant, see Figure 4, consists of a receiving bunker (78 m long, 12 m wide and 8 m deep) with a total volume of more than 7000 m^3. Two overhead travelling cranes with crab buckets feed the two redundant preparation lines. The crushing/ grinding is performed in two steps and magnetic sorting in three steps, before the boiler. M & J delivered the primary shredders and there are also two secondary shredders, which have replaced the hammer mills. The prepared waste is transported to an intermediate storage, an A-barn, before it is transported to the boiler silos. Sydkraft (today E.ON) has designed the waste preparation system, while the parts are delivered from a number of suppliers.

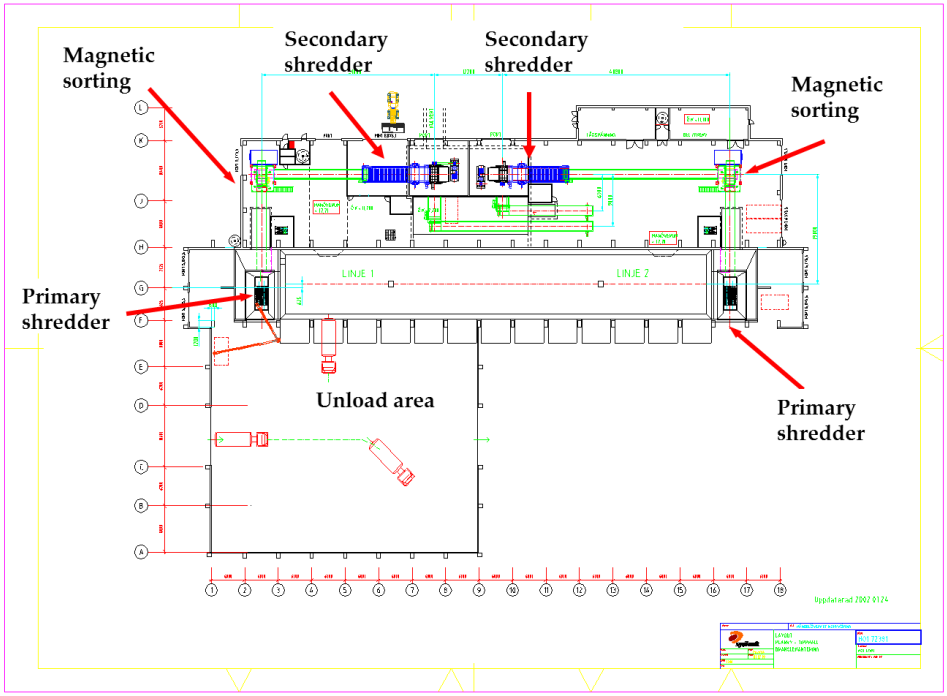

Figure 4. The fuel preparation

2.1.3 The flue gas cleaning

Alstom Power has delivered the flue gas cleaning system, see Figure 5, which is a semi-dry system without flue gas condensation. The NID-system includes a mixer, a reactor and a fabric filter. Burnt lime is mixed with water in an extinguisher. The hydrated lime is mixed with recirculated filter ash and additional water in a mixer. Next, the moisturized dust is fed into the flue gases in a reactor chamber where activated carbon is added. The particles are removed from the flue gas by a fabric filter. The lime binds to chlorine and sulphur while the activated carbon is used to remove dioxins and heavy metals. The major part of the removed fly ash is recirculated through the mixer and reactor system.

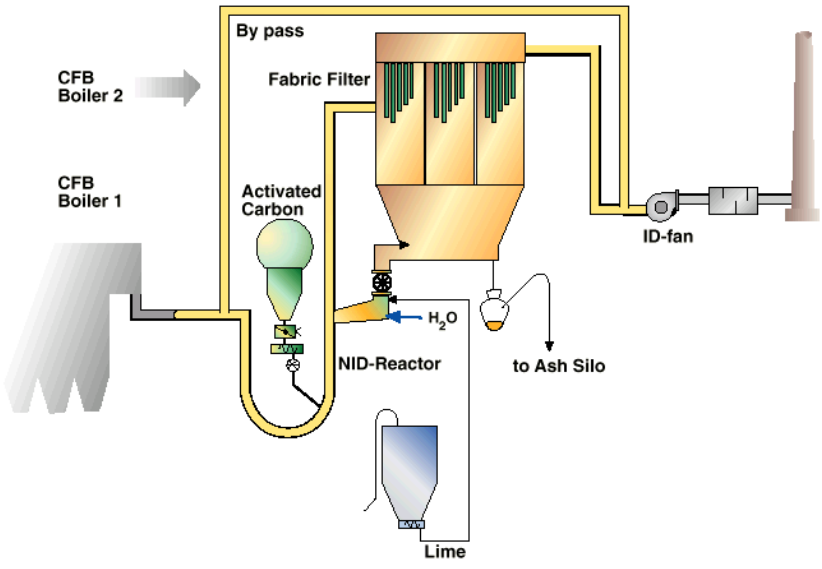

Figure 5. The flue gas cleaning

2.2 ÖRTOFTAVERKET

Örtoftaverket is a biomass-fired combined heat and power plant (CHP) that produces both district heating and electricity, shown in Figure 6. The plant consists of a steam boiler, steam turbine and flue gas condenser. The plant started its commercial operation in March 2014.

Figure 6. CHP plant Örtoftaverket.

The flue gas condenser utilizes the excess heat from the boiler flue gases. It is performed by condensing the water in the flue gases and transfer the recovered heat to the district heating network. Condensate water is then treated in water treatment processes to purity levels that correspond to feed water quality.

The steam turbine is a back-pressure turbine, which is cooled down during the condenser phase through the heat being transferred to the district heating network. Apart from using the turbine, all the steam can be dumped in a direct condenser. This can be used mainly during start-up and when electricity prices are low.

2.2.1 Boiler Örtoftaverket

The boiler is a circulating fluidized bed (CFB) boiler with a thermal capacity of 110 MW supplied by former Foster Wheeler (today: Sumitomo SHI FW).

Boiler capacity	110 MW_{th}
Steam pressure	112 bar
Steam temperature	540 °C
Steam flow	42,9 kg/s
Steam turbine	39 MWe
District heating network	74 MW_v
Flue gas condenser	20 MW_v
Total efficiency of the whole plant	91,4 % (103 % including flue gas condenser)

Table 4. Boiler data

The boiler design consist of the furnace and two water-cooled solid separators.

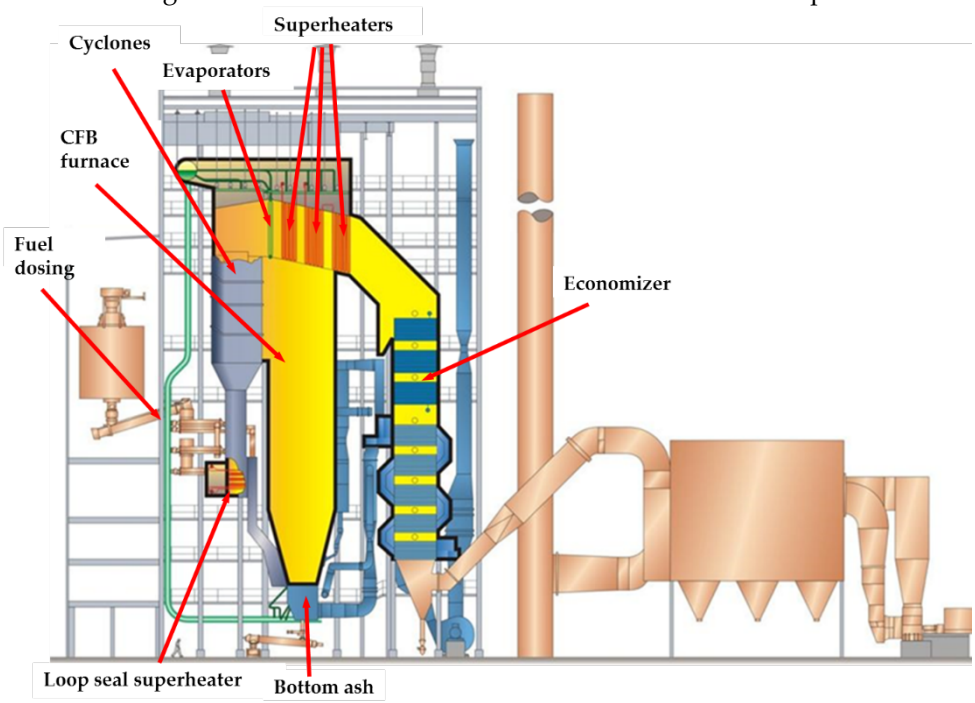

Figure 7. Overview of CFB boiler construction at Örtoftaverket.

The steam superheating process takes place in four stages; Superheater I (SH I), Superheater (SH II), Intrex Superheater III (SH III) and Intrex Superheater (SH IV). SH I – II tube bundles are of hanging type, located in the horizontal cross-over duct leading from solids separators to the back pass. Heat is transferred in SH I – SH II from the hot flue gas to the steam via convective heat transfer. SH III – IV are located in the sand loop seal. Heat is transferred to the steam in the Intrex superheaters from the circulating ash. Economizer and air preheater is located in the back pass.

2.2.2 Designed fuelmix Örtoftaverket

The fuel feeding systems consist of two feeding lines, each including a day silo with reclaimer, chain conveyors, robbing screws and feed chutes to solids return flow. Both feeding lines can feed all of the four feeding points.

The boiler is designed for firing forest wood chips, demolished wood and peat as the main fuels, but is also capable of firing sawdust, bark, salix and stump chips. The fuel mix changes depending on the needs and cost levels. The boiler load is dependent on the fuel mix and heating value. When firing waste, e.g. waste wood, the temperature shall be maintained above 850 °C for a minimum of 2 seconds in the furnace (European requirement when firing waste).

Waste wood is regarded as a challenging fuel due to high levels of impurities and highly inhomogeneous nature. CFB combustion was selected for the boiler for its fuel flexibility. Co-firing with peat reduces corrosion risks related to the biomass and demolished wood. Peat was fired during the first years of operation but will be phased out during firing season 2017/2018 since it is considered as a borderline fossil fuel. All of Kraftringen's production of district heating is planned to be fossil free no later than year 2020. Instead, Sulphur beads is added to the fuel to sulphurize any corrosive alkali chlorides.

Forest wood chips	0 – 100 %
Demolished wood	0 – 50 %
Peat	0 – 35 %
Sawdust	0 – 30 %
Bark	0 – 50 %
Salix	0 – 15 %
Stump chips	0 – 50 %

Table 5. Design fuel mixture range.

A greater amount of demolished wood is being mixed in the fuel for the boiler than in the beginning of operation. This is boosting the plant's yield since fuel price is low at the moment. The goal is to increase the faction of waste wood even further.

3 Experimental conditions

To be able to compare different corrosion testing methods (i.e. probes, coil/tubes and clamping), long term and short term exposures have been performed. In the waste fired boiler P15 at Händelö, the long term exposures included both clamps and coil/tubes testing. In the biomass fired boiler at Örtofta only clamp exposures were performed. The short term exposures with probes were performed at Händelö.

3.1 LONG TERM EXPOSURES

The main aim of the long term exposures was to investigate the extent of corrosion for a wide range of materials for up to three years. Thereby, the results give a solid ground for the progress of corrosion during a long period of time and thus, relevant material performance data. A schematic visualization of the long term exposures is shown in Figure 8.

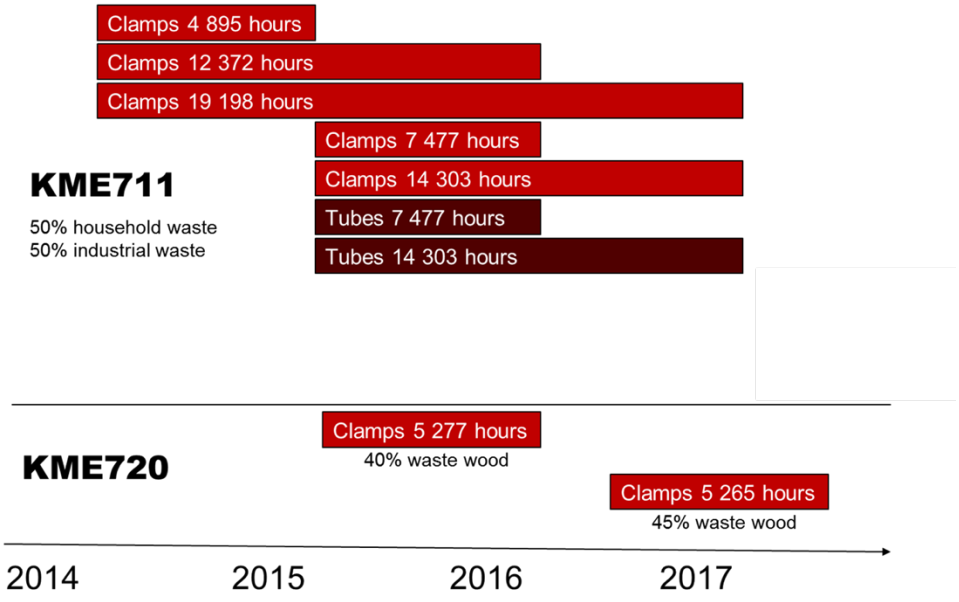

Figure 8. Schematic illustration of long term clamp and tube exposures. The "KME711" samples have been exposed in the waste fired P15 boiler at Händelöverket, Norrköping. The "KME720" samples have been exposed in the biomass fired Örtofta boiler, Lund.

3.1.1 Long term clamp exposures

The clamps were installed on the permanently installed superheater tubes during several revision periods, in both boilers. An example of the installed clamp samples can be seen in Figure 9. The temperature of the clamp will be dictated by the superheater temperature and surrounding flue gas temperature. An initial temperature measurement can be performed by an external thermoelement. Due to the corrosive environment inside the boiler this thermocouple is usually destroyed

within the testing period. The clamp samples can only be removed during revision, when the boiler is cooled down.

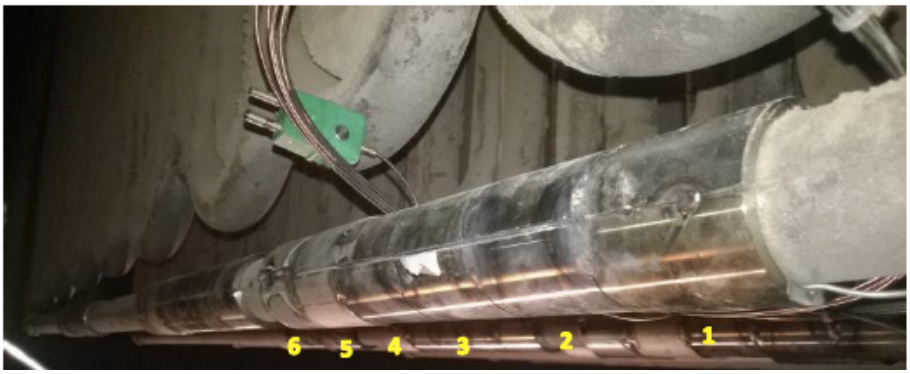

Figure 9. Image of clamp samples installed in the P15 Händelö boiler. The numbers represent different clamp samples.

3.1.2 Long term superheater tube exposures

The superheater tube samples were installed in the waste fired P15 Händelö boiler during a revision period, see Figure 10. The tube samples were welded together to each other and to the permantly installed superheater tubes. The tube samples can only be removed during revision, when the boiler is cooled down.

Figure 10. Image of superheater tube samples installed in the P15 Händelö boiler. The numbers represent different tube samples.

3.2 SHORT TERM PROBE EXPOSURES

The main aim of short term probe exposures are to investigate more in detail different aspects of the corrosion and/or techniques governing corrosion. The short term probe exposures were performed in two blocks; a first block only investigating the effect of the probe startup sequence and a second, more comprehensive, block where a number of studies were conducted in parallell. A schematic visualization of the studies in the second block is shown in Figure 11. In the second block, the effect of chlorine penetration through preformed oxide scales, new materials and "corrosion prediction" techniques were investigated. The prediction techniques

coupled to these exposures consist of a thermodynamical model (predicting alkali chloride levels in the flue gas), the IACM system (measuring alkali chloride levels in the flue gas) and an online corrosion probe (meaursing the corrosion rate online).

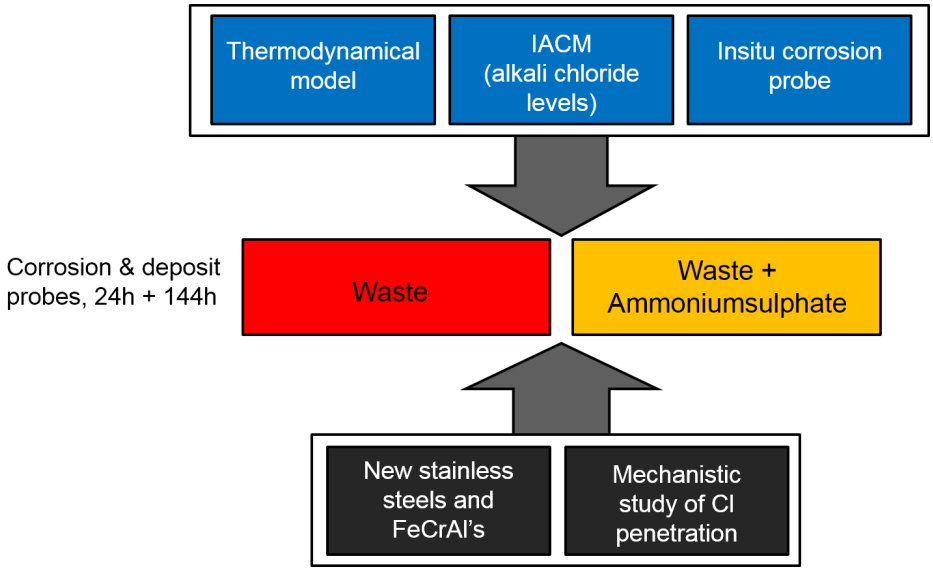

Figure 11. Schematic illustration of probe exposures

3.2.1 Probe exposures to study the startup effect

In order to study the effect of the startup sequence of probe exposures on the corrosion attack we performed short term probe exposures in the waste fired P15 Händelö boiler. Based on earlier experience, there was a concern that when a cold probe is inserted to a hot boiler the initial (minutes) will actually favour the condensation of a liquid water film on the cold probe (until the material temperature has reached 100 °C). The hypothesis was that the presence of a water film may facilitate an increased chlorine load as HCl(g) will dissolve readily in the water.

The probe type used for study the startup effect of cooled probes is shown in Figure 12. The probes hold 3x3 samples in three individually controlled temperature zones. The material temperature of each zone is controlled by a PID controller and pressurized air was used as cooling agent.

Figure 12. Three temperature zone probe used for start-up effect study

The exposed material was the stainless steel Sanicro 28. All samples were produced from tubes, shaped into its final dimensions using a lathe. The samples were cleaned in acetone and ethanol using an ultrasonic bath prior to exposure. The outer

diameter of the sample rings was 48 mm and the wall thickness was 2.9 mm. A total of 47 rings were exposed of which 12 rings were pre-oxidized in air at 700 °C during 24 hours in a laboratory box furnace. Each probe consisted of three individually controlled temperature zones (600, 500, and 400 °C), see figure Figure 13. The samples were characterized by means of SEM and XRD.

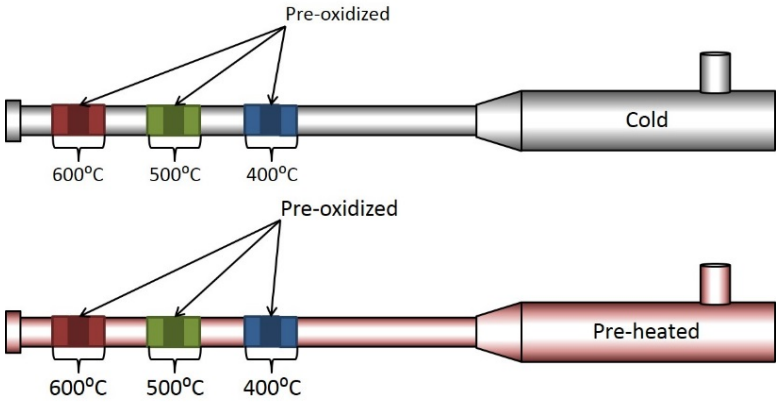

Figure 13. Schematic drawing of the exposed testing probes

3.2.2 Probe exposures to study chlorine penetration and new materials

One of the goals of the project is to correlate the corrosivity of the flue gas with the flue gas temperature in respect to the material temperature. Two sets of exposures were performed with respect towards corrosive environment. One set of exposures was performed during "reference" conditions in the waste fired boiler P15, the other set of exposures was performed with the addition of ammonium sulphate/ChlorOut® to the same boiler. The short term probe exposures consisted of a reference period (denoted "waste") and a period with additive (denoted "Waste + AmS"). In both periods, probes were exposed for 24 and 144 hours.

The probes used for the study of the effect of the chlorine, pre-oxidation and new materials hold 4 samples in two individually controlled temperature zones, as it is presented in Figure 14. The material temperature of each zone is controlled by a PID controller and pressurized air was used as cooling agent.

Figure 14. Schematic drawing of the two temperature zones probes

All samples were produced from tubes, shaped into its final dimensions using a lathe. The samples were cleaned in acetone and ethanol using an ultrasonic bath prior to exposure. The outer diameter of the sample rings was 38 mm and the wall thickness was 2.2 mm.

3.2.3 Online corrosion probe

The probe is designed to be installed into convective heat recovery areas to study corrosion of critical components of the boiler. During exposure probe can be cooled by air or water to control the metal temperatures of the samples. A schematic drawing of the probe is given in Figure 15. Probe set up consist of the following:

- corrosion probe
- control unit box with signal cable
- test coupons (test electrode 1 and 2, reference electrode, weight change specimens 1 and 2)
- ceramic pieces for galvanic separation of test coupons
- hoses for pressurized air or water.

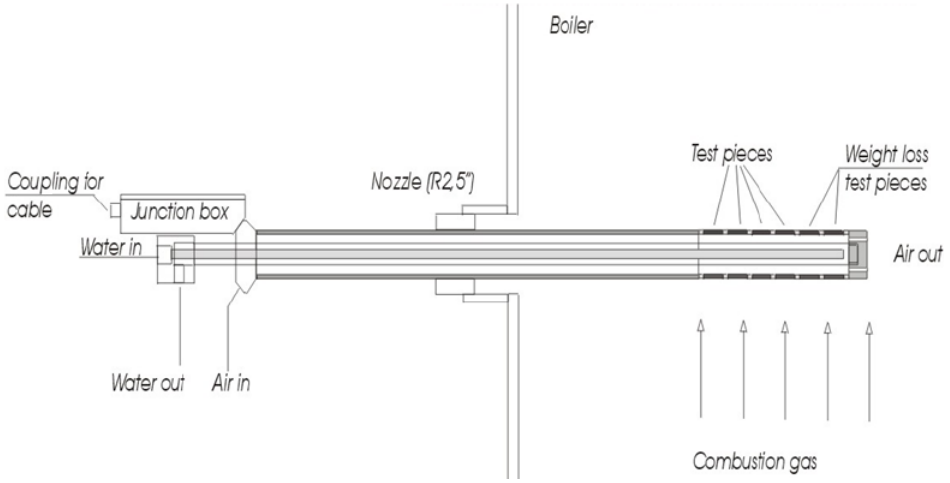

Figure 15. Schematic drawing of the online corrosion probe

A representative corrosion signal is received from the probe and the system automatically calculates corrosion rate values in cyclic periods by using linear polarization resistance method (LPR). System measures the resting potential between test electrode and reference electrode. Deflecting voltage is induced to the system and corrosion current is determined based on the polarization resistance. Weight loss of test pieces is measured and additionally XRF is used to analyse chemical compositions of deposits and metal surface.

3.3 MATERIALS

3.3.1 Description of materials

A wide material testing matrix have been performed in two boilers designed with a horizontal pass superheater region. The material matrix has included convential steels used today as well as newly developed stainless steels, FeCrAl model alloys and two different types of thermally sprayed coatings, namely HVOF and HVAF sprayed coatings. Below a short description of the use and benfits of each material type is presented.

The chosen materials are typical for superheaters, from low alloyed ferritic steel to nickel-based alloys. The choice of materials for the superheater depends on the quality of the fuel, placement of the superheater (dependent on the flue gas temperature), material temperature (dependent on the steam temperature), material cost etc. Chromium is often used to increase the corrosion resistance of the steel. Steels with more than 13 % chromium are often referred to as stainless steels. Nickel alloys are also commonly used in order to improve the corrosion resistance of the superheater. The price of low alloy steels may be up to 8 times cheaper than high nickel based alloys.

The alloys used within this project can be described as:

- **St35.8 III**
  This is a carbon steel used in boilers when the material temperature is kept low and the corrosive environment is mild.

- **16Mo3, EN10028**
  16Mo3 is a pressure vessel grade low alloyed steel for use in elevated working temperatures. The material is used as a weldable steel in boilers as well as steel pressurised vessels found in the oil, gas and chemical industry.

- **13CrMo4-5, EN10028**
  This is a commonly used Cr-Mo-alloyed low alloy steel in superheaters. It has better creep strength than non-alloyed steels.

- **10CrMo910, EN 10028**
  This alloy conatins increased levels of molybdenum and chromium compared to 16Mo3 & 13CrMo4-5 and is therefore expected to have a greater heat and corrosion resistance. The material is a pressure vessel grade steel for use in elevated temperature service. The steel has also good weldability.

- **X10CrMoVNb9-1, T91/P91, EN 10216-2**
  Grade T91 is a high Cr high strength ferritic-martensitic (9 % Cr, 1 % Mo) microalloyed steel (V, Nb, N) according to ASTM A 213, EN 10216-2 standard
  It can be used up to metal temperatures up to 580 °C - 600 °C. The high strength allows use at 80 °C - 100 °C higher temperatures than the 2.25%Cr (T22) material. The thinner walls/reduced weight of tubing, vs lower alloyed steels, means higher resistance to thermal fatigue. Compared with austenitic steels, grade T91 has higher heat transfer and lower thermal expansion coefficients.
  A drawback with T91 is that it requires PWHT which complicated / prolongs maintenance work. Buttwelds involving T91 need heat treatment after welding.

- **347H and 347HFG, EN1.4912 (6R44)**
  This is an austenitic stainless niobium stabilized stainless 18 10 chromium-nickel steel used in superheaters in steam powerplants allowed for metal temperatures up to to 600 °C - 620 °C. The grade also exists in a fine-grained mode, i.e. 347HFG. The fine grained mictrostructure is facilitating an increased transport of Cr to the oxide and thereby improves the corrosion properties of the steel.

- **Esshete1250, EN1.4982**
  This is an austenitic stainless chromium-nickel-manganese 15 9.5 6 steel used in superheaters & reheaters in coal and biomass powerplants. Its allowed foruse in metal temperatures up to to 600 °C - 620 °C. This alloy is verified in large installations in the UK coal fired power fleet operating at 568 °C superheat and reheat temperatures since the early 70's. Successfully used also in biomass fired boilers delivering superheat and reheat steam at 568°C. The alloy can be bent to tight radius as allowed by BS1113 without need for post bend heat treatment. This feature saves significant fabricator costs.

- **310H, EN1.4845**
  This is an austenitic stainless 25 % chromium 20% nickel type steel type. The material is suitable for use in superheaters operating in corrosive conditions at metal temperatures up to 525 °C - 540 °C. The grade is not yet included in the EN specification EN10216-5 and is therefore requiring a "single approval" for installation in boilers under the PED (European Pressure Directive).

- **Sanicro 28, EN 1.4563**
  This is an austenitic high alloyed Cr/Ni/Mo (27/31/3.5) very corrosion resistant steel. It was initially developed for wet corrosion applications. Its limited for use in metal temperatures up to 550 °C (VdTUV 483) and 450 °C (ASME Code Case1325-18). To facilitate fabrication/welding, to reduce thermal elongation, increase thermal transfer its also co-extruded over lower alloyed materials type 10Cr/T22, X10Cr/T91 to so called composite tubes. Such tubes are used both in superheaters and waterwalls when more corrosive fuels are used.

- **Sanicro 33**
  This is a newly developed high alloyed austenitic heat resistant stainless steel. It exhibits both high creep strength and high corrosion resistance. This allows the material to be used in environments with high temperature and high pressure in metal temperatures up to 650 °C. The material is not yet approved by any international standard. The grade is targeted for use in superheaters/reheaters in boilers in which more corrosive fuels are used.

- **KanthalAPMT**
  FeCrAl-alloys forms, depending on environment and temperature, a protective layer containing Al_2O_3. The FeCrAl-alloy Kanthal APMT is an advanced powder metallurgical, dispersion strengthened, ferritic iron-chromium-aluminum alloy. Typical applications for Kanthal APMT are as radiant tubes in electrically or gas fired furnaces. Recently, Kanthal APMT has been tested in environments related to biomass and waste fired boilers with good results, which makes FeCrAl alloys interesting to use also as superheater tubes.

- **FeCrAl model alloy, Fe10CrAl2Si**
  Kanthal has also delivered a FeCrAl model alloy for clamp testing and probe exposures. The model alloy has had the composition of Fe (bal), Cr (10%), Al (3%), Si (2%) and RE added. This alloy has also been exposed in the KME709 project.

- **Inconel625, (sometimes denoted alloy 625)**
  This alloy is a nickel base alloy contain both Chromium and Molybninum for corrosion protection. The alloy exhibits generally good corrosion resistance in chloride containing environments and is today a used to large extent in the boilers, primarily as overlay weldings and thermal spray coatings.

- **CorEr thermally sprayed coating**
  MH Engineering has devolped a nickel-based alloy, with a similiar composition as the Inconel625 alloy. However, micro-additvies has been added in order to promote precipitation hardening. This hardening process starts when the boiler is started up and after about 3 weeks at 300 °C material temperature the coating is fully hardened. This process increases the hardness to about 800 (HV300) as to compared to traditional Inconel625 which has a corresponding hardness of about 300. This increase in hardness is especially useful in CFB boilers burning difficult fuels and where corrosion and erosion is problematic. This coating has both been sprayed on to samples with the HVOF technique (High Velocity Oxy-Fuel) and the newer HVAF technique (High Velocity Air Fuel). The later coating technique is expected to produce more dense coatings and thereby higher corrosion resistance.

3.4 IACM

During the short-term tests, an IACM®-instrument was used. The IACM instrument (Online Alkali Chloride Monitor) measures the concentration of gaseous alkali chlorides (KCl and NaCl) on-line. The measurement principle is based on molecular absorption over a certain wavelength interval. IACM also enables measuring of the SO_2 levels. The instrument is often used in boilers for quality control of incoming fuel mixes as well as control of required amounts of the Vattenfall ChlorOut® additive. A schematic illustration of the IACM measuring system is shown in Figure 16.

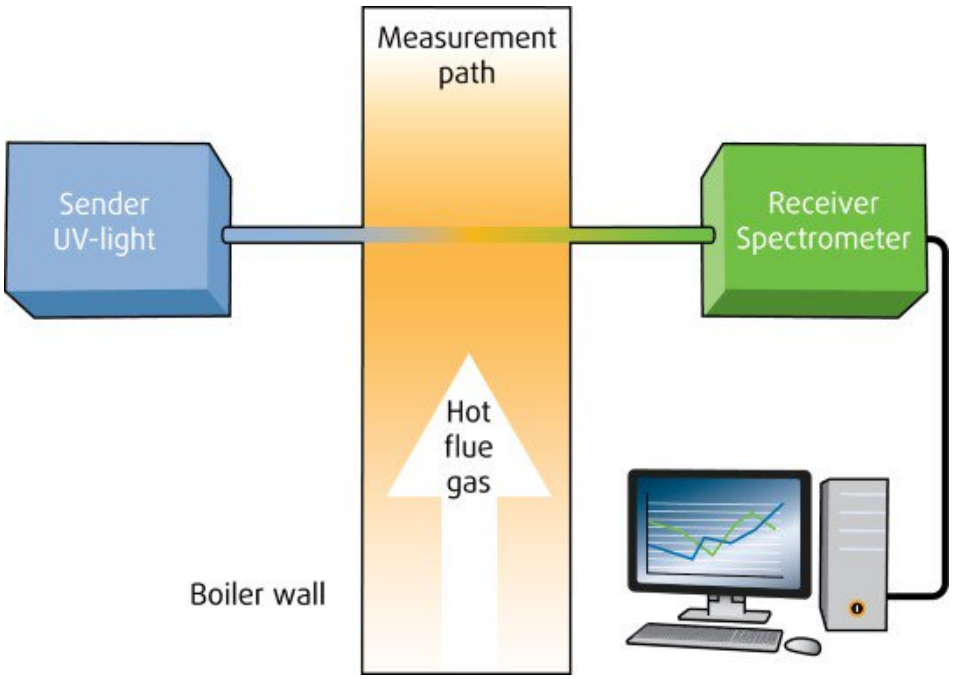

Figure 16. Schematic illustration of the IACM measuring system

The illustration shows schematically how the UV-transmitting unit on one side of the flue gas channel sends light to a receiving unit on the other side. It also shows the computerized signal evaluation leading to visualization of the results as KCl, NaCl and SO_2 levels. In the P15 boiler, the IACM was installed in the upper part of the empty pass, see Figure 17.

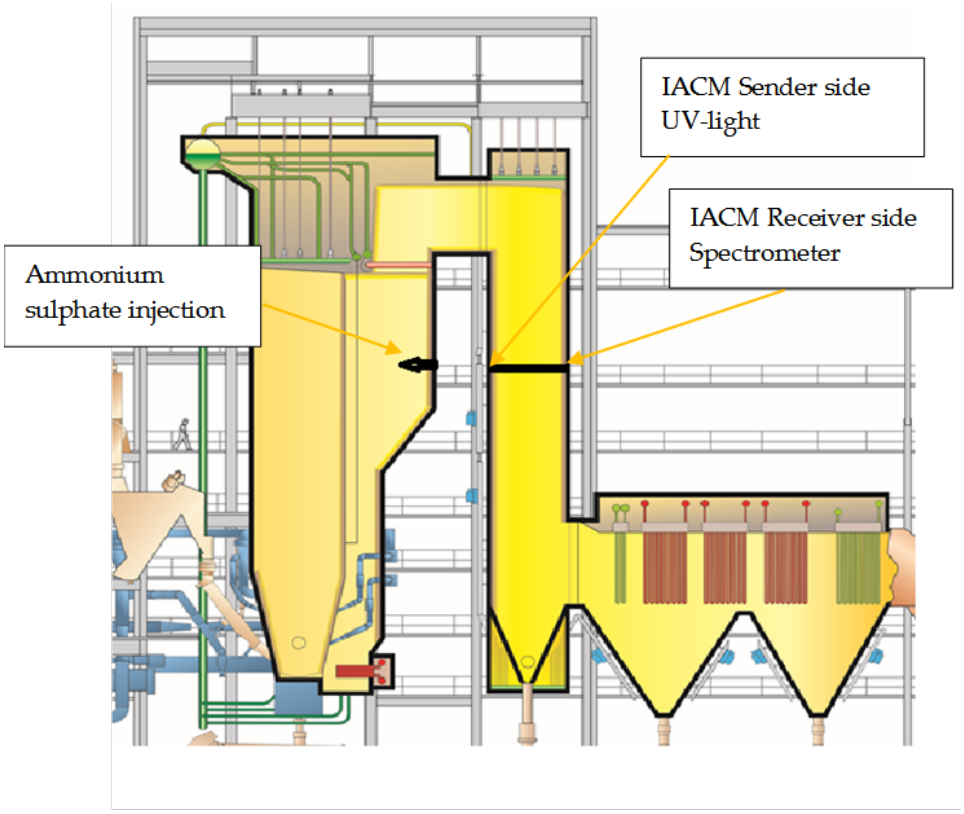

Figure 17. Placement of the IACM measuring system and Ammonium sulphate injection in the P15 boiler

The IACM system was used during the second block of short term probe exposures. In total, two exposure conditions were investigated; "Waste" and "Ammonium sulphate". The IACM measured the levels of gaseous alkali chlorides in the flue gas during both these exposures. In the reference exposure (Waste), normal operation conditions for the boiler was prevailing.

In order to inject ammonium sulphate to the boiler, existing ammonia injection system had to be used. The ammonium sulphate had to be stored in a separate tank, but the tank was connected to the injection system normally used for ammonia. The plan was to add corresponding amount of ammonium sulphate compared to ammonia to get the same NOx reduction, to avoid ammonia slip (increased levels of ammonia, too high levels of ammonia emissions). Except for the use of ammonium sulphate, normal operation conditions in the boiler was prevailing.

Samples of ash from different positions in the boiler and also samples of fuel were taken in both the reference exposure and in the Ammonium sulphate exposure.

3.5 THERMODYNAMIC MODELLING

3.5.1 Modelling approach

Figure 18 illustrates the modelling approach which was applied for the prediction of alkali chlorides (NaCl and KCl) concentration in the flue gas of the CFB boiler. The standard fuel analysis was carried out to determine the elemental composition of the solid waste. In addition, the chemical fractionation of the solid waste was performed to determine the reactive and less-reactive fractions of the ash-forming elements. It is known that the reactive fraction of the ash-forming elements primarily contribute to the formation of the flue gas, while the less-reactive fraction is assumed to form the bottom ash [1]. Thus, considering the total amount of the ash-forming elements (e.g. Na and K) for the equilibrium calculations may overestimate the concentrations of the alkali chlorides in the flue gas. Furthermore, this approach will minimize the restrictions regarding the kinetics of the reactions which are not taken into account by the thermodynamic equilibrium models.

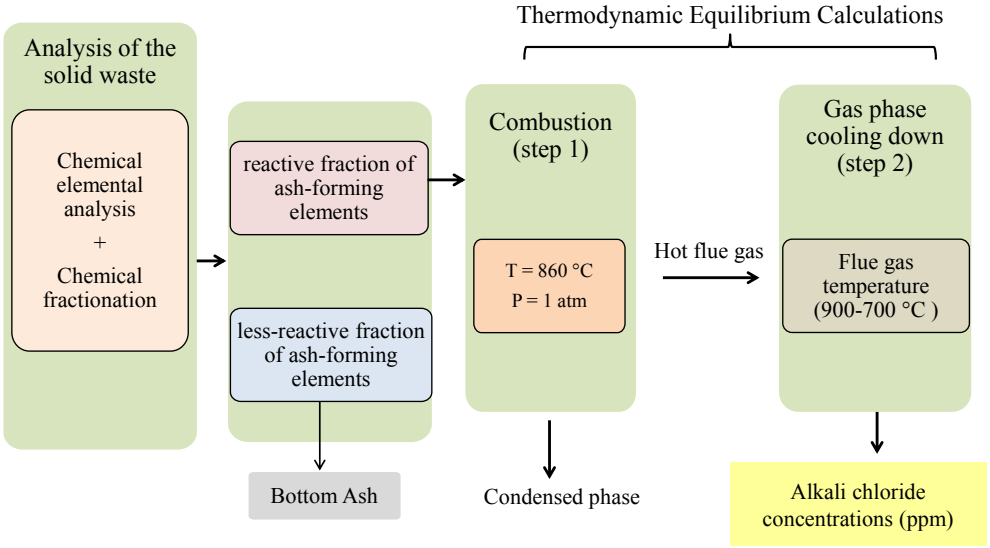

Figure 18. Schematic representation of the modelling approach applied for prediction of alkali chloride concentration in the hot flue gas of the CFB boiler

The thermodynamic equilibrium calculations were carried out in two steps. Step 1 simulates the combustion of the solid waste in the furnace and predicts the chemical composition of the hot flue gas leaving the furnace, considering the fuel composition (combustible fraction and reactive fraction of the ash-forming elements), combustion temperature and pressure, as well as air/fuel ratio. The condensed phase (solid and liquid phases) was withdrawn from the system, and the gas phase (the calculated hot flue gas) was used as input for the modelling of the gas phase cooling down (step 2). Step 2 evaluates the changes in the chemical composition and physical state of the hot flue gas as the temperature decreases from 900-700 °C, which determines the alkali chloride concentration in the flue gas prior to the superheater.

3.5.2 Thermodynamic equilibrium calculations

FactSage 7, the thermochemical software and databases, was employed for the thermodynamic equilibrium calculations. All input data for the equilibrium calculations, including fuel elemental composition, combustion temperature and pressure, as well as air/fuel ratio are based on operational data which were obtained from full-scale sampling and measurements. Therefore, it is possible to compare the equilibrium calculation results with the full-scale measurements data (e.g. IACM data) and evaluate the accuracy of the predictive model. This was mainly focused on comparison between the alkali chloride concentration in the flue gas calculated by the predictive model and measured by the IACM.

As described in Figure 18, the thermodynamic equilibrium calculations were carried out in two steps. Step 1 simulates the combustion of the solid waste in the furnace of the CFB boiler. Note that the combustion of the solid waste in the CFB boiler was modeled in one step, considering the relatively uniform temperature profile in the furnace, as the logged data did not show significant temperature difference in the bed zone and freeboard. For the step 1 of the equilibrium calculations, the input elements and their total amount in the solid waste were selected based on the standard fuel analysis (ultimate analysis) of the fuel (SWA and SWB). For the ash-forming elements, the reactive fraction was recalculated based on the chemical fractionation results. In total, 14 elements were considered: C, H, N, O, Cl, S, K, Na, Ca, Mg, Si, P, Zn and Pb. Other elements present in the chemical composition of the solid waste were excluded, owing to their less-reactive nature or very low concentrations. The total concentrations of the C, H, N and O in the fuel were assumed to be reactive. All calculations were carried out under the atmospheric pressure (1 atm). The air/fuel ratio was adjusted based on the logged data, resulting in approximately 6 vol % excess O_2 in the flue gas. Thermodynamic databases FactPS, FToxid and FTsalt were employed for the calculations and prediction of the gas and condensed phases. Further information regarding the selected FactSage's databases for simulation of the combustion process and flue gas composition can be found in Moradian et al [2].

3.6 ANALYTICAL TECHNIQUES

The exposed samples were investigated by means of quantative as well as qualitative analytical techniques. The quantitative measures have involved material loss determination and the qualitatively analysis have primarily involved cross sectional SEM/EDX analysis and XRD analysis. Most of the analyses were performed by HTC/Chalmers. The exception being chemical fractionation which were performed by University of Borås.

3.6.1 Material loss

The samples were evaluated by means of metal loss determination, performed with an Olympus 38DL Plus ultrasonic thickness gage with a 0.01mm resolution. Complementary material loss determinations was performed by OM and SEM measurements.

3.6.2 Scanning Electron Micriscopy/Energy Dispersive X-Rays (SEM/EDX)

After exposure, some selected samples were prepared for cross sectional SEM/EDX analysis. These samples were casted in epoxy, cut and polished prior to the SEM/EDX investigation. The samples were casted by first descending them in epoxy resin. Both sample and mould were then subjected to a 10-bar pressure to avoid the formation of bubbles during the hardening of the resin. The hardening time was fixed at 24 hours. After the hardening of the epoxy resin was complete, the samples were cut using a silicon carbide disc and a lubricant without any water due to the delicate corrosion products. The samples were then polished dry with Silicon Carbide P4000. The cross-section was coated with gold to avoid charging in the SEM. The polished cross-sections of the samples were subsequently investigated by scanning electron microscopy, SEM. In addition, an Energy Dispersive X-rays (EDX) system was used enabling analysis of the elemental composition of the sample in the SEM image. The resolution and depth of focus in an SEM is much higher than in an optical microscope, revealing more details of the corrosion attack. The samples were examined with an FEI Quanta 200 FEG ESEM. The SEM has a field emission electron gun (FEG) and is equipped with an Oxford Inca energy dispersive X-ray (EDX) system. SEM/EDX was used for elemental mapping and quantification. For imaging and EDX analysis an accelerating voltage of 20 kV was used.

3.6.3 X-Ray Diffraction (XRD)

In order to determine the crystalline phases in the deposit and corrosion layer, XRD was used. The diffractometer was a Siemens D5000 powder diffractometer, equipped with grazing – incidence beam attachment and a Göbelmirror. Cu – Kα radiation was used and the angle of incidence was 2. The measuring range of the detector was $10°<2\theta<65°$.

3.6.4 Chemical Fractionation

Chemical fractionation is a stepwise leaching technique which is used to determine the chemical association of the ash-forming elements in solid fuels, as is illustrated in Figure 19. The water-soluble and ammonium acetate-soluble ash-forming matter of solid fuels are mainly in the form of dissolved salts (e.g. alkali chlorides, sulphates, carbonates, etc.) and organically bound metal cations, respectively. These fractions are assumed to be volatilized and participate in combustion reactions and form gas phase, fine ash particles or condense on cool surfaces. The acid- soluble fraction of the ash-forming matter and also the solid residue (non-soluble rest) are mainly consisted of salts of alkaline-earth metals, silicates and other minerals, which are known to be less-reactive during combustion and remain as bottom ash in the boiler. Note that elements covalently bound to the organic fuel matrix, such as S, Cl, and P may stay in the solid residue but are considered to be reactive during combustion [1].

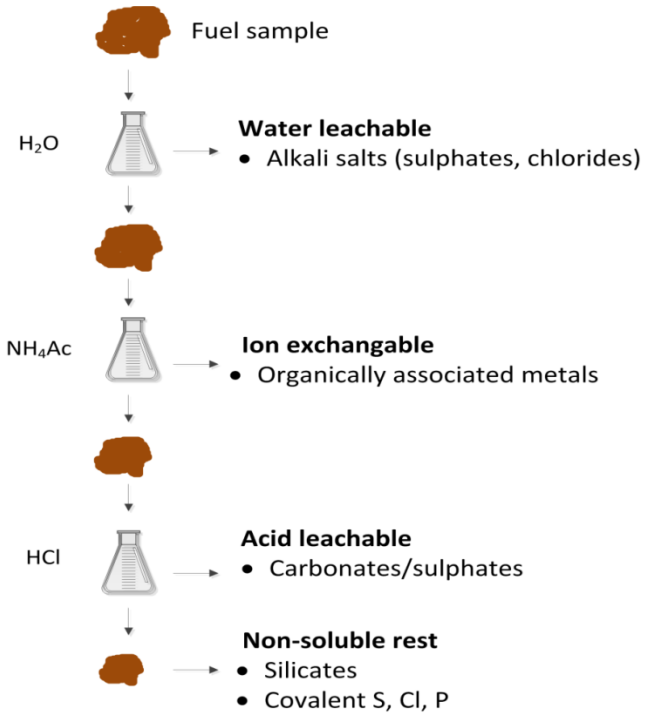

Figure 19. The chemical fractionation procedure leaches a fuel with water, ammonium acetate, and hydrochloric acid

Chemical fractionation was carried out for two samples of the solid waste which were sampled from the CFB boiler in two time intervals, namely, solid waste A (sample #162386) and solid waste B (sample #162632). Solid waste A (SWA) and solid waste B (SWB) were analyzed by chemical fractionation twice, in order to investigate the reproduciblity of the results.

4 Results

4.1 BOILER OPERATION, FLUE GAS MEASUREMENTS AND FUELMIX

4.1.1 Örtoftaverket

Sulphur is added (sulphur beads and co-firing of peat) to the fuel to sulphurize any corrosive alkali chloride. The volume of sulphur added is determined so an excess of SO_2 is maintained in relation to HCl. The flue gas chemistry is monitored in the empty pass before the flue gas cleaning, see Figure 20 and Figure 21.

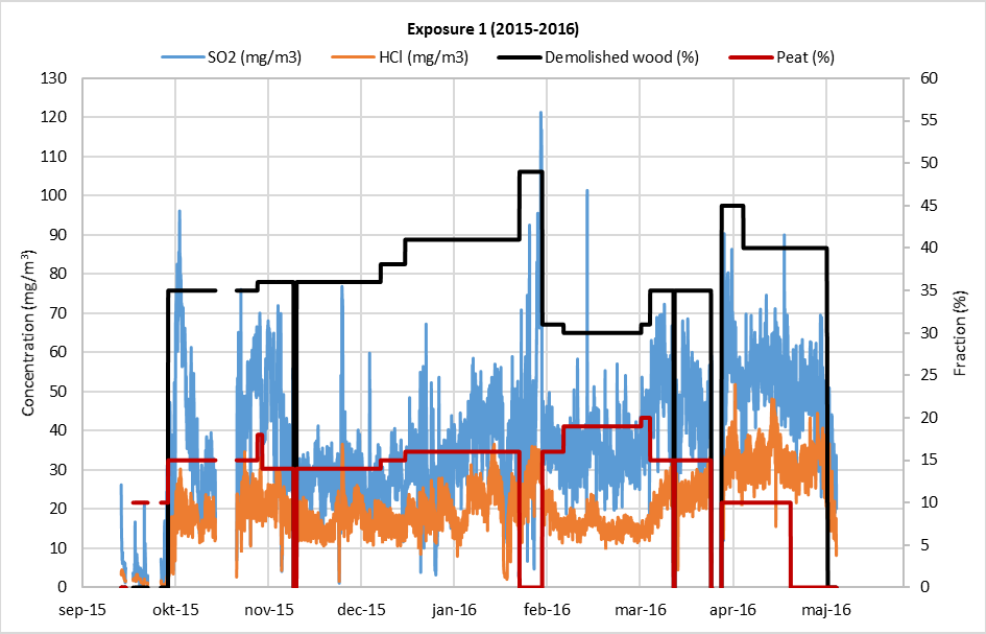

Figure 20. Flue gas data during 2015-2016.

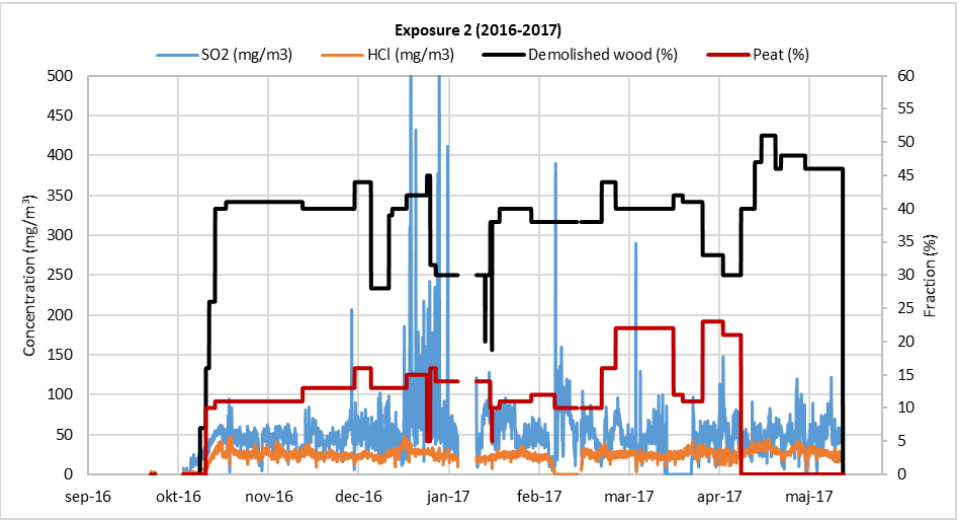

Figure 21. Flue gas data during 2016-2017.

The distribution between the different types of fuels has been as presented below during the years of operation.

	2014	2015	2016	2017
Forestry residue	38	33	25	28
Demolished wood	28	32	40	45
Peat	13	11	8	8
Sawdust	9	16	17	11
Bark	13	8	11	8

Table 6. Distribution of fuel (volume fraction).

Two sets of long term clamp exposures were conducted at the plant. Installation of clamps in the superheater were performed during the maintenance stop 2015 and 2016.

	Boiler operation (h)
Exposure 2015-2016	5 277 (Sep 2015 – May 2016)
Exposure 2016-2017	5 265 (Sep 2016 – May 2017)

Table 7. Boiler operation hours during exposure time 2015-2016 and 2016-2017.

Some disturbances did occur during the tests. Some disturbances of interests for the exposures are:

- December 2016: Deposits in cyclones, sand return leg, Intrex and convective pass. Deposits were formed because of rearrangement of airflows that caused combustion further back in the furnace. The problems were improved by increasing the volume of added sulphur, increasing sootblowing, increasing sand removal and supply, reduce load etc.
- January 2017: Sintering of bed material caused by mistake when reheating the bed after downtime.

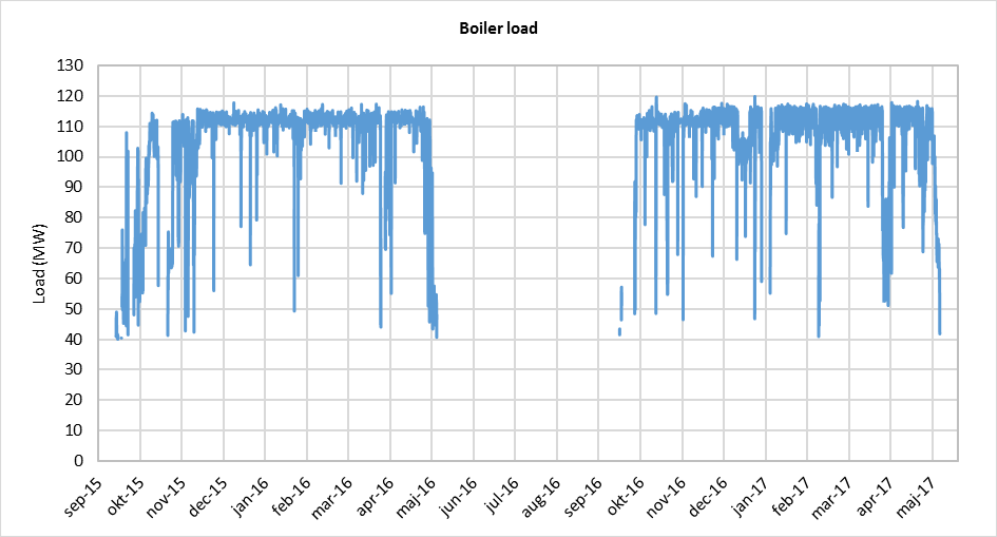

Figure 22. Boiler load at Örtoftaverket during exposure time 2015-2017.

The clamps were installed on SH I and SH II. The material temperature is measured with thermocouples attached on the SH-tubes. The material temperature for SH I are shown in Figure 23 and the material temperatures for SH II are shown in Figure 24.

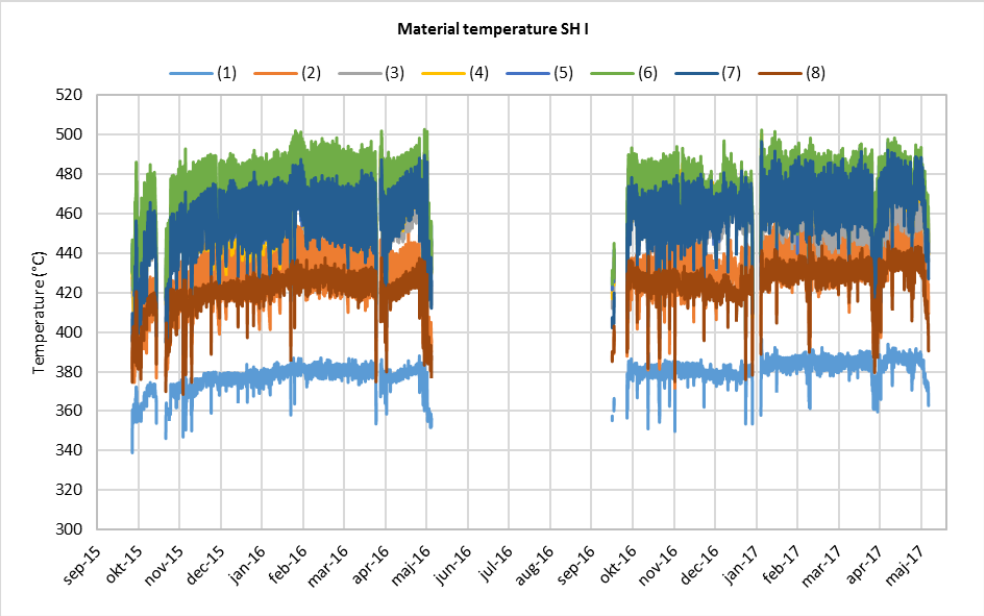

Figure 23. Material temperature SH I at Örtoftaverket during exposure time 2015-2017. The position of the installed clamp samples corresponds to tag #5 in the graph, the average temperature being about 450 °C 2015-2016 and about 460 °C 2016-2017.

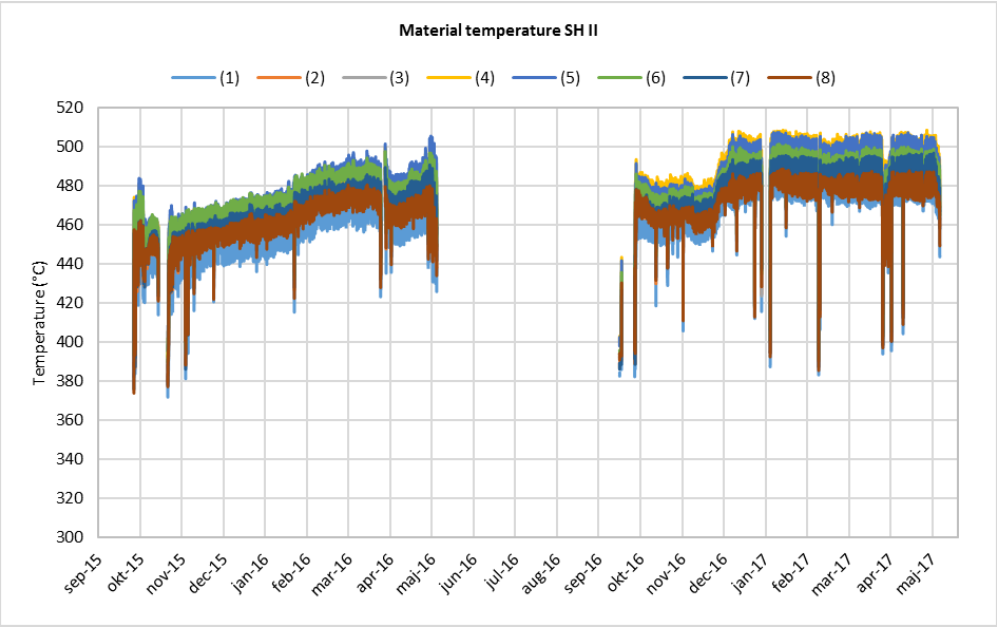

Figure 24. Material temperature SH II at Örtoftaverket during exposure time 2015-2017. The position of the installed clamp samples corresponds to tag #5 in the graph, the average temperature being about 475 °C 2015-2016 and about 495 °C 2016-2017. The average temperature for the clamp samples with 1 round of insulation have been about 505 °C 2015-2016 and about 525 °C 2016-2017.

4.1.2 P15 Händelöverket

Both long term and short-term tests were performed in the P15 Händelö boiler.

Long term tests

The long term tests took place from the summer 2014 until spring 2017, see Table 8. Both clamp testing and tube testing were performed. The clamp and tube samples were installed and dismantled during maintenance stops and revisions.

Clamp testing	**Boiler operation***	
Exposure 2014-2015	4 895 hours	(July 2014 – March 2015)
Exposure 2014-2016	12 372 hours	(July 2014 – May 2016)
Exposure 2014-2017	19 198 hours	(July 2014 – April 2017)
Exposure 2015-2016	7 477 hours	(March 2015 – May 2016)
Exposure 2015-2017	14 303 hours	(March 2015 – April 2017)
Tube testing	**Boiler operation***	
Exposure 2015-2016	7 477 hours	(March 2015 – May 2016)
Exposure 2015-2017	14 303 hours	(March 2015 – April 2017)
*Boiler hours are defined as boiler load exceeding 10 MW, mean value for one hour.		

Table 8. Boiler operation hours during exposure times

The performance of the boiler is shown in Figure 25 - Figure 27, see below. Figure 25 shows the load of the boiler during the period July 2014 until March 2017, the temperature of the flue gas in the empty pass just before entering the horizontal pass and the levels of SO_2 and HCl in the raw gas before filter. Both planned and unplanned shutdowns of the boiler are shown in the figure. The planned shutdowns take place twice a year; every autumn and every spring (except for 2014 when the spring shutdown was moved to the summer). The shorter shutdowns in the figure are mainly unplanned shutdowns. The two most common reasons for unplanned shutdowns during the project exposures are leakage in the pressure vessel (three times 2014, three times 2015 and once 2016) and clogging in different flue gas passes (once during 2015, 2016 and 2017).

The online corrosion probe testing was performed in three campaigns, see chapter 4.4.1. The boiler performance during these campaigns is shown in the same figure as for the long-term testing, Figure 25, below.

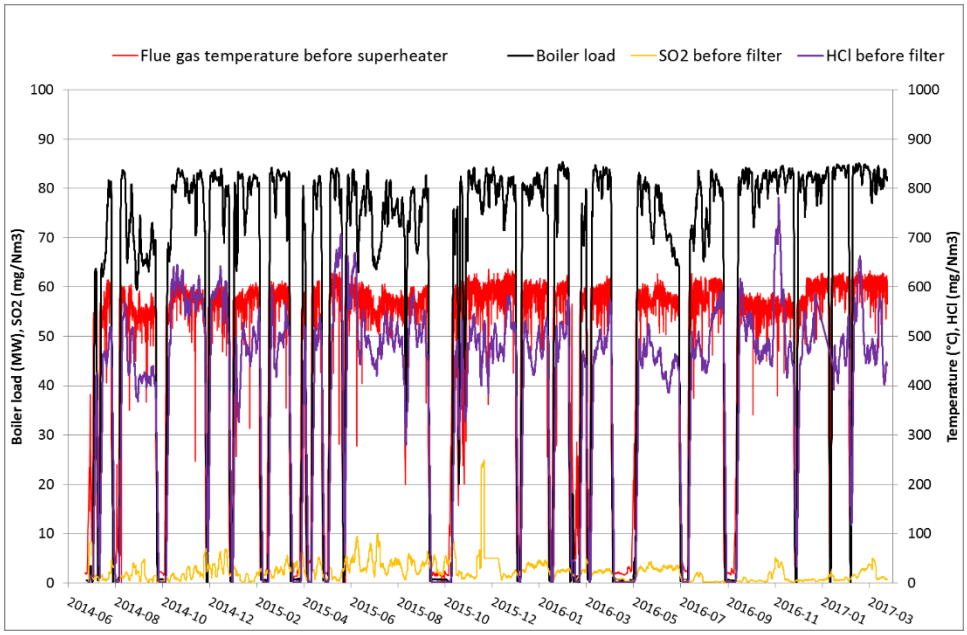

Figure 25. Boiler operation and flue gas data during 2014 – 2017.

The distribution between the different types of fuels has been as presented below during the years of testing, see Table 9.

	2014	2015	2016	2017
Household waste	53	52	46	47
Industrial waste	40	43	49	47
Impregnated wood (CCA)	3	1	2	3
Forest residues/recycled wood	2	2	1	1
Fuel oil	2	2	2	2

Table 9. Boiler operation hours during exposure times

Short term tests

The short term tests took place during the autumn 2016. The IACM instrument was measuring gaseous alkali chlorides in the empty pass during both one reference period and during the period when ammonium sulphate was added. The boiler performance during these two periods is shown in Figure 26 and Figure 27, respectively.

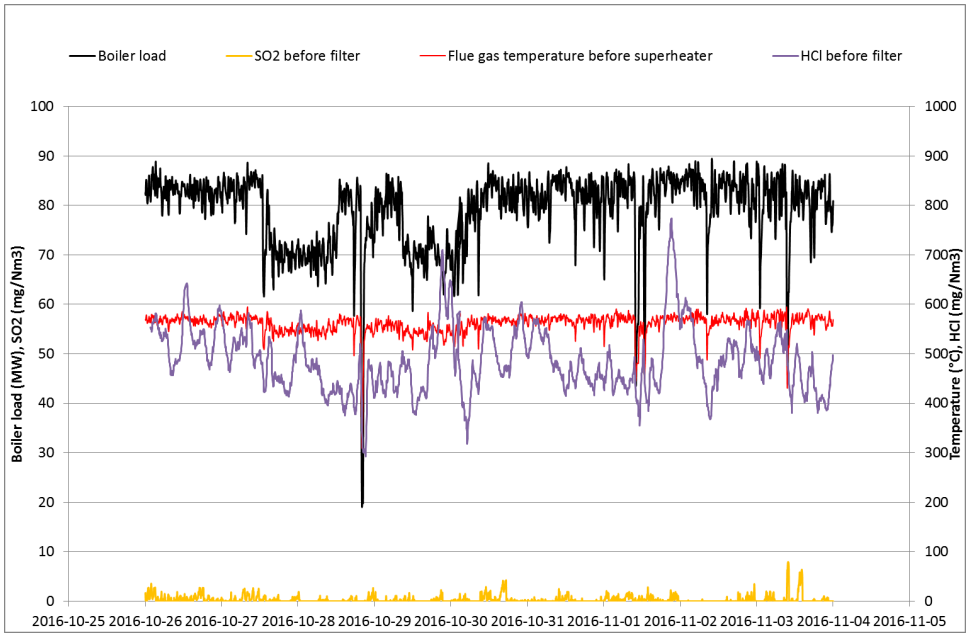

Figure 26. Boiler operation and flue gas data during the short tem tests (Reference exposure)

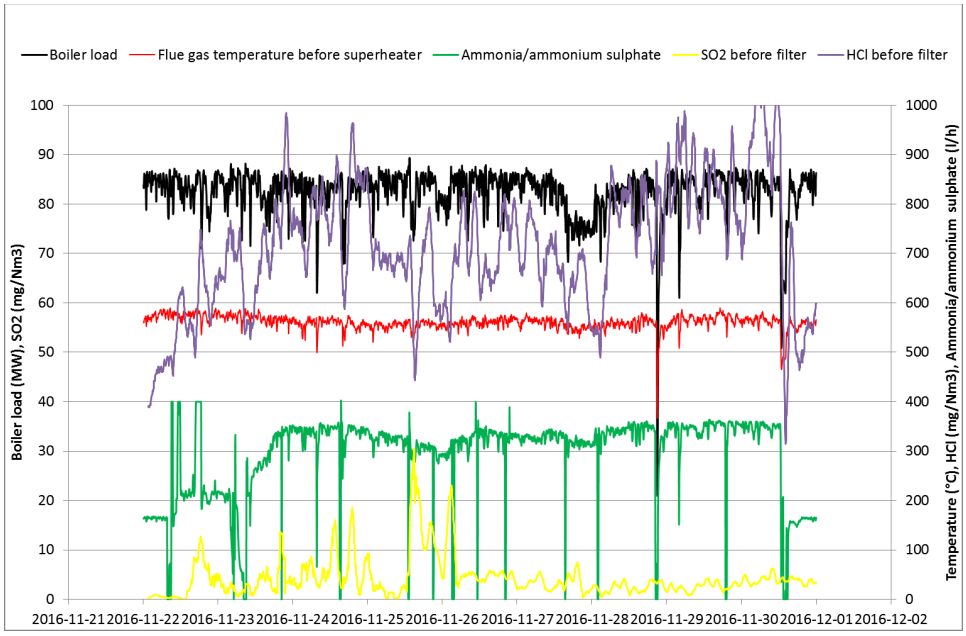

Figure 27. Boiler operation and flue gas data during the short tem tests (AmS exposure)

4.2 LONG TERM CORROSION EVALUATION

4.2.1 Clamp exposures

Clamp exposures has been conducted in both projects. In the KME711 project, the clamp exposures has been in a continuous mode lasting for 1, 2 and 3 years respectively. In the KME720 project, all clamp exposures has lasted for 1 year (i.e. one firing season august – may). In the KME720 project, the fraction of waste wood has been increased for each clamp exposure. In the KME711 project, the fuel mix has remained the same throughout the exposure.

A overview of all long term exposures in the two projects is shown in Figure 8, in chapter 3.1.

4 895 hours clamp exposure in the waste fired boiler P15 Händelö

The clamp samples exposed for 4 895 hours (July 2014 – March 2015) in the waste fired P15 boiler in Händelö are shown in Figure 28. The material loss is in general very low, regardless of material and/or position. Corrosion rates below 0.1 mm/year are in many cases regarded as an acceptable level of material wastage, marked as a dashed line in the figure. Slightly higher corrosion rates can be noticed for the SH1b samples. However, the corrosion rates are still below 0.1 mm/year.

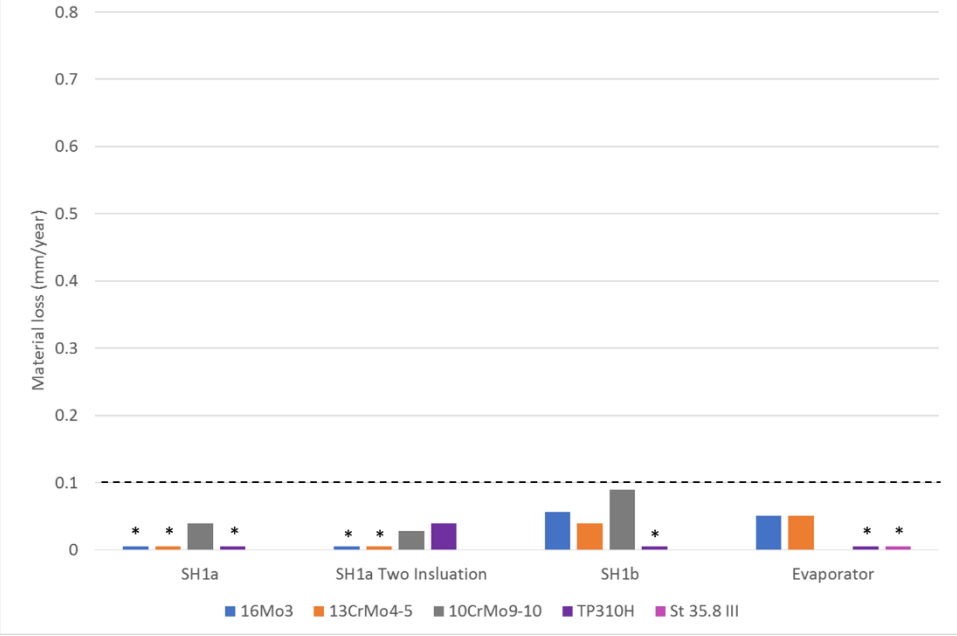

Figure 28. Material loss of the clamps removed from the P15 boiler in Händelö after 4 895 hours. The material temperature has been 360-380 °C. * No noticeable corrosion

5 277 hours clamp exposure with 40% waste wood fraction, Örtoftaverket

The clamp samples exposed for 5 277 hours (Sep 2015 – May 2016) in the biomass fired Örtoftaverket boiler with 40% waste wood are shown in Figure 29. Compared to the waste fired boiler P15 Händelöverket, the material loss is higher for the low

alloyed steels (16Mo3, 10CrMo910 and 13CrMo4-5). The corrosion rates are about 0.3 – 0.5 mm/year. The stainless steels, including the coated samples, exhibit lower corrosion rates compared to the low alloyed steels, being around 0-0.15 mm/year. There is no general trend in corrosion rate and position/material temperature. Corrosion rates below 0.1 mm/year are in many cases regarded as an acceptable level of material wastage, marked as a dashed line in the figure.

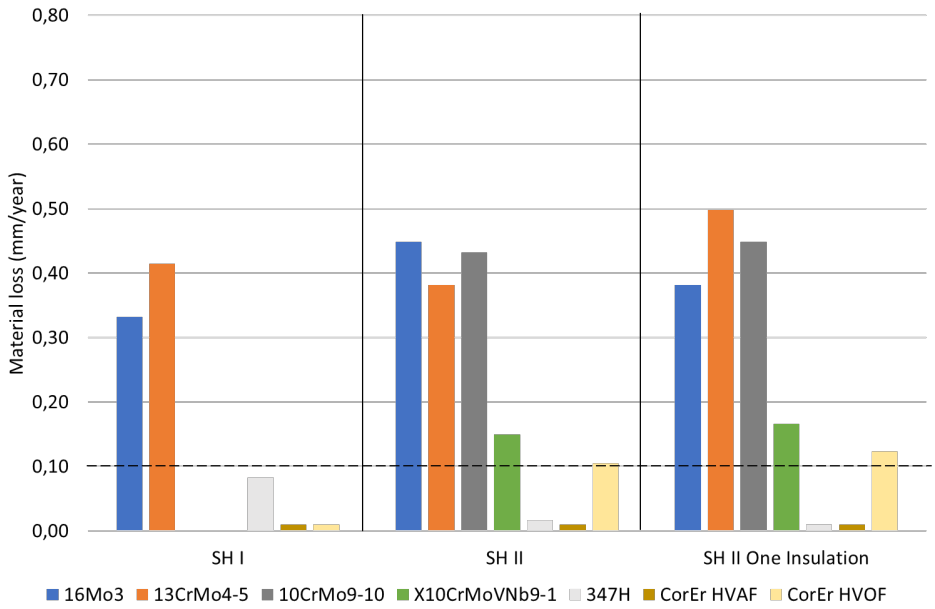

Figure 29. Material loss of the clamps exposed for 5277 hours with 40% waste wood in Örtoftaverket. The material temperature of the clamps has been about 450 °C (SH I), 475 °C (SH II) and 505 °C (SH II One Insulation), respectively.

5 265 hours clamp exposure with 45% waste wood fraction, Örtoftaverket

The clamp samples exposed for 5 265 hours (Sep 2016 – May 2017) in the biomass fired Örtoftaverket boiler with 45% waste wood are shown in Figure 30. The increase of the waste wood fraction by 5% resulted also in an increase in corrosion rate for the majority of the tested materials. The corrosion rate for e.g. the low alloyed steel 16Mo3 increased between 20-60%. However, still the corrosion rate is low for several, more highly alloyed materials; the corrosion rate of e.g. the stainless steel 347H is for all positions/temperatures around 0.1 mm/year or lower. For the coated samples, HVAF performs better compared to the HVOF sample.

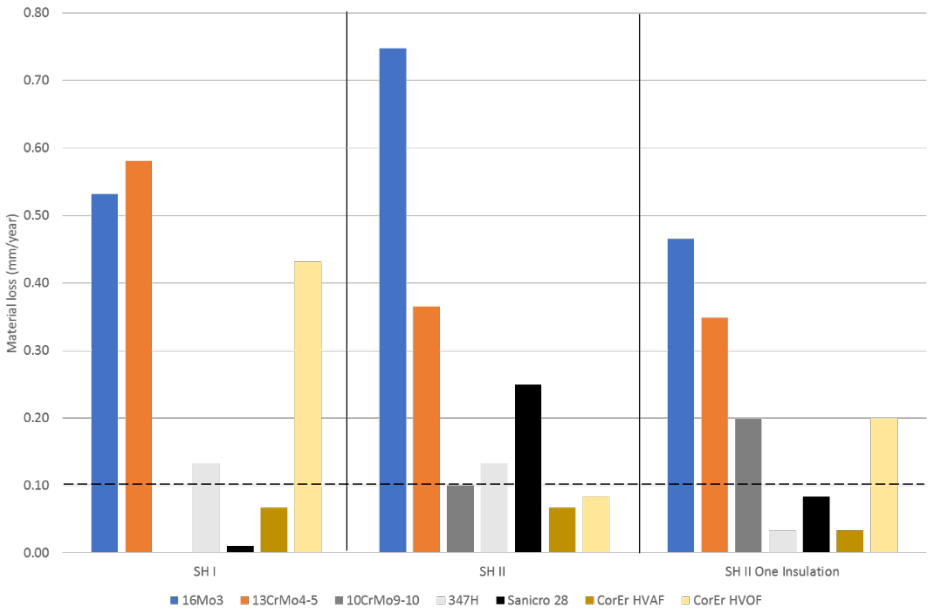

Figure 30. Material loss of the clamps exposed for 5265 hours with 45% waste wood in Örtoftaverket. The material temperature of the clamps has been about 450 °C (SH I), 475 °C (SH II) and 505 °C (SH II One Insulation), respectively.

Long term corrosion of the clamp samples exposed in the waste fired boiler

In the waste fired P15 Händelö boiler a large material matrix has been exposed for several positions and up to three years (19 198 hours), see Figure 31. The corrosion rate of the all the tested materials is in general low, with the exception of the low alloyed 10CrMo910 exposed in the SH1b position. The corrosion rate for this material at this position was slightly less than 0.25 mm/year. For most materials, the corrosion rate was rather constant over the years, indicating a linear corrosion rate. The exception being TP310H where the three years exposed sample showed a marked increase in corrosion rate (from negligible to about 0.2 mm/year). However, this sample may be viewed as an outlier since all other TP310H samples exhibited very low corrosion rates. For other materials, e.g. 16Mo3 and 13CrMo4-5 at the SH1b position, the corrosion rate decreases with time. This would imply that the corrosion attack is slowing down after the initial attack. However, since the corrosion rates are rather low the progress of the corrosion attack is rather hard to extrapolate.

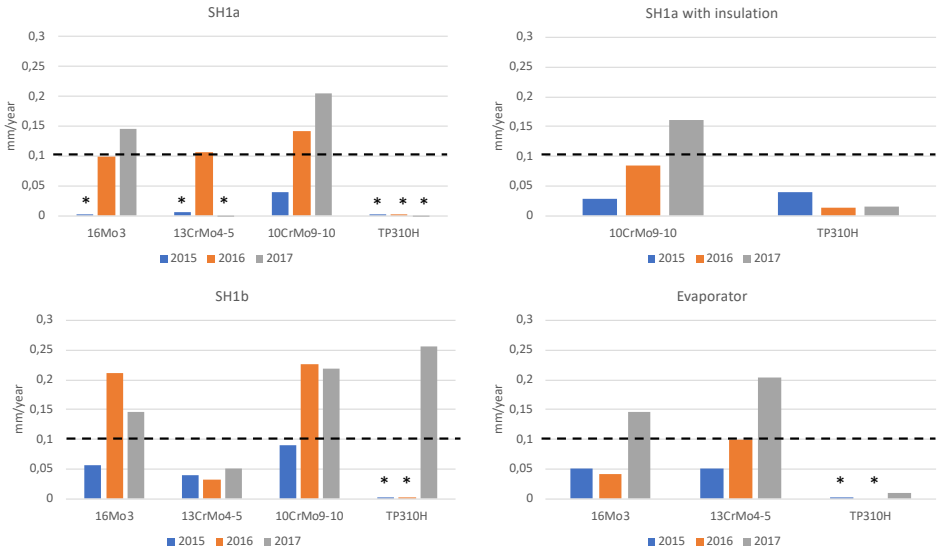

Figure 31. Material loss of the clamps exposed on several positions in the superheater region in the waste fired boiler P15 Händelö. The years refers to time for outtake from the boiler. * No noticeable corrosion

SEM/EDX analysis of clamp exposures

The clamps exposed in the waste fired P15 Händelö boiler exhibit all low corrosion rates, even at the longest exposure time. The exposed clamp samples has also been subject towards SEM/EDX analysis. As the corrosion attack has been rather low, only the 10CrMo910 is shown in this report, see Figure 32. The corrosion rate of these two samples have been 0.12 and 0.1 mm/year, respectively. As can be seen, there are some corrosion products forming and the sample surface is slightly undulating. The EDX analysis (not shown) reveals that the corrosion products that formed consist of iron oxides and iron chlorides. It is expected that part of the corrosion products and deposit has spalled off from the samples after outtake from the boiler.

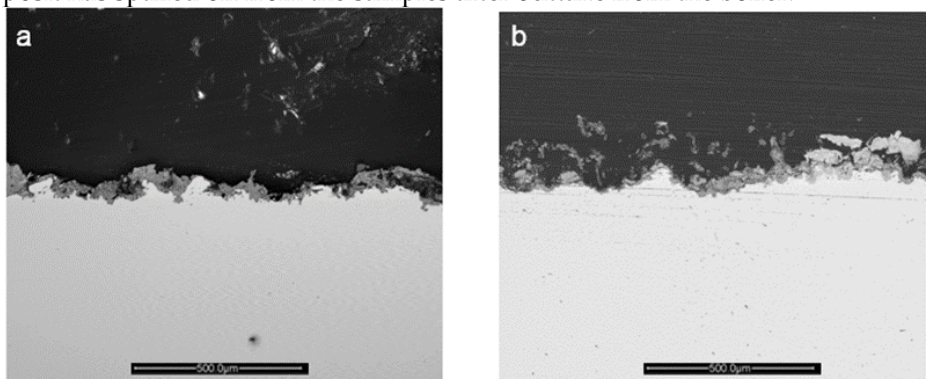

Figure 32. SEM cross section of 10CrMo910 exposed for a) 4 895 hours and b) 12 372 hours exposed in the waste fired P15 Händelö boiler on SH1a (about 360 °C material temperature).

A comparison of the the CorEr coating applied by the HVOF or HVAF technique on 310H base material was performed in the biomass fired Örtoftaverket boiler. The newly developed HVAF coating technique is expected to produce more dense coatings compared to the HVOF technique. As shown by the material loss determinations (Figure 29 and Figure 30), both coatings performed well in the tested

superheater region of the Örtofta boiler. The corrosion rate of the HVAF was neglible and the HVOF showed small wastages, up to 0.4 mm/year. The initial thicknesses of the coatings were about 350 – 360 µm and 440 – 460 µm of the HVAF and HVOF coatings, respectively.

The SEM/EDX cross section of the HVAF coating exposed for 5277 hours on SH I (about 450 °C material temperature) is seen in Figure 33. The HVAF coating is characterized as dense and homogeneous. In general, very low or almost no corrosion attack was observed, According to the EDX analysis, part of the deposit present on top of the coating contains mainly S, K and some Ca, probably present as K_2SO_4. The presence of Cl is low. In addition, a layer rich in phosphorous is observed in the deposit closest to the coating. The S map is overlapping with Mo and "S" content in the coating and base material is to be regarded as Mo.

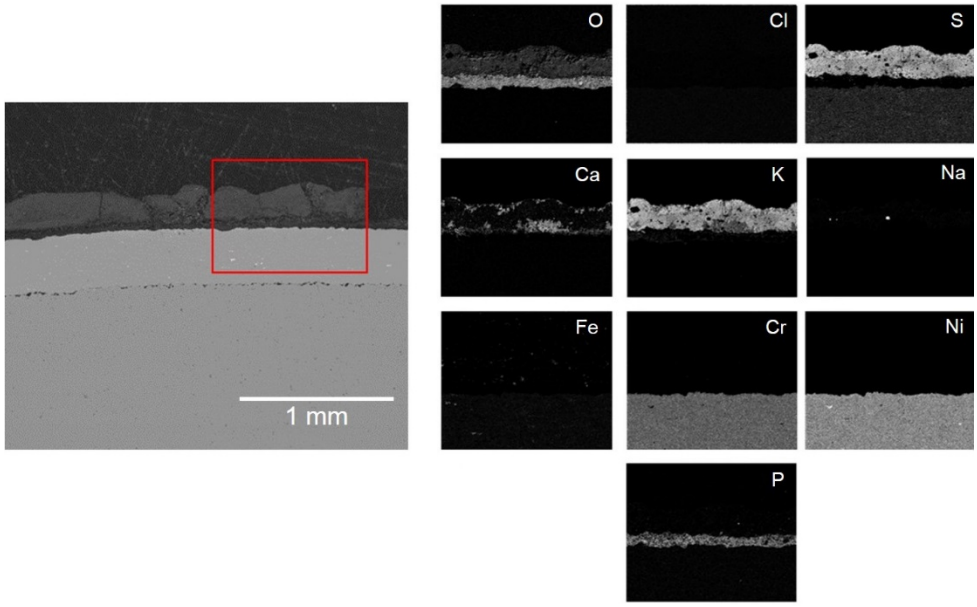

Figure 33. SEM/EDX cross section of CorEr HVAF coating exposed for 5277 hours with 40% waste wood on SH I (about 450 °C material temperature). The red square marks the EDX map region.

The corresponding HVOF applied coating exposed on SH I is shown in Figure 34. Compared to the HVAF coating, the HVOF coating is slightly more porous and the coating surface is more rough. The EDX analysis shows a well adherent deposit layer. The deposit layer is again dominated by K and S. The inner part of the deposit is enriched in P, originating from the coating application process. The S map is overlapping with Mo and the "S" content in the coating and base material is to be regarded as Mo.

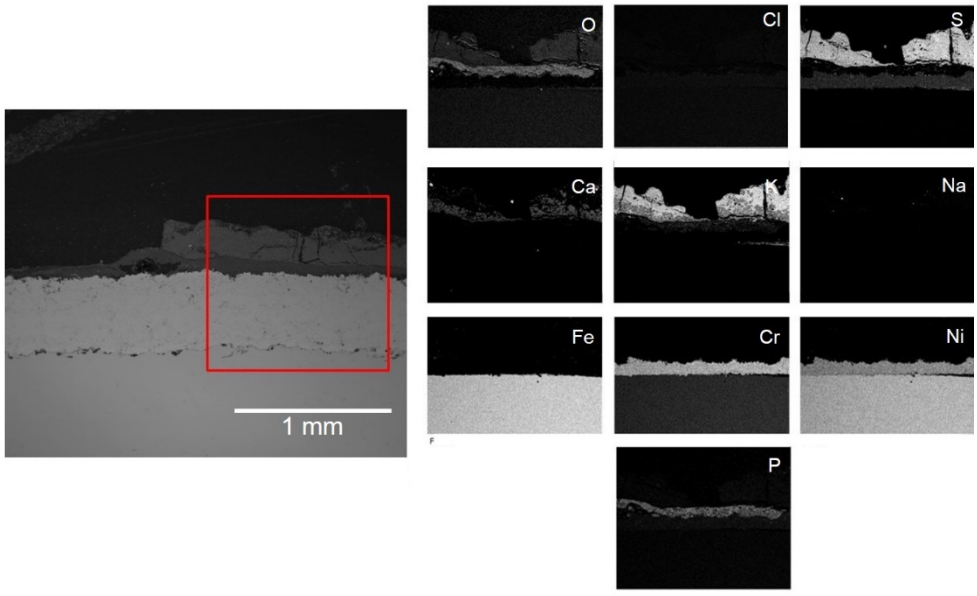

Figure 34. SEM/EDX cross section of CorEr HVOF coating exposed for 5277 hours with 40% waste wood on SH I (about 450 °C material temperature). The red square marks the EDX map region.

The coatings were also exposed at SH II, with and without insulation between the clamp and the superheater tube, corresponding to a material temperature of about 475 °C and 505 °C, respectively. In Figure 35, the HVAF coating without insulation is shown. Similar to the SH I position, the HVAF coating performs well in this environment, the coating remains dense and homogeneous. There is no indication of the corrosion attack being initiated. As on the samples exposed on the SH I position, the deposit is dominated by sulphates of potassium and calcium. The content of chlorine is below the detection limit. A P enriched layer is detected at the coating/deposit interface. This layer seems to be correlated to the presence of Al according to the EDX analysis. Both Al and P orginates from the coating application process.

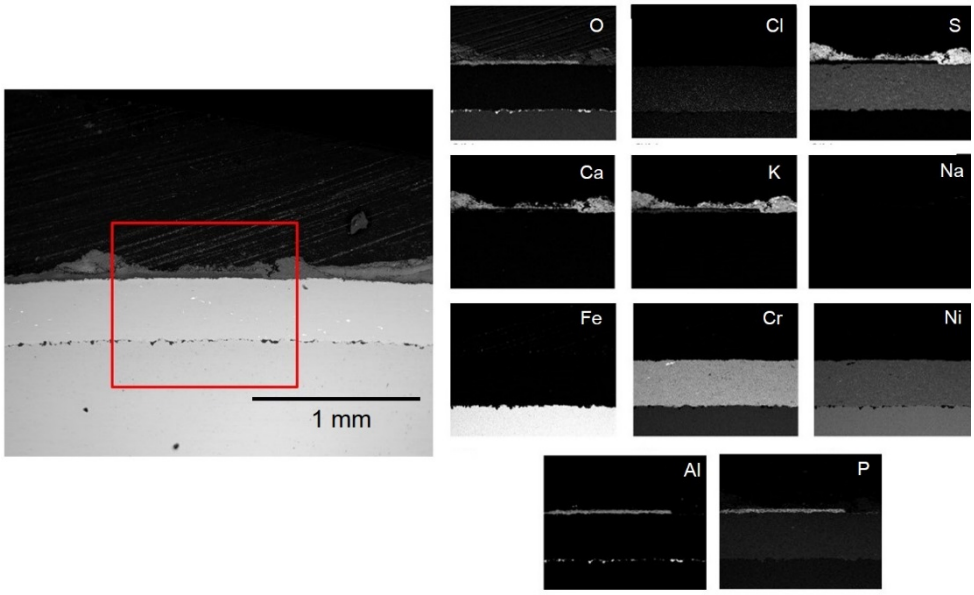

Figure 35. SEM/EDX cross section of CorEr HVAF coating exposed for 5277 hours with 40% waste wood on SH II (about 475 °C material temperature). The red square marks the EDX map region.

In the case of the HVOF coating exposed on SH II without insulation, the performance of the coating was poor as the coating lost its adherence to the base material, see Figure 36. However, the underlying base material (310H) seems rather unaffected, i.e. no corrosion products have formed where the coating has been lost. Thus, the coating failure may be a result of the sample preparation prior to analysis rather than the corrosive environment in the boiler.

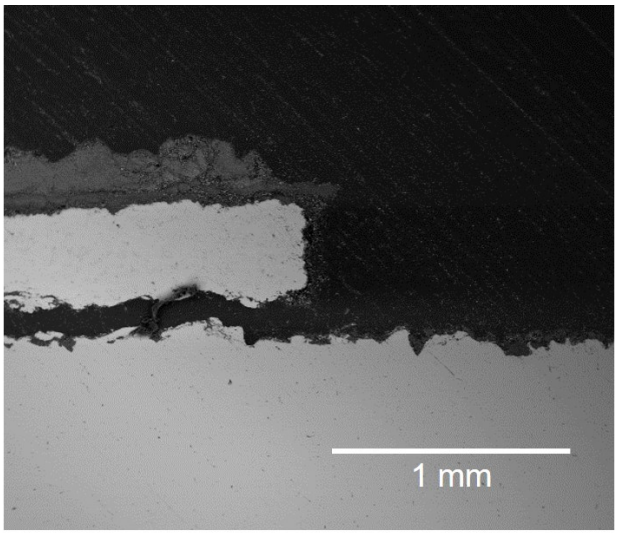

Figure 36. SEM cross section of CorEr HVOF coating exposed for 5277 hours with 40% waste wood on SH II (about 475 °C material temperature).

In Figure 37, a SEM/EDX cross section of the HVAF coating exposed on SH II with insulation between the clamp and the underlying superheater tube is shown. The material temperature (about 505 °C) is slightly higher compared to the

corresponding samples exposed without the insulation layer. Despite the increase in temperature, the coating performs well and a relatively thin layer of well adherent deposit is observed and no indication of an accelerated corrosion attack can be observed. The slightly higher material temperature did not induce any differences in deposit composition; the deposit is dominated by potassium and calcium sulphates and the chlorine content is low. The "S" content in the coating and base material is to be regarded as Mo.

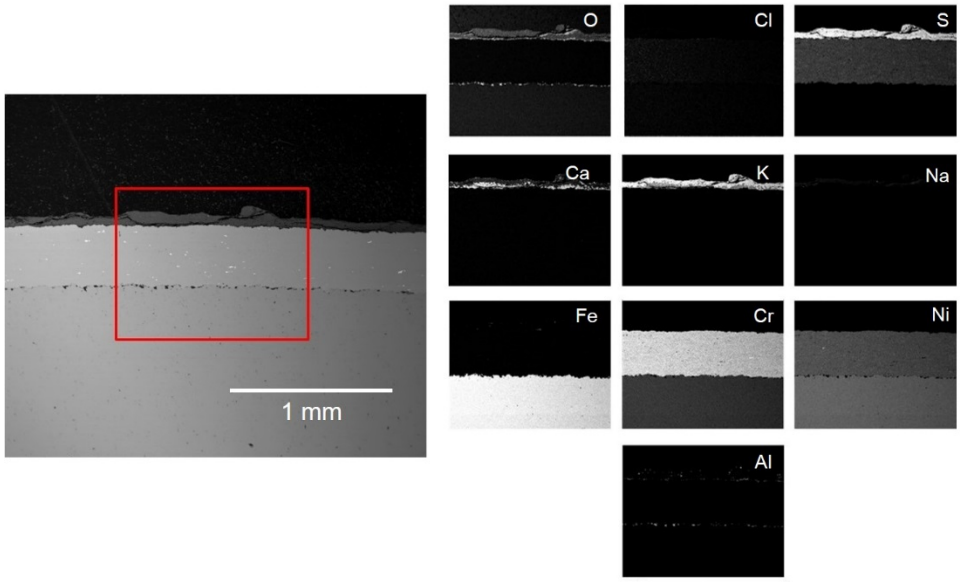

Figure 37. SEM/EDX cross section of CorEr HVAF coating exposed for 5277 hours with 40% waste wood on SH II with one round of insulation (about 505 °C material temperature). The red square marks the EDX map region.

The SEM/EDX analysis of corresponding HVOF coating exposed on SH II with insulation, detected almost no deposit on top of the coating, see Figure 38. In addition, the surface of the coating seems to be slightly rougher and more porous than the HVAF coating. According to the material loss determination, this sample experienced the highest material loss of the exposed coatings, being about 0.12 mm/year. However, the corrosion rate is still rather low compared to the low alloyed steels.

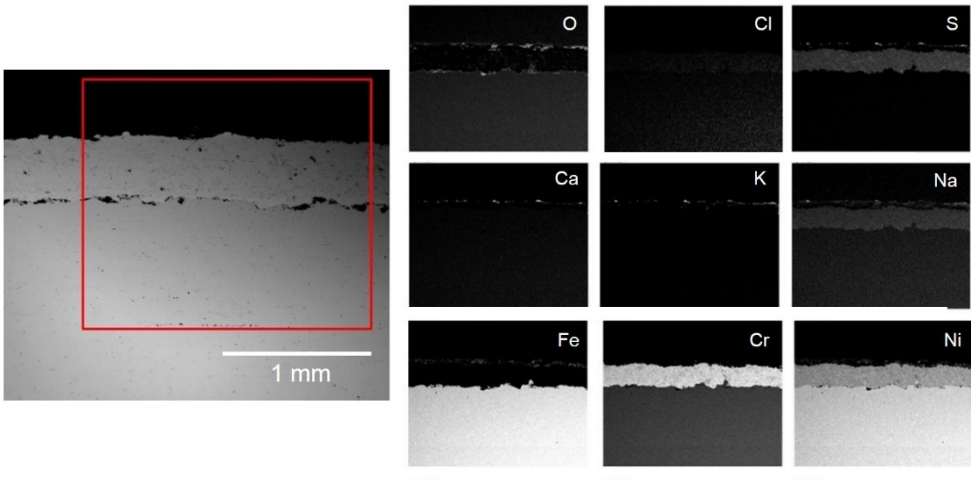

Figure 38. SEM/EDX cross section of CorEr HVOF coating exposed for 5277 hours with 40% waste wood on SH II with one round of insulation (about 505 °C material temperature). The red square marks the EDX map region.

To summarize, both the HVAF and the HVOF coatings performed well in this environment, the corrosion rate was negligible for the HVAF coating and at acceptable levels for the HVOF coating. On the SH I, having the lowest material temperatures, the corrosion was negligible for both coatings. The environment was also to be regarded as relatively mild, the deposit was mainly composed of potassium and calcium sulphates. The addition/co-combustion of sulphur/peat to fuel mix in the Örtofta boiler is most probably the reason for this relatively benign deposit.

4.2.2 Tube exposures

One of the goals of this study is to compare different corrosion measurement techniques, e.g. clamp exposures, probe exposures and tube exposures. In particular, the novel clamp exposure technique is important to compare with actual superheater tube exposures. This since the clamp samples are aimed directly to reveal the corrosion rate of the superheater tubes, without the need of dismantling any pressure bearing parts of the boiler when the exposures ends. Hence, it is of great importance that the clamp samples exhibit a similar corrosion attack and corrosion rate as the tubes.

In the waste fired P15 Händelö boiler a large material matrix consisting of clamp samples has been exposed for several positions and up to three years (19 198 hours), see Figure 31. Some of these clamp samples has mirrored as a tube sample, having as far as possible same exposure time, temperature and position in the boiler. The material loss data of the test tube sections are presented in Figure 43 below.

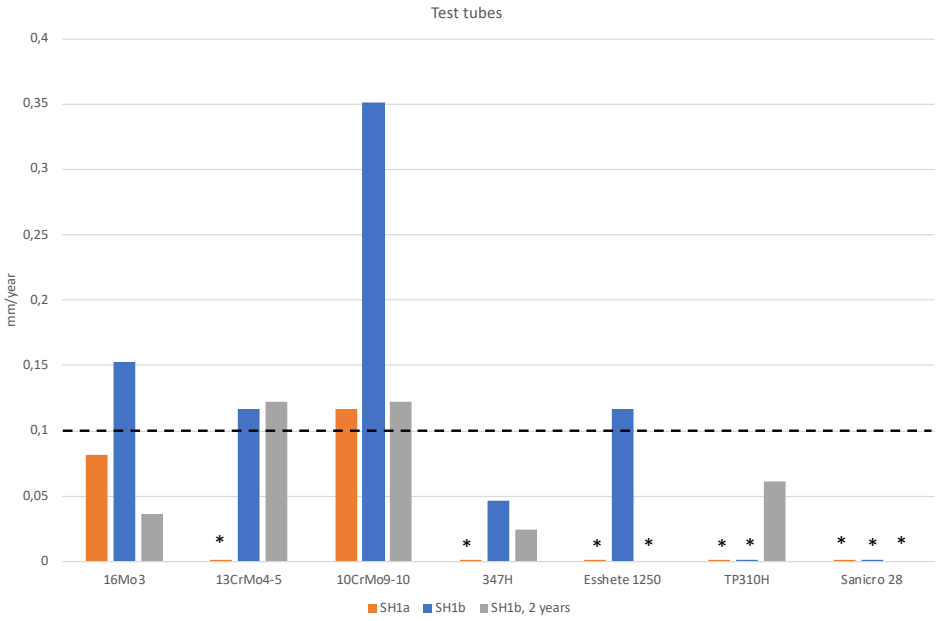

Figure 39. Material loss of the test tubes exposed on several positions in the superheater region in the waste fired boiler P15 Händelö. The years refers to time for outtake from the boiler. * No noticeable corrosion

The installed test tubes exhibit a similar corrosion trend as the clamp samples. The low alloyed steels (16Mo3, 13CrMo4-5 and 10CrMo9-10) exhibit higher corrosion rate compared to the more high alloyed steels (347H, Esshete1250, TP310H and Sanicro 28). However, the corrosion rate is in general low. The dashed line marks an acceptable corrosion rate. As for the clamp samples, the highest corrosion rates are noticed for the SH1b tube section, where a corrosion rate of 0.35 mm/year is noticed for the 10CrMo9-10 sample. For this particular sample, the corrosion rate is about a factor of 3 higher for the tube sample compared to the corresponding clamp sample. However, the corrosion rate has decreased for the tube sample exposed for 2 years, being close to 0.1 mm/year, which is close to what has been observed for the corresponding clamp sample.

4.3 SHORT TERM CORROSION EVALUATION BY PROBE EXPOSURES

4.3.1 The effect of start-up sequence on probe exposures

Commonly in order to predict the service life of boilers components suffering from corrosion, e.g. superheaters tubes, air-cooled probes are used. However, it is well known that corrosion rates measured with cooled probes are higher than the corrosion rate of the permanently installed tubes in the superheater bundle. This phenomenon is poorly understood and the number of studies is scarce. One hypothesis has been that the probe startup is of great importance. This since a normal procedure during probe exposures is that the probe, holding room temperature, is inserted directly into the hot boiler and the corrosive environment to be investigated. However, by doing so the probe will during a short period of time, until reaching higher temperatures, be exposed to gases condensing on the

surface, e.g. water vapour. If a liquid film of water is present on the probe surface, HCl(g) is expected to dissolve here within and thus, causing a chlorine enriched environment. By exposing two identical probes simultaneously where one of the probes has been subject to an external preheating procedure prior insertion to the boiler we aim to study this hypothesis.

Exposures of corrosion test probes were performed in order to compare two different startup sequences. The exposure times were 15 min, 2 hours and 24 hours. For the 2 hours and 24 hours exposures, two probes were exposed simultaneously having different startup sequences. One probe was inserted into the operating boiler directly from room temperature whereas the other probe was pre-heated to above 100 °C before inserted into the boiler. An IR-furnace was used for the pre-heating. After exposure, the probes were withdrawn from the boiler allowing them to cool down to room temperature. The following table shows the matrix of the exposures performed.

Probe	Number of samples		Material Temperature	Time
	Non pre-oxidized	Pre-oxidized*		
Cold	9	-	400, 500, 600 °C	15 min (until probe reached set temperature)
Cold	6	3	400, 500, 600 °C	2 hours
	6	3	400, 500, 600 °C	24 hours
Pre-heated	6	3	400, 500, 600 °C	2 hours
	6	3	400, 500, 600 °C	24 hours
*Pre-Oxidation: 700°C, 24 hours, lab air; **Pre-heating: over 100 °C				

Table 10. Sample matrix and experimental conditions.

Each probe consisted of two individually controlled temperature zones, only one zone was used for this part of the experiment, see the following figure. The material temperature was 600 °C. The samples were characterized by means of SEM and EDX.

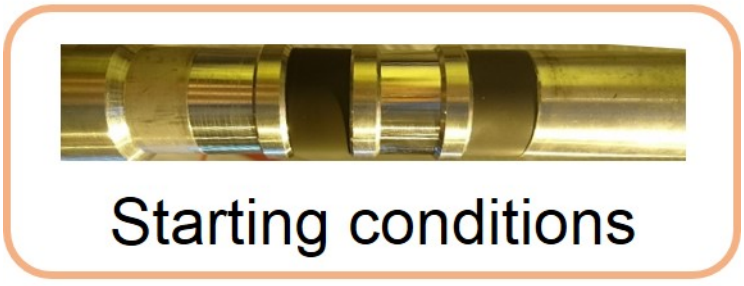

Figure 40. Initial conditions of the ring samples prior expoure; clean / pre-oxidized / clean / pre-oxidized.

During the exposure campaign the boiler were operated at full load and exhibited stable operation conditions. The following figure, shows the initial temperature profile of the two probes exposed for 24 hours. The cold probe reached its target temperature after 4 min and 7 min for 400 °C and 600 °C, respectively. The cold

probe exhibited a heating rate between 79-94 °C/min. The preheated probe was prior to the exposure installed in an IR furnace for 4 min in order to reach a material temperature above 100 °C. Once reached, the probe was swiftly, without decreasing more than 5 °C in material temperature, installed in the boiler and after additional 4-7 min the intended set temperatures was reached. The preheated probe exhibited (inside the boiler) a heating rate between 50-75 °C/min.

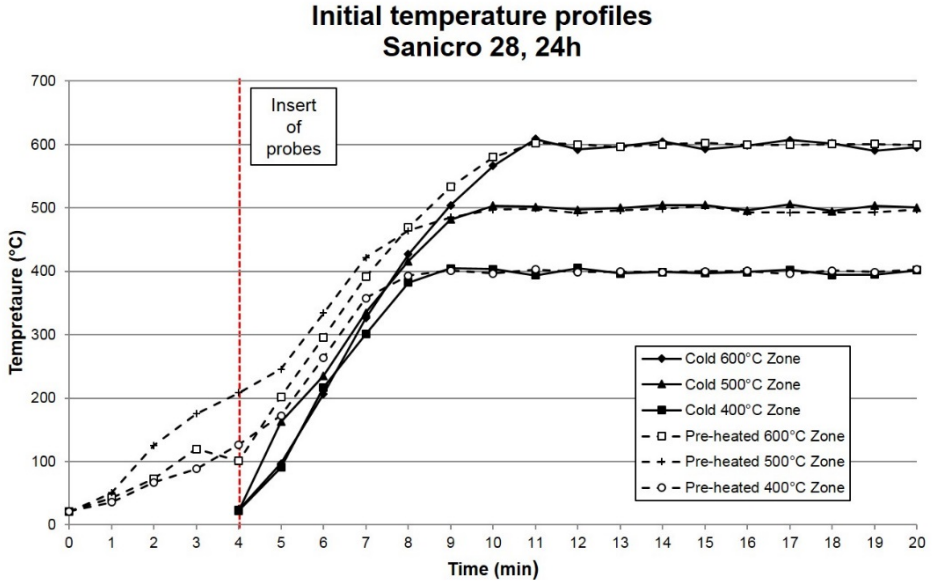

Figure 41. Temperature profile from the initial 24-hour exposures.

Images of the samples after the 24 hours exposure are shown in Figure 42. A bright beige deposit formed on the samples during exposure. The thickness and appearance of the deposit layer was rather uniform in all the samples. The adherence of the deposit was poor, regardless of material temperature and/or preheating. Due to the spallation, the obtained mass gains of the samples were arbitrary and therefore not included in this study. However, it may be noted that the spallation is not equally pronounced for the samples that were pre-oxidized prior to exposure. In the areas where the deposit layer has spalled off a red-greyish region could be observed indicating the presence of a corrosion layer.

Figure 42. Optical images of samples exposed for 24 hours.

The amount of deposit forming on the sample surfaces is rapidly increasing with exposure time. After 24 hours, the deposit layer was roughly 500-1000 μm in the thickest part. However, both deposit and corrosion products spalled readily off the sample and large metallic areas were revealed. According to EDX analysis the main species in the deposit are Ca, S, Na, K, Cl, Al, Si and O. The XRD analysis primarily detected $CaSO_4$, NaCl and KCl. This was true for both the cold and the preheated probe samples.

In addition to the 2 and 24 hours exposures, the cold probe was exposed for a very short time (15 min). The aim of this exposure was to analyze any deposition material during the first minutes of the exposure, when the heating of the test material takes place. The exposure was ended once the temperature material reached the set temperature of 600 °C. A thin layer of deposit (~40 μm) was observed on the sample. There were no direct signs of a corrosion attack. The EDX map of a cross section of a non-pre-oxidized sample briefly exposed is shown below, see Figure 43. The EDX map shows that the deposit material mainly contained chlorine and calcium along with some traces of potassium and sulphur. This suggests direct contact between chlorine and the metal surface from the first minutes of exposure.

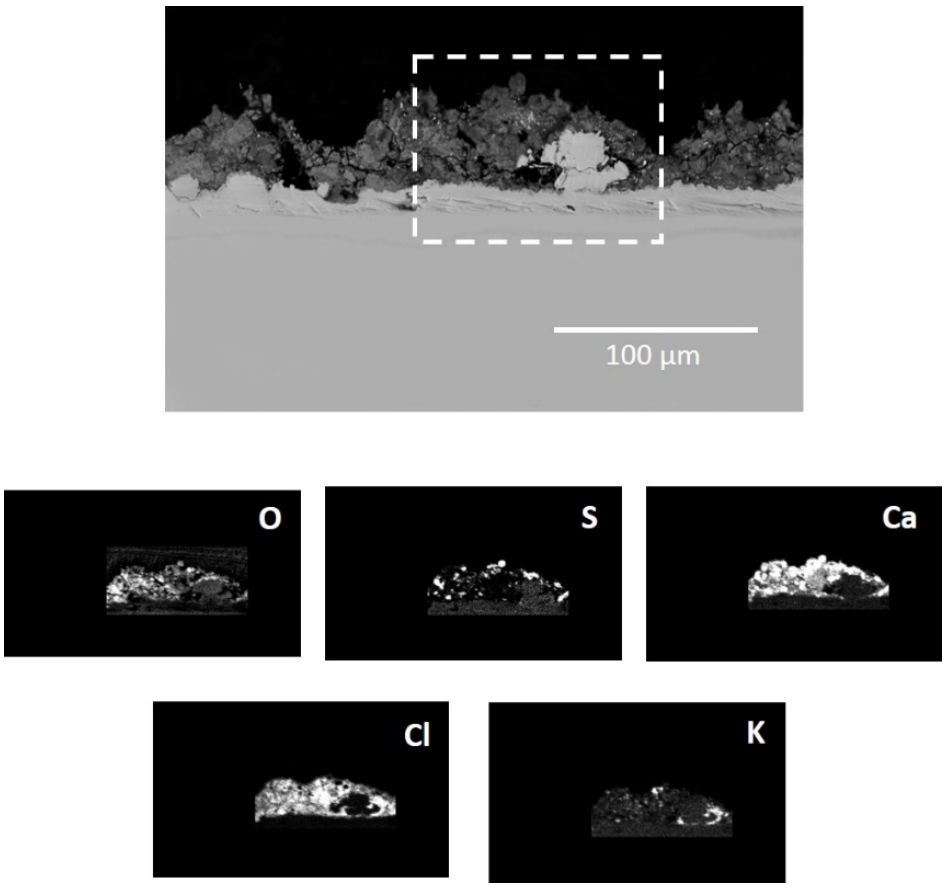

Figure 43. EDX mapping from cross section of sample exposed 15 minutes, material temperature 600°C; cold testing probe.

The sample exposed for 24 hours (Figure 44) exhibits a poorly adherent deposit/corrosion product layer. The detached oxide layer consists primarily of Fe, Cr and O. Still attached to the sample, a thin Fe,Cr,Ni oxide could be seen (see Figure 45). Below this oxide, a Fe and Cr depleted zone, enriched in Ni is present. This zone is about 175 µm in thickness and the oxygen level is around 10-15% in this region. In the middle of this nickel enriched metal, a Cr-rich oxide was detected. Furthermore, metal chlorides were observed at the oxide/metal interface. According to the EDX analysis, the metal chlorides are suggested to consist of chromium chlorides.

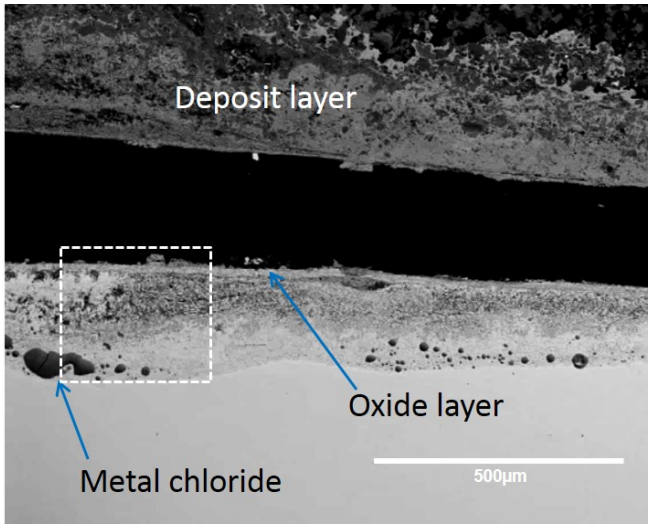

Figure 44. Cross section of samples exposed for 24 hours, material temperature 600 °C, cold testing probe.

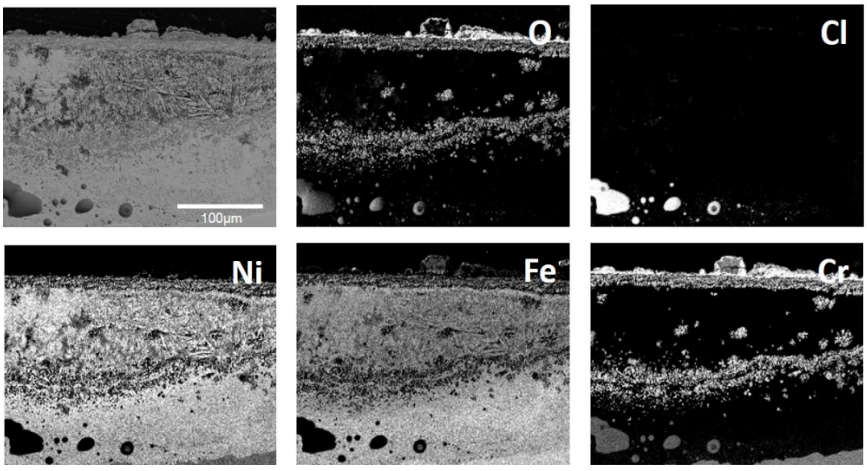

Figure 45. EDX mapping of samples exposed for 24 hours, material temperature 600 °C, cold testing probe.

In order to study the effect of initial probe temperature on the deposit formation and corrosion, probes preheated above 100 °C were exposed. These exposures were performed in parallel with the probe exposures started cold, using two different inlets on the same man door. SEM/BSE images of polished cross-section of the pre-heated samples exposed for 24 hours are shown in Figure 46. Similar to the

corresponding cold samples, the oxide layers formed exhibits poor adherence. According to EDX analysis the main species in the deposit are Ca, S, Na, Al, Si and O. The majority of the oxide layers has detached from the steel substrate. In the top of the steel substrate, a Ni-rich region is observed. The low levels of oxygen in this region suggest the presence of a nickel enriched metal area. In the bottom of this area, the presence of chlorides can be seen. However, compared to the corresponding samples exposed on the cold probe the results indicate slightly less metal chlorides.

The preheated samples exposed for 24 hours (see Figure 46) do suffer from spallation and the corrosion product layer/deposit layer is detached from steel substrate. The EDX analysis shows that the main elements in the deposit layer are Ca, S and O, indicating the presence of $CaSO_4$ (not shown). Dense oxide layers are formed underneath the deposit layer, see Figure 47. The oxide layer is enriched in Fe in the upper part and Cr in the inner part. The top part of the steel substrate consists of nickel enriched metal. However, compared to the corresponding samples exposed on the cold probe, the nickel enriched area on the preheated 24 hours sample was thinner. The thickness in the preheated case being about 75 µm, compared to 175 µm for the sample exposed from cold conditions. The presence of metal chlorides is again observed at the metal/oxide interface. The distribution of the chlorine in the metal/oxide interface differs slightly from the corresponding sample exposed on the cold probe, being less localized for the sample exposed on the preheated probe. The EDX results also indicate that the total amount of metal chlorides is slightly less on the samples exposed on the preheated probe. However, it should be noted that the difference between the two cases is rather minor. The formation of metal chlorides in the metal/oxide interface is severe in both cases.

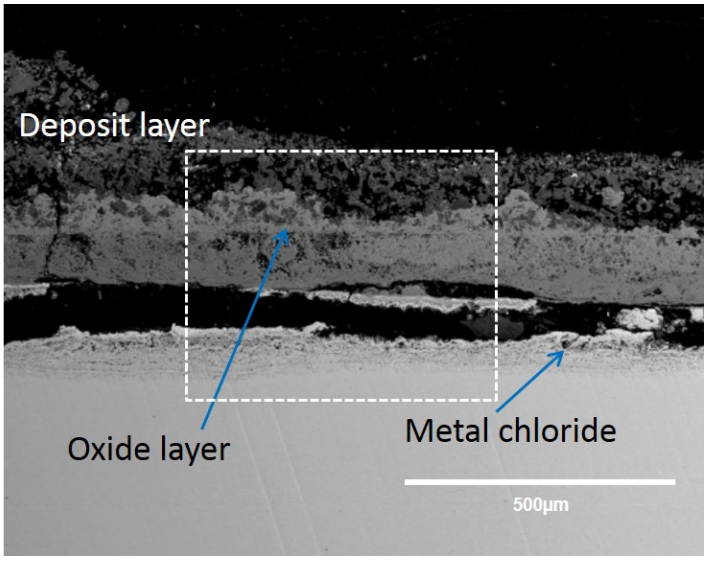

Figure 46. Cross section of sample exposed 24 hours, material temperature 600 °C; pre-heated testing probe.

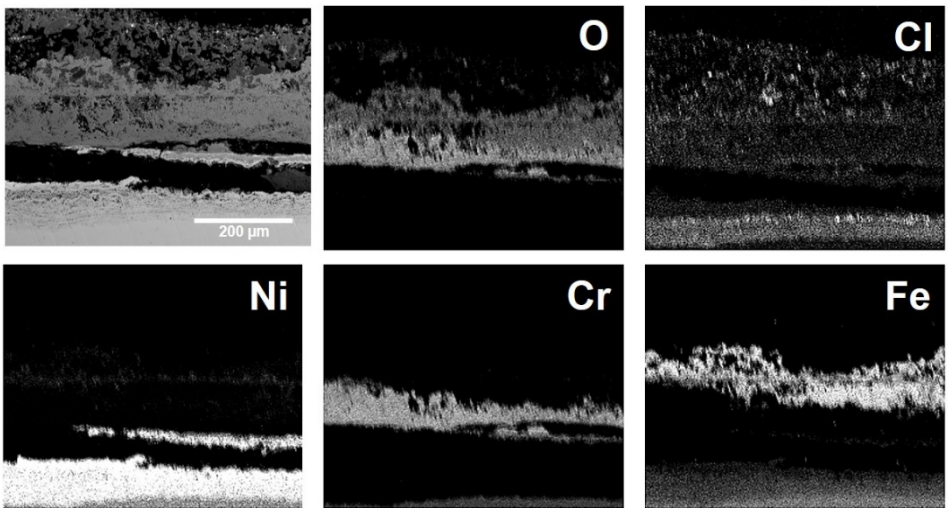

Figure 47. EDX mapping from cross section of sample exposed 24 hours, material temperature 600 °C; pre-heated testing probe.

A comparison of different startup sequences is shown in Figure 48, i.e. startup with cold probe, preheated probe and preheated probe and pre-oxidized samples. The effect of preheating the probe on the overall exposure is according to the results minor (compare Figure 48a and Figure 48b). In both cases the samples suffers greatly from spallation and an accelerated corrosion attack. Metal chlorides were detected on both samples. However, the results indicate that presence of these chlorides is slightly less on the preheated sample. Furthermore, the Fe and Cr depleted zone (enriched in nickel) in the outermost part of the steel are different between the samples. This nickel enriched zone is more than twice as thick on the samples exposed on the cold probe compared to the samples exposed on the preheated zone; the thicknesses are about 175 µm and 75 µm respectively. In Figure 48c a pre-oxidized sample exposed on a preheated probe is shown. Compared to samples shown in Figure 48a and Figure 48b the corrosion product layer is thinner and better adherent. The corrosion layer consists of a dense duplex oxide scale. The outer part consists of a Fe-rich oxide while the inner part is dominated by a Cr-rich oxide. Similar to the samples shown in Figure 48a and Figure 48b the outer part of the steel is depleted in Fe and Cr, leaving behind a nickel enriched steel substrate. However, this region, with a thickness of about 40 µm, is considerably thinner compared to the previous samples. At the front of this region, metal chlorides could be detected. The deposit composition is similar in all three cases, being dominated by calcium sulphate and alkali chlorides.

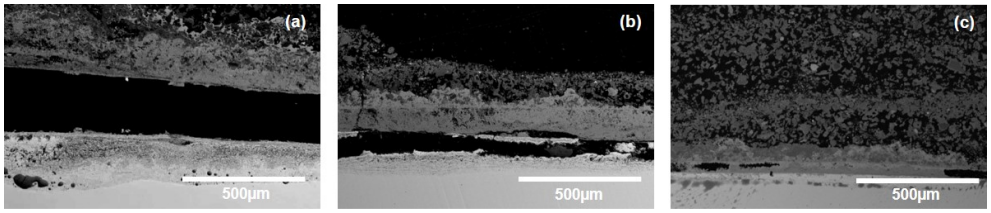

Figure 48. Cross section of samples exposed for 24 hours, material temperature 600 °C; (a) cold testing probe, (b) pre-heated testing probe, (c) pre-oxidized samples.

The lack of a protective oxide scale becomes apparent in both the cold probe and preheated probe exposures as metal chlorides are detected in corrosion front in both cases. According to the SEM/EDX cross sections the presence of metal chlorides is more pronounced for the samples exposed on the cold probe. In addition to samples exposed on the cold probe and preheated probe, pre-oxidized samples were exposed on the preheated probe. Thus, samples were prior to the boiler exposure pre-oxidized in a box furnace at 600 °C for 24 hours using lab air. The oxide scale formed consisted of a Cr-rich oxide in the sub-micron range. The pre-oxidized samples were pre-heated over 100 °C and thereafter exposed for 24 hours in the waste fired boiler. According to Figure 48c, the original oxide scale from the preoxidation has grown and the corrosion attack has been initiated. However, the adherence of the oxide scale as well as the deposit on the pre-oxidized sample seems to be good, which indicates that the initial corrosion has been less aggressive compared to the samples not being pre-oxidized. Despite this, transition metal chlorides are detected at the oxide/metal interface and poor adhesion may be expected after prolonged exposures.

The results imply that the initial stages of exposure in a waste fired boiler can be rather aggressive. Regardless of preheating or pre-oxidizing the sample probe the corrosion attack is still very fast leading to thick oxide scales and formation of metal chlorides resulting in poor scale adhesion. By preheating and pre-oxidation, the attack as well as the amount of metal chlorides was decreased slightly. Thus, the startup sequence seems to have a minor effect on the initial stages of exposure.

4.3.2 The effect of chlorine penetration through oxide scales

The environment in biomass- and waste-fired boilers is very complex. Some of the compounds that are commonly detected in considerably high levels in the flue gas of a boiler are chlorine species, such as alkali chlorides and HCl. The high corrosivity of the boiler atmosphere is partially attributed to the presence of chlorine species, which are considered hazardous to the metallic parts of the boiler. The metallic parts are mainly made of stainless and low alloy steels. Since steels rely on the oxide scale formed during the first hours of boiler operation, it is of great importance to understand the propagation of a corrosion attack, see Figure 49.

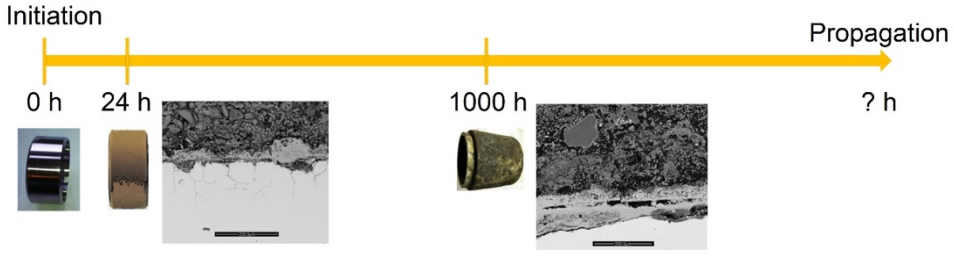

Figure 49. Schematic progress of the corrosion attack in harsh environments versus time. As can be seen, the corrosion attack starts almost immediately and in order to make better estimations of the predicted life time, the properties of the initially formed oxide scales are of great importance.

Propagation refers to the part of the corrosion attack when the material has passed through the initiation of the attack and lost its primary oxide protection (e.g. the chromium rich oxide initially formed on stainless steels). The resulting, often multilayered oxide scale, is referred to as the secondary oxide protection. For

materials exposed in harsh environments, such as biomass and waste fired boilers, the propagation step starts very fast after startup. This multilayered oxide scale is susceptible for chlorine penetration and an accelerated corrosion attack. In order to investigate the propagation of the corrosion attack induced by the presence of chlorine species, pre-formation of well-known oxide layers is necessary. The pre-oxidation was followed by exposures in aggressive environment. Thus, it may be possible to relate the observations done on field studies with the mechanistic study of the transport of chlorine performed in the laboratory.

Pre-oxidation: Fe-Cr-Ni oxides of stainless steel

The effect of pre-oxidation on the corrosion behavior of steels in presence of chlorine species has already been studied by different authors [3-6]. However, these studies were mainly focused on the protective properties of the oxide scales and none of them addresses the transport of chlorine through the oxide scale.

In this study the material used was the 347H stainless steel. In order to mimic the oxidation taking place during the first operation hours of the boiler, it is necessary to understand the pre-oxidation step previously investigated in the laboratory exposures. It is well known that stainless steels rely on the formation of a protective Cr-rich oxide to withstand a corrosion attack. This type of oxide is usually referred to as the primary protection of a steel. When stainless steels are exposed to a highly corrosive atmosphere in the presence of alkali chlorides and water vapor, the protective Cr-rich oxide layer is destroyed. Future protection of the steel will depend on the composition and microstructure of this new oxide layer(s). This type of oxide scales are referred to as the secondary protection of the steel. Our aim with this study is to investigate how chlorine may penetrate these different types of oxide scales. With a corrosion knowledge of laboratory exposed samples it is possible to form a well-defined Fe-rich oxide scale on the stainless steel.

In a former study, the oxidation of the stainless steel 347H was performed to obtain an oxide scale defined by an outward growing Fe-rich oxide and inward growing spinel oxide. The pre-oxidation was performed in an atmosphere consisting of 5% O_2 and 95% N_2 at 600 °C during 168 hours. To accelerate the breakdown of the Cr-rich oxide, 1.35 μmol K^+/cm^2 in the form of K_2CO_3 was deposited on the sample surface prior to exposure. The pre-oxidation parameters were selected based on earlier work of Pettersson, et.al. [7], Jonsson, et.al. [8] and Lehmusto, et.al. [9]. The resulting oxide was well adherent to the substrate. The thickness of the oxide was about 5-6 μm, see Figure 50. The alkali ion, in this case K^+, reacted with the Cr-rich oxide formed during the first hours of pre-oxidation. This reaction leads to the formation of K_2CrO_4 which promotes the breakdown of the protective oxide [7]. K_2CO_3 was selected as a deposit in order to accelerate the breakdown of the Cr-rich oxide without presence of chlorine. The exposure time of 168 hours was selected to ensure complete coverage of the substrate by the Fe-rich oxide. According to XRD, K_2CrO_4 was not detected. This agrees with earlier studies that have reported low stability in the formed K_2CrO_4. After a long period, i.e. 168 hours, chromate is seldom detected [9-11].

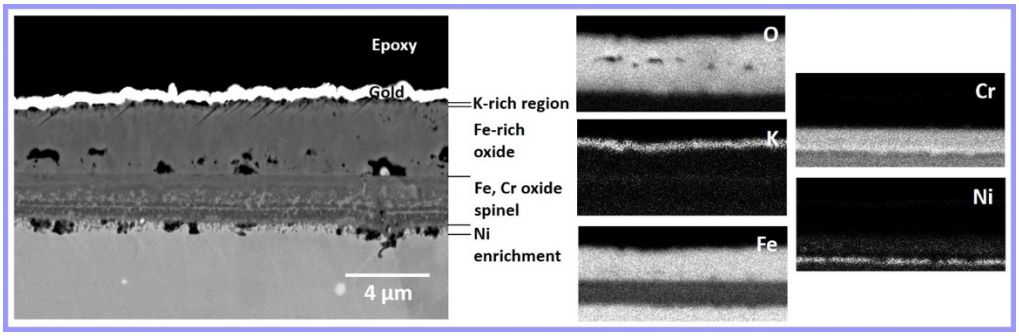

Figure 50. SEM of cross-sectional view of pre-oxidized 347H steel in 5% O_2 + N_2 with deposition of 1.35 µmol K^+/cm^2 in the form of K_2CO_3.

After oxidation of the stainless steel 347H, the oxide layers consisted of an outward growing Fe-rich corundum type oxide and an inward growing spinel oxide. The oxide scale was about 3.7 µm of the Fe-rich oxide and 1.8 µm of the Fe,Cr spinel oxide. The Fe-rich oxide layered showed some pores close to the original metal surface of the metal. According to the XRD results, the Fe-rich oxide was identified as Fe_2O_3. EDX analysis was performed (see Figure 50) on this sample. The results showed a K-rich region that correlates with the Fe on the top of the Fe-rich oxide; and $KFeO_2$ was detected using XRD. Furthermore, Ni enrichment in the metal was detected at the oxide/metal interface. This has been reported earlier for FeCrNi alloys [12, 13].

Based on the pre-oxidation of the stainless steel 347H in the lab, the pre-oxidation of the ring samples was performed in a 3 temperature zone tube furnace. K_2CO_3 was deposited on the samples surface prior exposure to 5%O_2+95%N_2, the temperature of the 3 zones was all kept at 600 °C. The samples were placed one at each zone. The following image shows a cross section of the initial condition of the pre-oxidized samples. According to EDX analysis (not shown) the pre-formed oxide consisted mainly of iron-rich oxide with small amounts of chromium and potassium. Enrichment of nickel at the metal close to the oxide was observed, which is a common behavior of stainless steels also observed in laboratory samples.

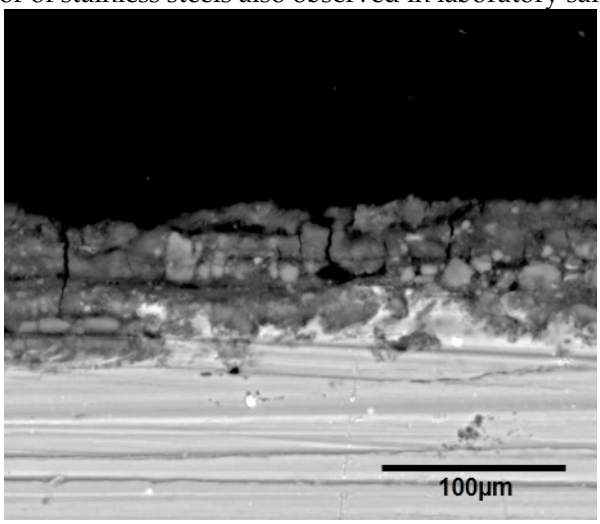

Figure 51. SEM of cross-sectional view of pre-oxidized 347H steel ring in 5% O_2 + N_2 with deposition of K_2CO_3 at 600 °C.

Field tests evaluating the effect of peroxidation on chlorine diffusion

The corrosion test was performed during winter 2016 in the E.ON boiler P15 in Händelö (Norrköping). The tests lasted for 24 hours and 144 hours, respectively. A reference exposure with regular fuel conditions was performed followed by the ammonium sulphate added exposure.

Figure 52 shows the probe after being exposed during 24 and 144 hours with waste as fuel. All the samples were covered with deposit material. The deposit stayed attached to the samples during the outtake of the probes from the boiler. The amount of deposit material seemed not to vary between the 24 and the 144 hours exposure. The samples were removed from the test probe once the probe was cooled down. The samples were stored in individual boxes in a desiccator to avoid contact to ambient water.

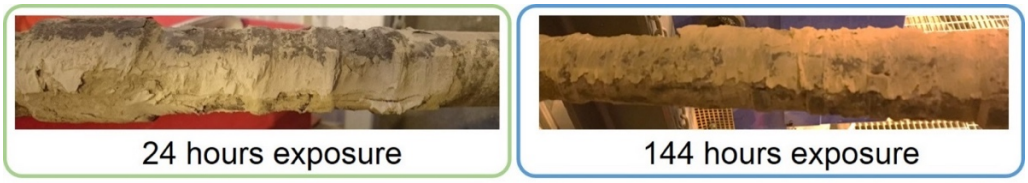

Figure 52. Testing probes after reference exposures.

Optical examination of the samples was performed. However, when the samples were removed from the test probe almost all the deposit material was detached from the sample surface. According to the Figure 53, only few areas of the samples surfaces kept deposit material attached. No visible difference can be observed between the pre-oxidized and non-pre-oxidized samples.

Figure 53. Optical images of exposed samples after 24 hours and 144 hours with and without ammonium sulphate

The samples were casted in epoxy, cut and prepared in order to examine their cross sections. After preparation the samples were stored in a desiccator in order to avoid ambient humidity.

- SEM/EDX analysis of samples exposed with waste as fuel mix

The total thickness of the still attached oxide after 24 hours varies along the sample surface, the thickest oxide being approximately 230 μm. The flue gas side of the sample shows a general corrosion attack. Cracks in the oxide were observed. Indication of grain boundary attack is noticeable already after 24 hours. In some regions the grain boundary attack is so severe that part of the metal is clearly defragmented, see Figure 54.

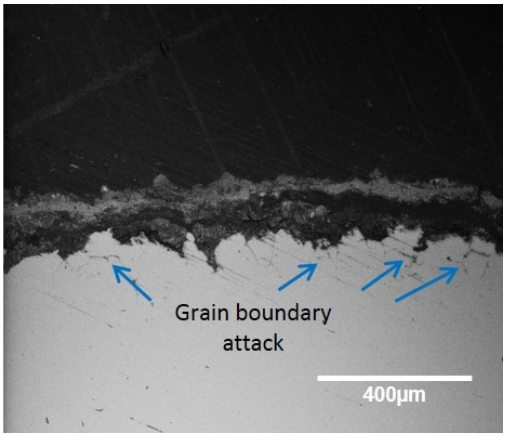

Figure 54. 347H reference exposure after 24 hours.

The deposit was rich in chlorine leading to an extended corrosion attack over the material surface. According to EDX analysis chlorine was observed in the oxide reaching the oxide/metal interface. Point analysis shows that iron, chromium and nickel are detected at the chlorine-rich layer. Accumulation of chromium and nickel is detected over the chlorine-rich layer. At the oxide/metal interface oxygen, iron and nickel are detected, however the amount of chromium is low.

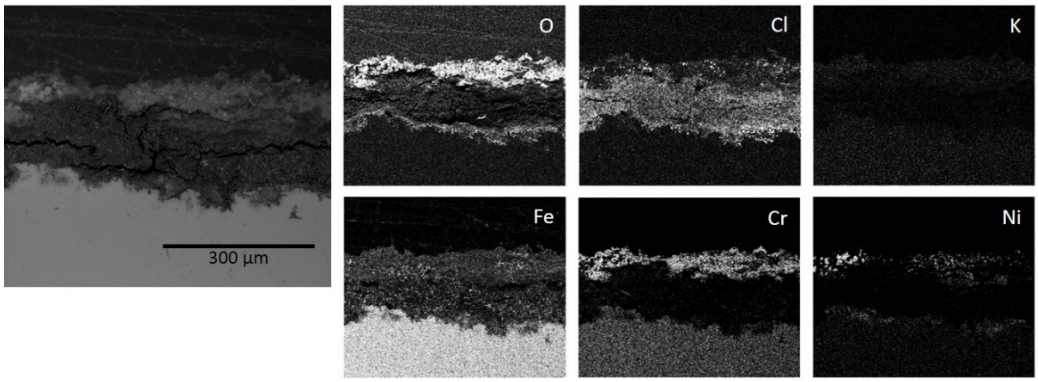

Figure 55. EDX analysis of 347H reference exposure after 24 hours.

Pre-oxidized 347H was also exposed. The deposit formed on top of the samples was highly corrosive, promoting an aggressive corrosion attack on the samples. However, the pre-oxidized 347H showed a slightly better corrosion resistance in this environment compared to the corresponding non-pre-oxidized 347H sample. The preoxidized sample did also suffer from steel grain boundary corrosion attack in some regions, as shown in Figure 56a. In other areas, the preformed oxide was able

to withstand the corrosive environment during the 24 hours exposure, see Figure 56b. Thus, the metal underneath the pre-formed oxide scale was not attacked during this time. The adherence and integrity of the oxide layers seems to be important factors in the decreasing the extent of the corrosion attack.

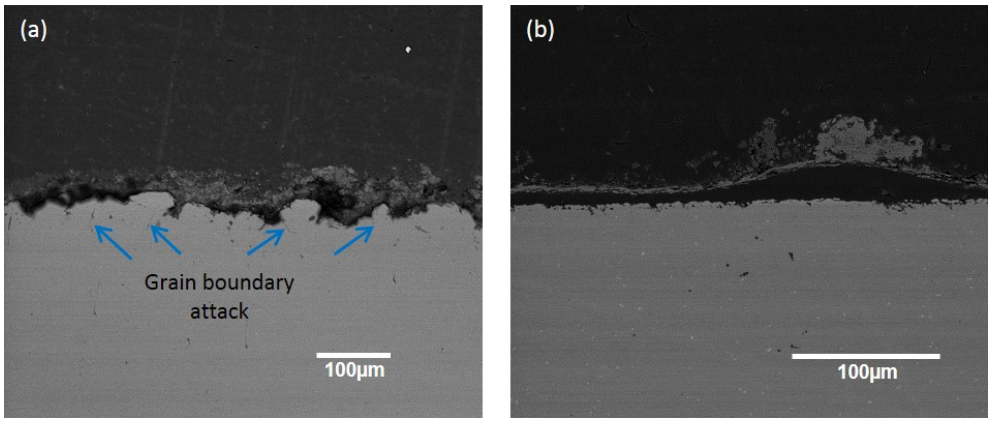

Figure 56. Pre-oxidized 347H reference exposure after 24 hours, a) an area where the corrosion attack has been initiated b) an area where the pre-formed oxide still has withstand the corrosion attack.

According to EDX analysis accumulation of chlorine close to the metal is detected. Iron, chromium and nickel are present in the oxide scale, however higher amount of chromium is located on the top of the oxide layer. Potassium was not detected in the scale which means that the potassium accumulated during the pre-oxidation reacted with the deposit material. According to the laboratory study that set the matrix for the current exposures, the potassium rich layer on the top of the oxide scale is suggested to react in presence of HCl(g) forming KCl(g) making potassium non-detectable in the oxide scale.

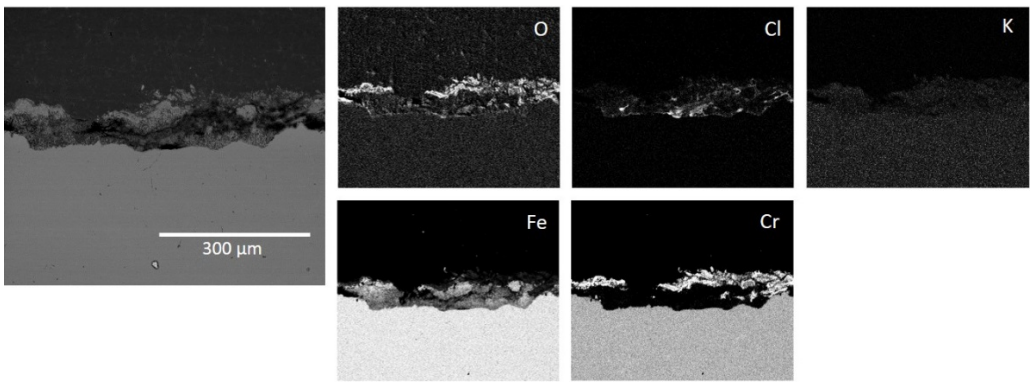

Figure 57. EDX analysis of pre-oxidized 347H reference exposure after 24 hours.

The samples were also exposed for longer times, 144 hours. Even though, the optical examination showed that all samples looked similar regardless the exposure time, cross sectional views of the samples revealed the actual corrosion attack after longer exposure times. Figure 58, shows again grain boundary corrosion, however it is observed that after 144 hours the corrosion attack reached deeper into the metal. The SEM image shows clearly the corrosion attack in the grain boundaries, presence of

metal chlorides were detected all over the oxide scale but also at the oxide/metal interface.

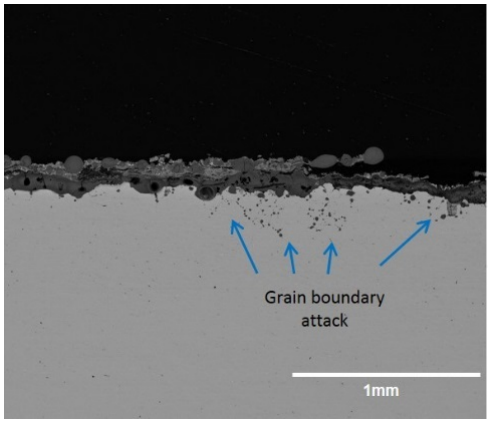

Figure 58. 347H reference exposure after 144 hours.

In the EDX analysis showed below, it is confirmed that chlorine is spread all over the oxide scale, the highest concentration of chlorine was detected at the surface of the scale. Chlorine was also detected in the attacked grain boundaries. Regarding the oxide scale, same behavior as the samples exposed during 24 hours was observed. The oxide consists of iron rich oxide. Accumulation of chromium at the scale surface and grain boundaries of the oxide in the bottom layer. Enrichment of nickel was detected at metal close to the oxide/metal interface.

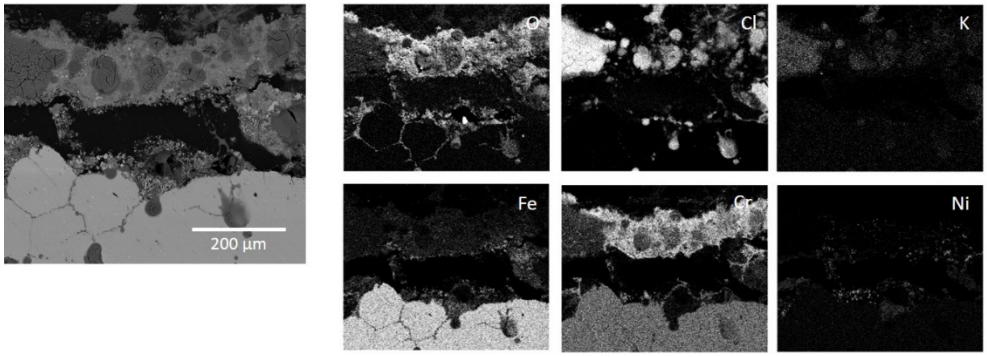

Figure 59. EDX analysis of 347H reference exposure after 144 hours.

In the case of the pre-oxidized sample exposed during 144 hours, it was observed that areas where the pre-formed oxide scale was still present with deposit material. Even though SEM image of the cross section shows that the oxide scale is detached from the metal, grain boundary attack was not observed. Moreover, regions of the ring sample where the pre-formed oxide scale was lost, presence of metal chlorides was detected as well as grain boundary attack, see Figure 60.

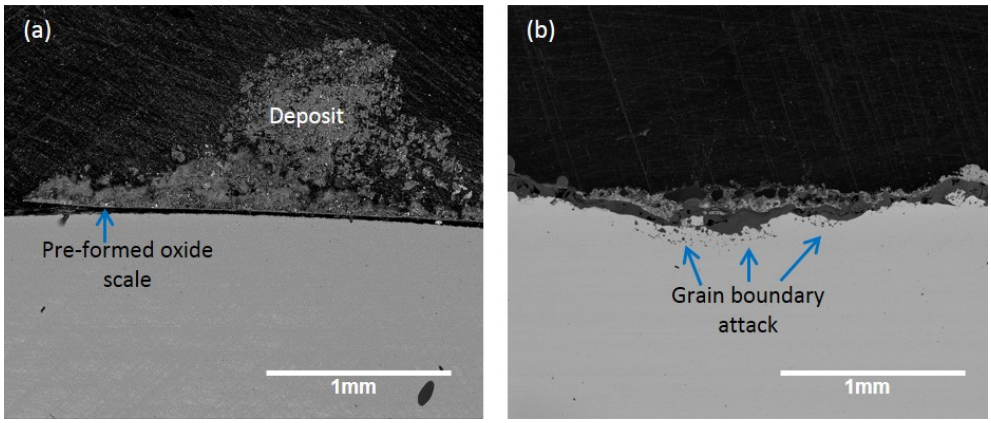

Figure 60. Pre-oxidized 347H reference exposure after 144 hours a) an area where where the pre-formed oxide still has withstand the corrosion attack. b) an area where an accelerated corrosion attack is seen. Steel grain boundary attack is observed as well as the formation of metal chlorides.

EDX analysis was performed in the region where the pre-formed oxide spalled off. The layer of corrosion products formed during exposure, two areas in the scale are observed. The top layer is rich in chromium and iron. In the bottom layer, the content of chromium decreases while the iron content is the same. Concentration of chlorine was detected in the bottom layer of the scale and the metal where grain boundary corrosion was observed. Presence of potassium was low, this was also observed after 24 hours.

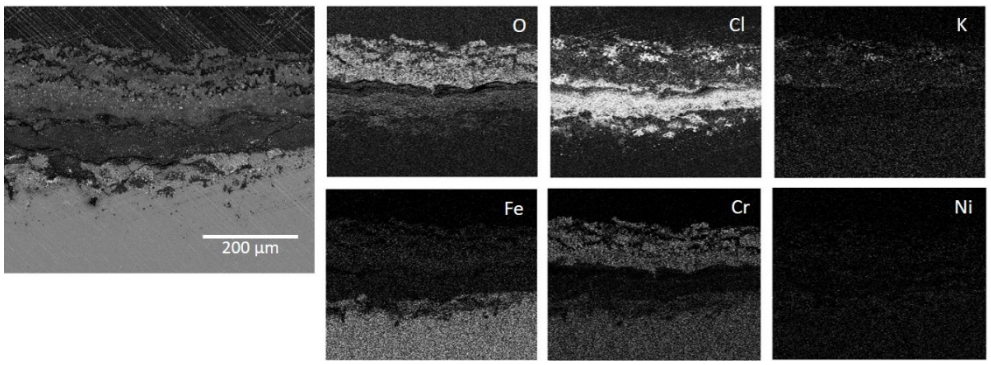

Figure 61. EDX analysis of pre-oxidized 347H reference exposure after 144 hours.

- Ammonium sulphate exposures

Similar exposures were performed with addition of ammonium sulphate, in order to test any mitigation of the corrosion attack of the metallic samples. Deposit material detached from the sample surface according to the optical examination, see Figure 62.

The SEM image below shows the cross section of a 347H sample after 24 hours exposure. It shows a uniform corrosion attack on the samples surface. The corrosion attack is similar to the one observed in the reference exposure in absence of ammonium sulphate. Indication of grain boundary corrosion was also observed. Partial detachment of the deposit material and oxide scale. The sample surface suffered of material lost in different areas.

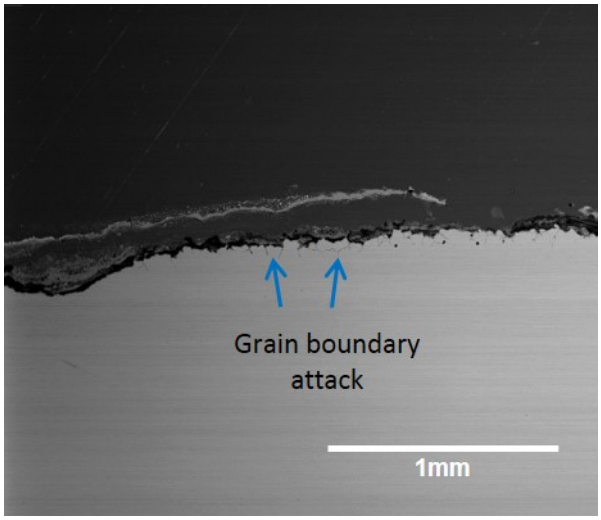

Figure 62. 347H exposure with ammonium sulphate addition after 24 hours.

The following figure shows the EDX analysis of the sample. The oxide scale after 24 hours exposure has a similar chemical content compared to the sample exposed without the ammonium sulphate addition exposures. However, it is noticeable that the concentration of chlorine seems to be lower than the reference.

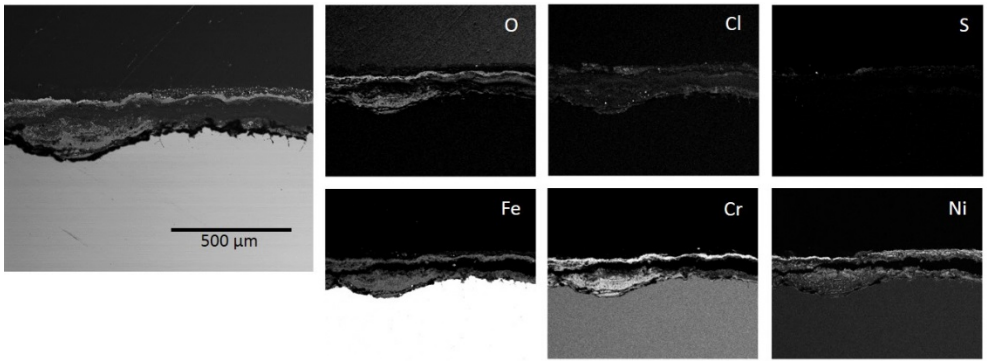

Figure 63. EDX analysis of 347H exposure with ammonium sulphate addition after 24 hours.

In the case of the pre-oxidized 347H exposed in presence of ammonium sulphate, the deposit material was detached in some regions of the samples. It was still possible to find regions where the initial pre-formed oxide was present. Even though it was observed the same type of corrosion attack it was noticed that the attack was slightly milder than the one observed for the non-pre-oxidized sample. The most affected part of the sample was seen on the flue gas side, where significant material loss was be observed.

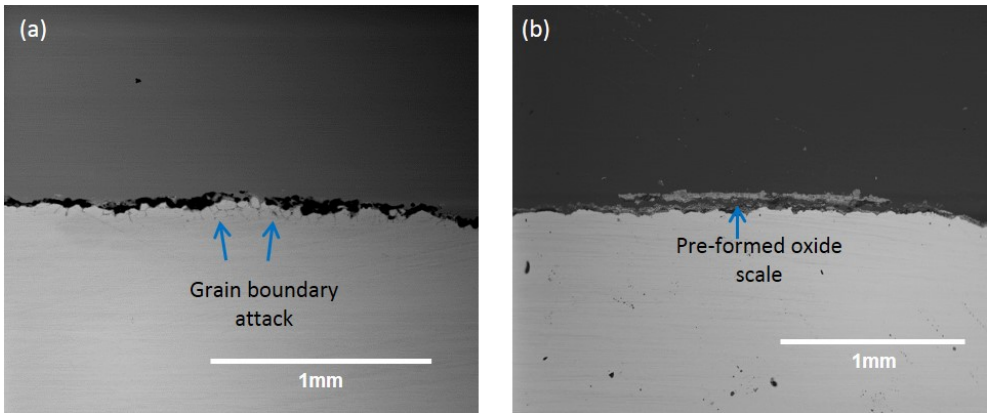

Figure 64. Pre-oxidized 347H exposure with ammonium sulphate addition after 24 hours, a) an area where the corrosion attack has been initiated b) an area where the pre-formed oxide still has withstand the corrosion attack.

It is important to emphasize that only small amounts of chlorine were detected at the metal/oxide interface and KCl particles were found at the scale surface. The remained oxide scale seemed to be the oxide formed prior exposure according to the chemical analysis. However, the potassium rich region at the top of the scale was not detected, this was also observed in the samples exposed in absence of ammonium sulphate.

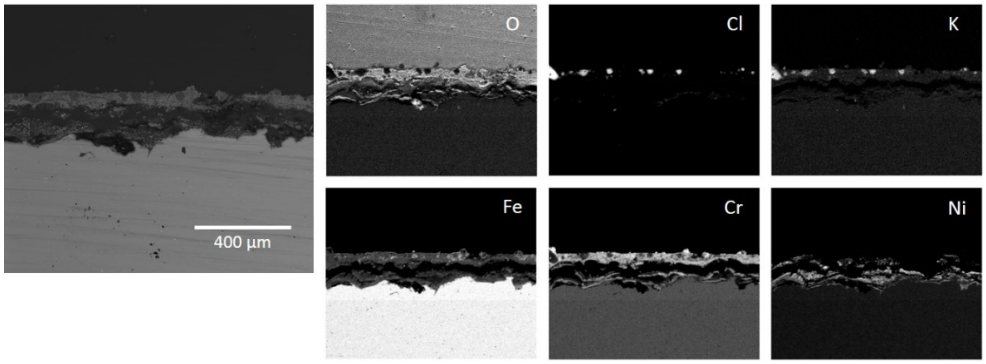

Figure 65. EDX analysis of pre-oxidized 347H exposure with ammonium sulphate addition after 24 hours.

Samples exposed during 144 hours in presence of ammonium sulphate are shown below. Figure 66 shows an SEM cross section of the non-pre-oxidized sample. As seen in the optical examination, most of the deposit material has been lost. The SEM image shows a part where some deposit material still is attached to the sample. Indication of grain boundary attack is observed, however the number of attacked grain boundaries seems to be lower compared to the samples exposed for shorter times.

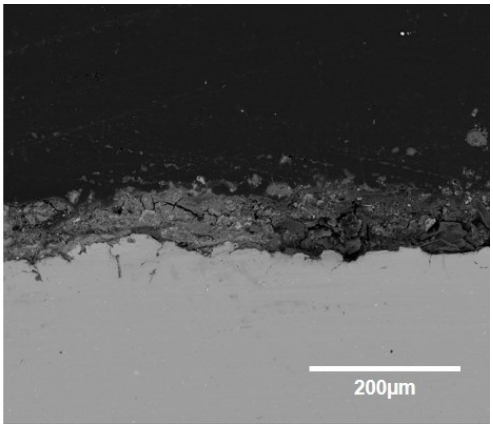

Figure 66. 347H exposure with ammonium sulphate addition after 144 hours.

Chlorine was detected along the deposit/oxide layer all the way to the oxide/metal interface. On the top part of the layer iron, chromium and nickel were detected, which suggests the formation of the oxide scale typical of stainless steels.

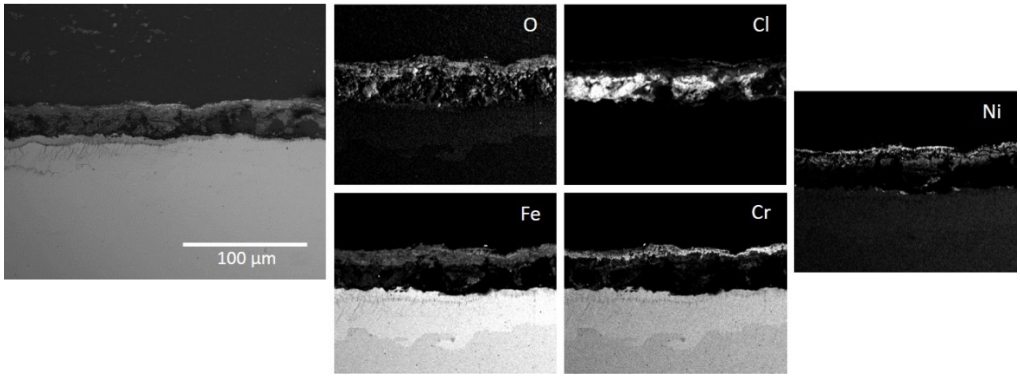

Figure 67. EDX analysis of 347H exposure with ammonium sulphate addition after 144 hours.

The pre-oxidized 347H exposed after 144 hours showed a uniform mild corrosion attack. The pre-formed oxide scale seemed to be partially lost together with the deposit material.

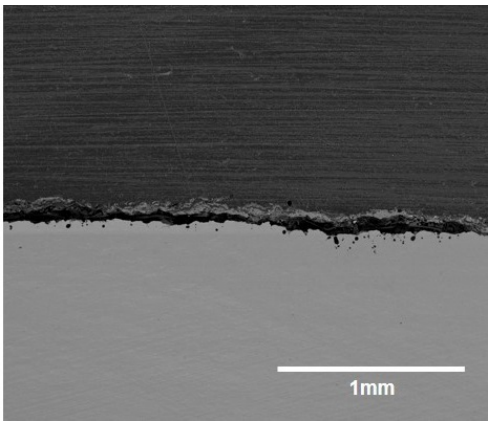

Figure 68. Pre-oxidized 347H exposure with ammonium sulphate addition after 144 hours.

The EDX analysis shows that part of the oxide scale is still attached since the analyzed layer consisted of iron, chromium and some enrichments of nickel. Penetration of chlorine is detected at the oxide/metal interface and at the grain boundary attack. This behavior was also observed in the corresponding sample in absence of ammonium sulphate.

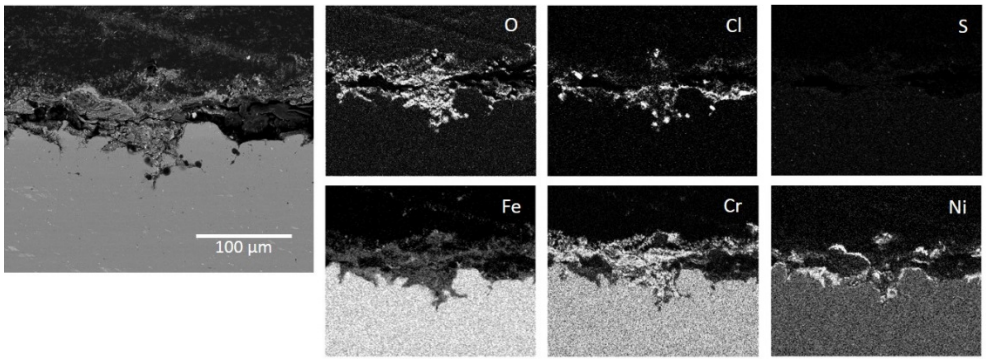

Figure 69. EDX analysis of pre-oxidized 347H exposure with ammonium sulphate addition after 144 hours.

To summarize, for the pre-oxidized and non-pre-oxidized samples there seems to be an effect of the preformed oxide in decreasing the inward diffusion of chlorine, even though the preformed oxide scale is actually the normal corrosion product layer formed in alkali rich environments. The samples without pre-oxidation exhibited a slightly more accelerated corrosion attack and a thicker chlorine enriched corrosion product layer. However, the corrosion attack was in general very fast, regardless of how the samples were pre-treated.

4.3.3 Short term evaluation of new materials

The short term corrosion evaluation of new materials was performed during winter 2016 in the E.ON boiler P15 in Händelö (Norrköping). The new materials exposed were the stainless steel Sanicro 33 and a FeCrAl Model Alloy Fe10Cr3Al2Si, 347H and Kanthal APMT were used as reference materials, respectively. The aim of these probe exposures was also to compare the corrosion results with the modelling and the corrosion prediction tools results, also performed in the present project. The tests were performed at two different times: a short 24 hours test and a longer 144 hours test. A reference exposure with regular fuel conditions was performed followed by an exposures where ammonium sulphate was added.

Material loss

Material loss determination was performed for the samples exposed for 144 hours in both the Reference and the Ammonium sulphate addition exposures. The results are shown in Figure 70. The presented results are shown in mm material loss. Recalculated to mm/year, the corrosion rate is very high, being up to 17 mm/year. Compared to the long term clamp exposures, which exhibited corrosion rates of up to 0.1 mm/year, the corrosion attack is several order of magnitude larger for the short term exposed samples. However, there are some major differences between these two investigations. The short term exposures has been performed in a more corrosive environment (higher flue gas temperature and higher particle density in

the flue gas) and with higher material temperature (600 °C on the probe exposures compared to 380 °C on the clamp exposures). Thus, the graph below is presented with the material losses in mm, instead of mm/year. The aim of these short term exposures was to investigate the initial corrosion attack of the newly developed material (the stainless steel Sanicro33 and the FeCrAl Model alloy) and compare it to corresponding commercial steels, the stainless steel 347H and the alumina former KanthalAPMT, respectively.

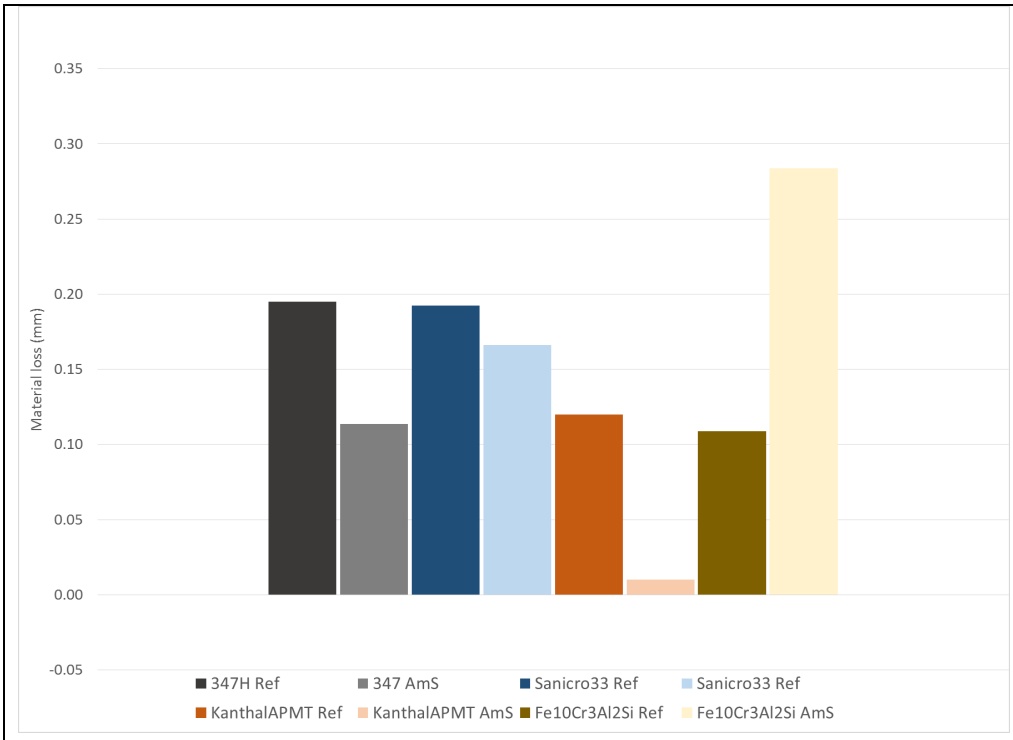

Figure 70. Comparison of the material loss of several materials in the reference (denoted ref) exposure and in the Ammonium sulphate addition exposure (denoted AmS)

According to the material loss data presented in Figure 70, there is a general trend that the corrosion was slightly milder in the Ammonium sulphate exposure, the exception being the FeCrAl model alloy which exhibited a higher mass loss in the Ammonium sulphate exposure. The Sanicro33 showed similar or slightly higher material losses compared to the 347H. For the alumina forming materials, KanthalAPMT and the FeCrAl model alloy, KanthalAPMT performed better compared to newly developed model alloy in the AmS exposure. In the reference exposure, the material loss was similar for the two materials.

SEM/EDX analysis on samples exposed in the reference exposure for 24 hours

Figure 71 shows the probe (a) before and (b) after the 24 hours exposure. Both zones of the probe were set at 600 °C. The new material samples were placed in the zone closest to the tip. All samples are covered in rather loosely attached deposit after the exposure. As a consequence, a major part of the deposit was lost during the removal after exposure.

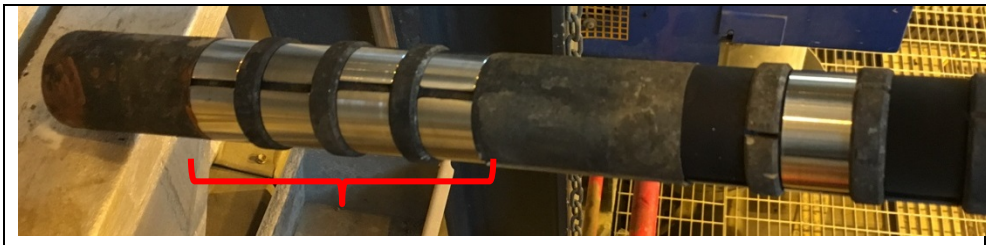

(a)

(b)

Figure 71 (a) Probe with the samples before exposure (b) Probe with the samples after 24 hours exposure in regular fuel conditions

After 24 hours exposure all the samples were removed and stored in desiccators in order to preserve them until the performance of the analyses. Figure 72 shows an optical image of the rings after removing them from the probes.

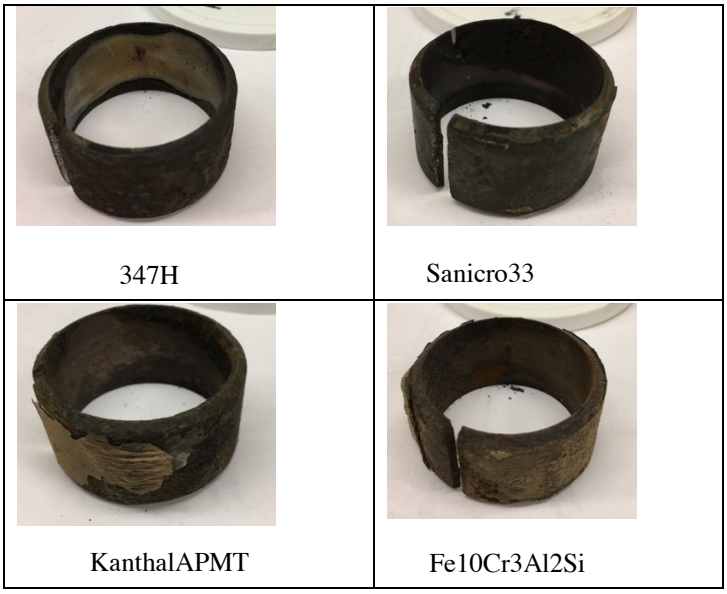

Figure 72. Optical images of the samples after 24 hours in the reference exposure

In order to study the corrosion attack of the different materials, cross sections of the samples were prepared to SEM/EDX analysis.

- 347H

The cross section of the sample shows that some of the deposit is still present on top of the surface, see Figure 73. The EDX analysis presented in Figure 74 shows a non-homogeneous layer of corrosion products, dominated by chlorine. The chlorine is detected primarily in rather thick layer in the metal/oxide interface. Above this a mixed oxide containing chromium, iron and nickel oxides can be seen. The total thickness of the corrosion product layer is roughly 140 µm, already after 24 hours of exposure showing a very fast corrosion attack. The chloride layer could be seen following a steel grain boundary into the steel substrate. Thus, the corrosion attack in the steel grain boundaries seems to be associated with chlorine, see Figure 73.

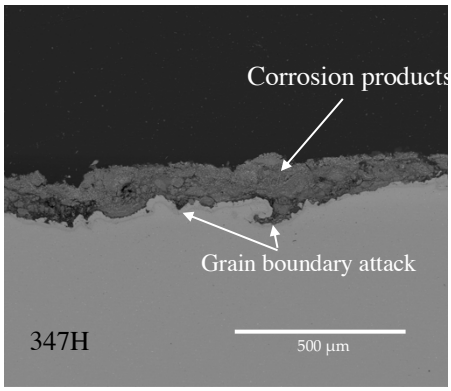

Figure 73. Backscattered SEM image of the 347H sample after 24 hours exposure in regular fuel conditions

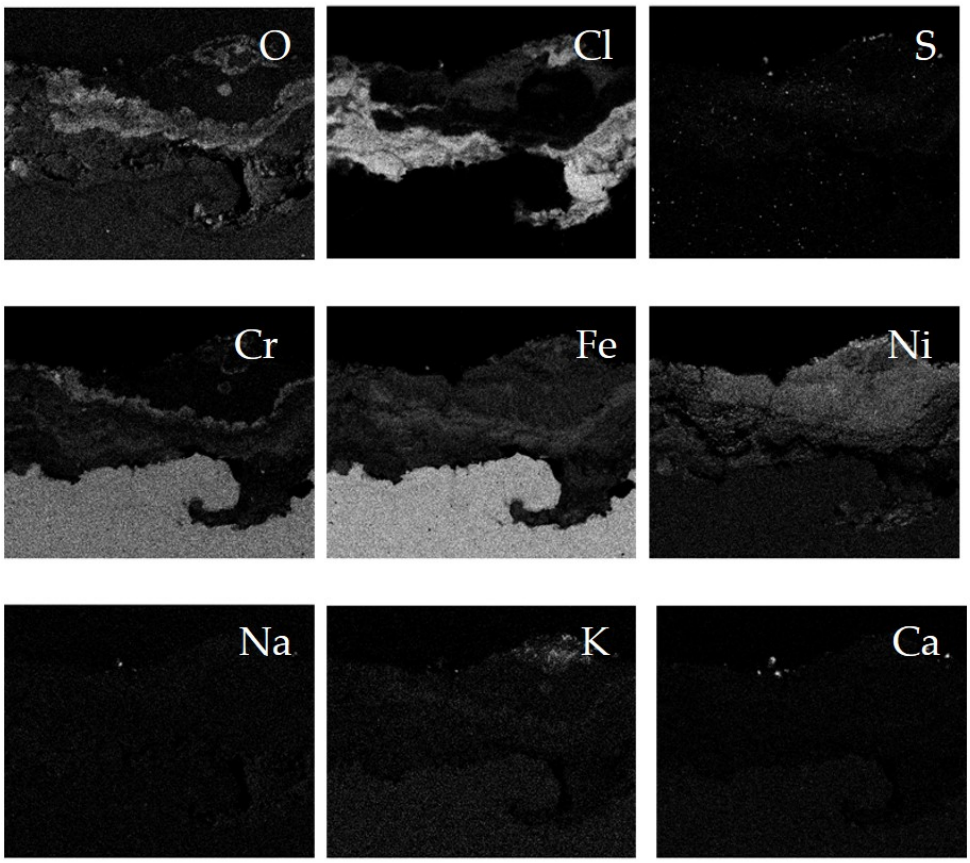

Figure 74. EDX mapping analysis of the 347H sample after 24 hours exposure in regular fuel conditions

- Sanicro 33

Figure 75 shows a SEM cross section of the Sanicro 33 sample after 24 hours in the reference exposure. The oxide scale is formed by a nickel rich non-homogeneous oxide which is present all over the surface, see Figure 76. The oxide layer is in the order of 20-30 μm.

Some of the deposit formed during the exposure is still present on the sample. The EDX analysis shows that the deposit is dominated in chlorine and some metal chlorides has started to grow in the metal/oxide interface. The accumulation of metal chlorides are especially high in the steel grain boundaries. Compared to the corresponding 347H sample, the initial corrosion attack of Sanicro33 is more modest. However, the corrosion attack has started for both materials already after 24 hours of exposure.

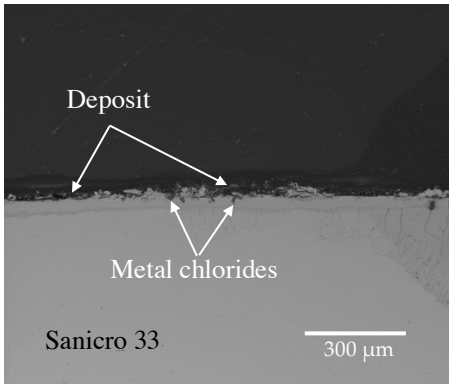

Figure 75. Backscattered SEM image of the Sanicro 33 sample after 24 hours exposure in regular fuel conditions

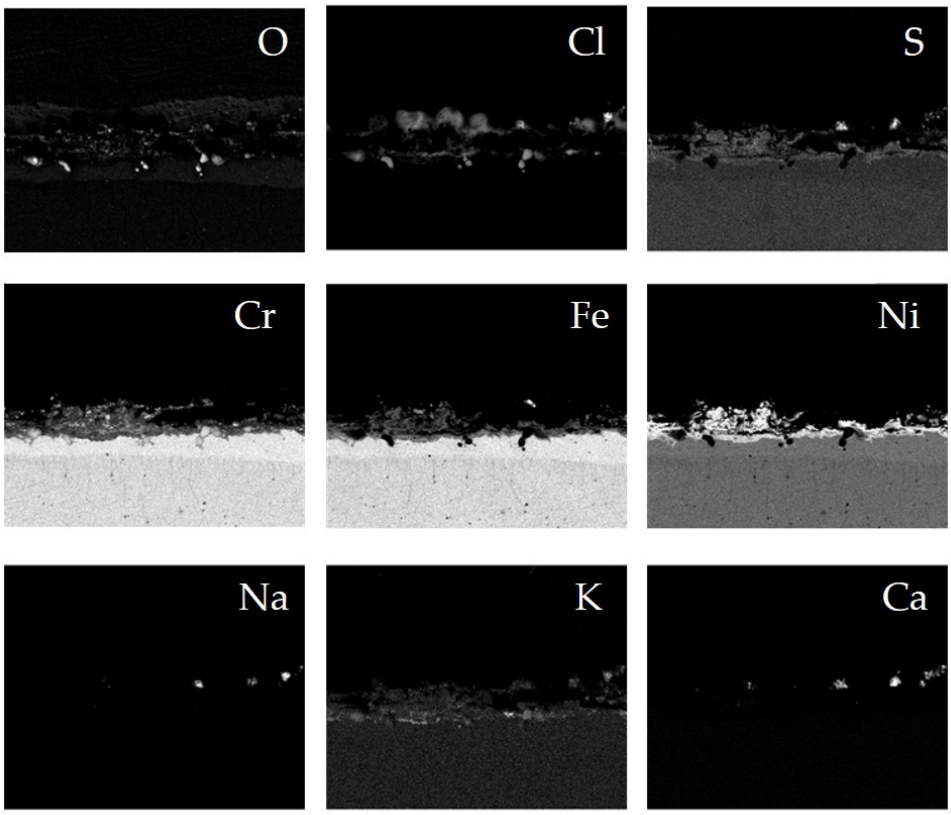

Figure 76. EDX mapping analysis of the Sanicro 33 sample after 24 hours exposure in regular fuel conditions

- KanthalAPMT

Figure 77 shows the KanthalAPMT sample after 24 hours in the reference exposure. A discontinuous chromium and iron inward growing oxide was detected over the surface, followed by an approximately 150 μm thick outward growing iron oxide. No alumina was found over the surface after 24 hours exposure. The EDX maps presented in Figure 78 show that some deposit was still present over the sample after the preparation. It is mainly composed by sodium and potassium chlorides were found and also some calcium remains were detected.

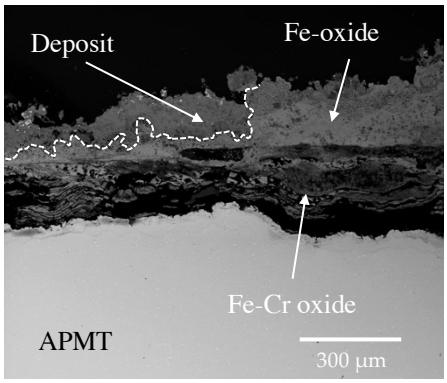

Figure 77. Backscattered SEM image of the APMT sample after 24 hours exposure in the reference exposures

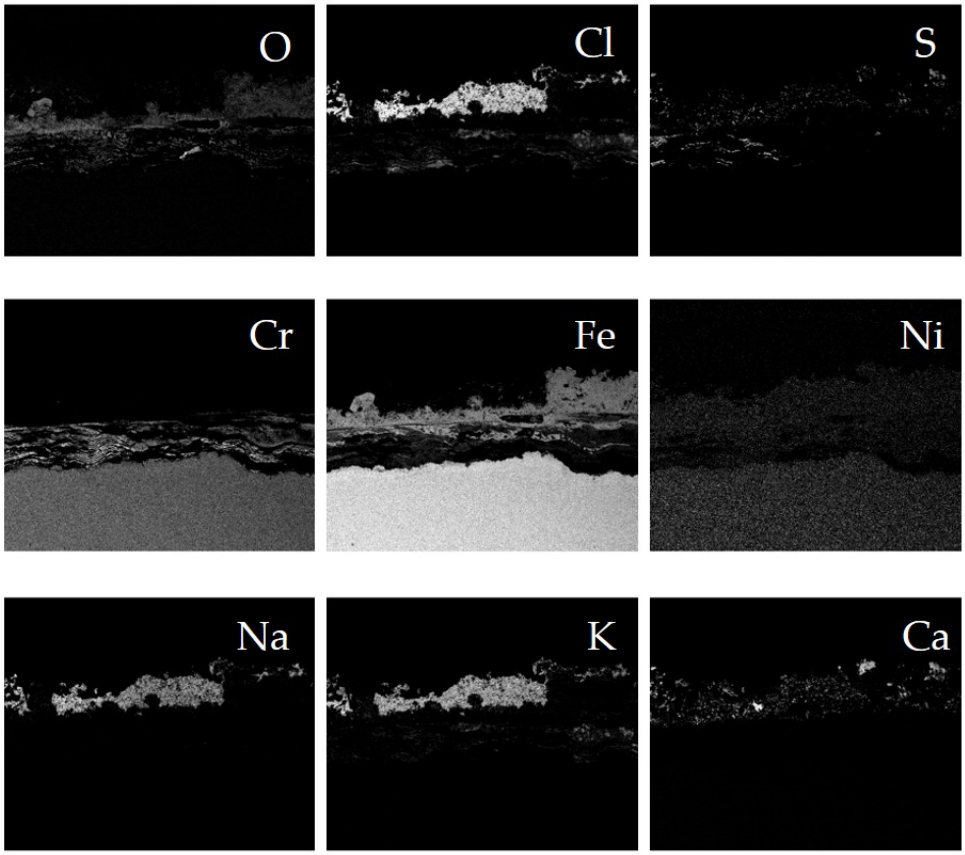

Figure 78. EDX mapping analysis of KanthalAPMT after 24 hours in the reference exposure

- FeCrAl model alloy (10% Cr, 3% Al, 2% Si, Fe Bal)

The Figure 79 shows the FeCrAl model alloy sample after 24 hours in the reference exposure. There is no visible corrosion attack according to the SEM cross section (Figure 79) and the corresponding EDX maps (Figure 80). Due to an electrical charge up of the sample in the SEM the EDX maps are slightly blurred. The gap between the deposit and the sample surface is an effect of the sample preparation. The analysis reveal no information of the formation of a oxide layer. Instead, the EDX maps detects a 300 µm layer of deposit composed mainly of sodium, potassium, calcium and chloride was detected in the deposit. The results of the FeCrAl model alloy is compared to the commercial KanthalAPMT. According to the corrosion results of the initial phases, the FeCrAl model alloy performs better compared to KanthalAPMT.

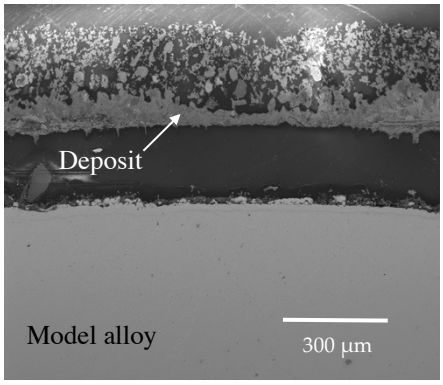

Figure 79. Backscattered SEM image of the model alloy sample after 24 hours exposure in regular fuel conditions

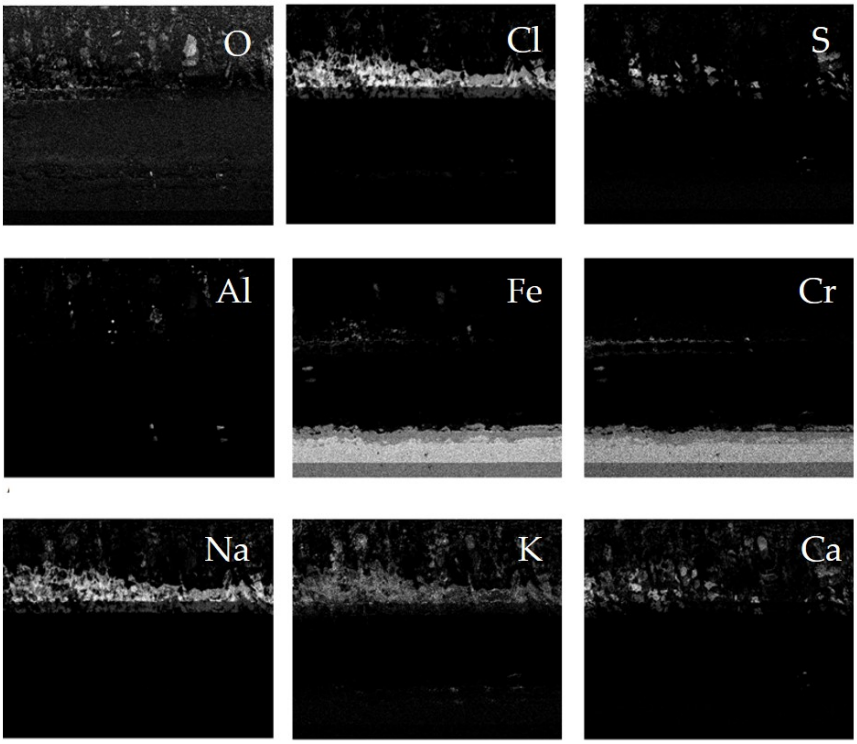

Figure 80. EDX mapping analysis of the model alloy sample after 24 hours in regular fuel conditions

SEM/EDX analysis on samples exposed in the reference exposure for 144 hours

Figure 81 shows the probe (a) before and (b) after the 144 hours exposure. Both zones of the probe were set at 600 °C. The new material samples were placed in the zone closest to the tip.

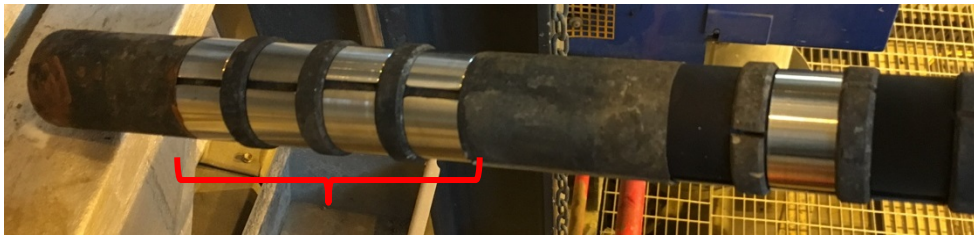

(a)

(b)

Figure 81. Probe with the samples (a) before and (b) after 144 hours exposure in the reference exposure

After the 144 hours exposure all the samples were removed and stored in desiccators in order to preserve them until the performance of the analyses. Figure 82 shows an optical image of the rings after removing them from the probes.

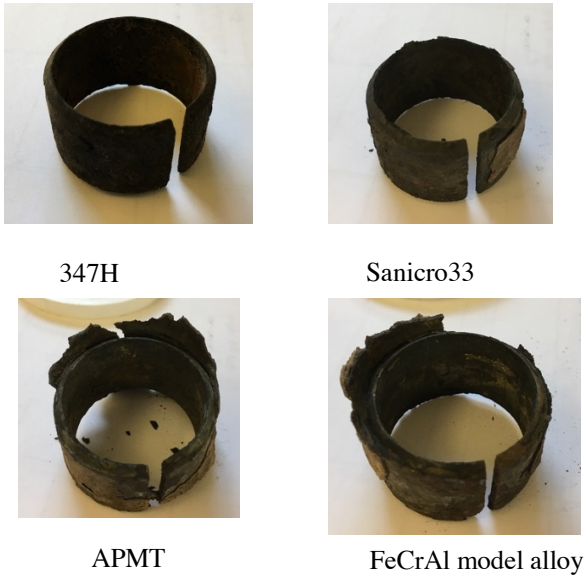

Figure 82. Optical image of the samples after 144 hours exposure in the reference exposure

In order to study the corrosion attack of the different materials, cross sections of the samples were prepared to SEM/EDX analysis.

- 347H

The cross section of the sample shows that the deposit layer had spalled off. However, some corrosion products are still attached on the sample, see Figure 83. The EDX analysis presented in Figure 84 shows that the presence of chlorine in the corrosion products is high. Similar to the corresponding sample exposed for 24 hours, the chlorine enrichment is primarily detected in the metal/oxide interface. Chromium, iron and nickel oxides are present above this chlorine enriched level. It is difficult to distinguish separate oxide layers in the oxide scale. It is therefore suggested that this oxide layer is a mixture of a spinel type oxide containing Fe, Cr and Ni. This type of oxide is usually growing inwardly to the metal, suggesting that the outer part of the corrosion product layer has been lost. The SEM/EDX analysis of the 347H sample does also show that the steel suffers from grain boundary attack (Figure 83). This is common when the deposit is rich in chlorine. The thickness of the remaining corrosion product layer is roughly 240 µm, showing that the corrosion has progressed compared to the 24 hours exposure.

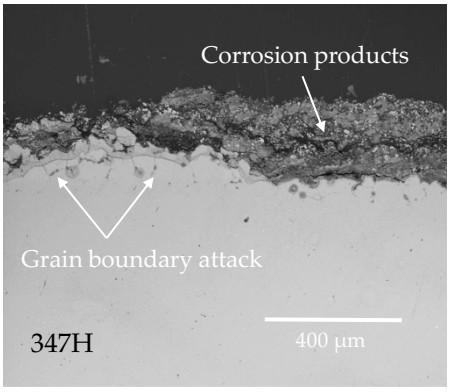

Figure 83. Backscattered SEM image of the 347H sample after 144 hours exposure in the reference exposure

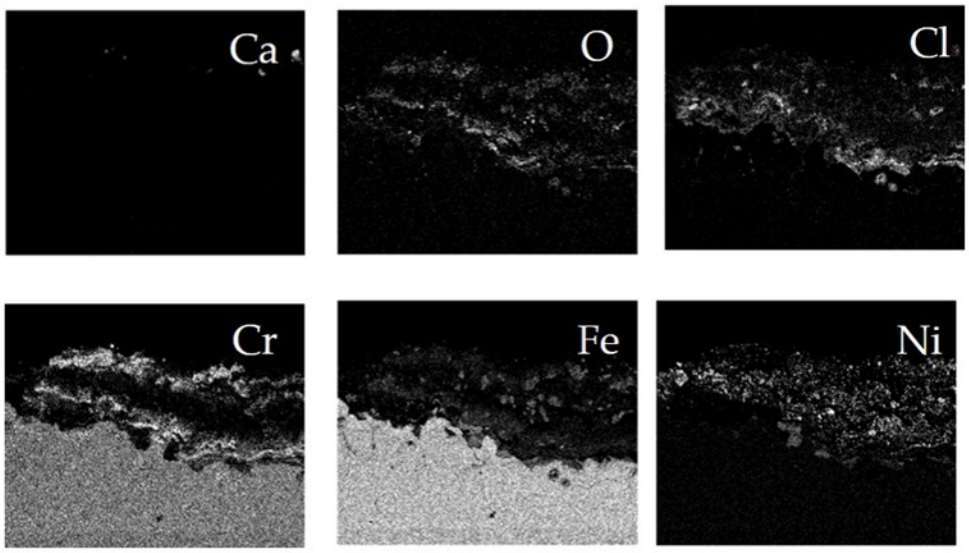

Figure 84. EDX mapping analysis of the 347H sample after 144 hours exposure in the reference exposure

The thickness of the sample was measured before and after the exposure. The results are presented in Figure 85. The sample presents a maximum material loss of 0.32 mm on the flue gas side. The material loss is close to zero on the lee side of the sample.

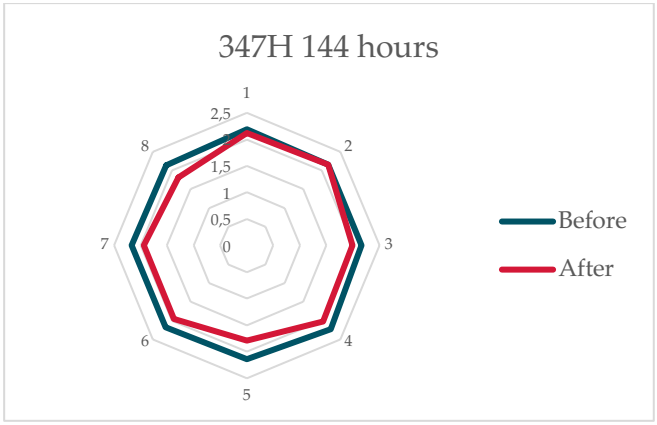

Figure 85. Thickness of the 347H sample before (blue) and after (red) 144 hours exposure in the reference exposure.

- Sanicro 33

Figure 86 shows an SEM cross section of the Sanicro 33 sample after 144 hours exposure in the reference exposure. A nickel rich non-homogeneous oxide is present all over the surface. Similar to the 24 hours exposure, a chromium rich non-homogeneous oxide was detected on the top of the Ni-rich oxide.

None of the deposit formed during the exposure is still present over the oxide due to sample preparation issues. The EDX analysis presented in Figure 87 shows large

chromium chloride particles growing under the surface of the sample. This effect was also seen after 24 hours exposure, however, to a less extent.

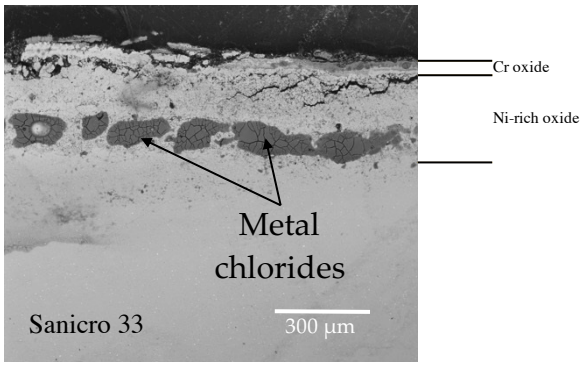

Figure 86. Backscattered SEM image of the Sanicro 33 sample after 144 hours exposure in regular fuel conditions

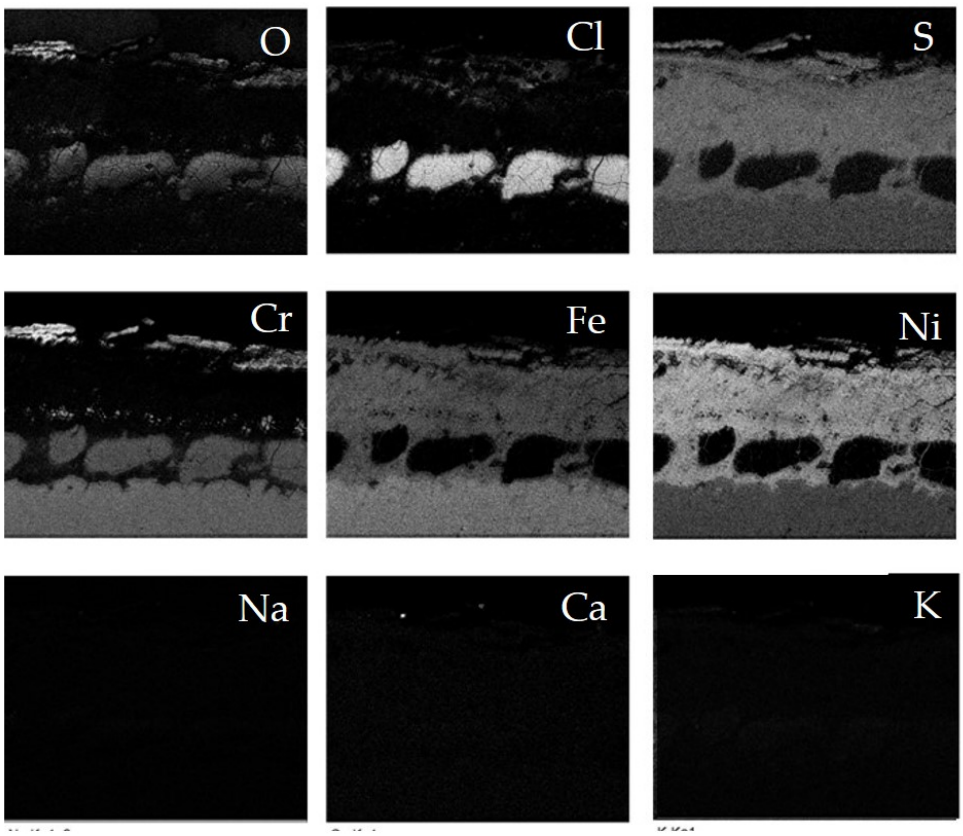

Figure 87. EDX mapping analysis of the Sanicro 33 sample after 144 hours exposure in the reference exposure

The thickness of the sample was measured before and after the exposure. The results are presented in Figure 88. The sample presents a maximum material loss of 0.22 mm in the flue gas side. The material loss is close to zero on the lee side of the sample.

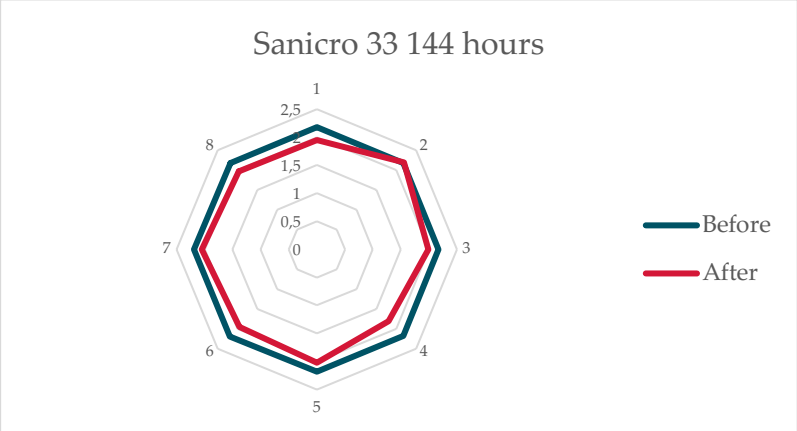

Figure 88. Thickness of the Sanicro 33 sample before (blue) and after (red) 144 hours exposure in the reference exposure

- Kanthal APMT

Figure 89 shows the Kanthal APMT sample after 144 hours exposure in regular fuel conditions. An approximately 200 µm thick deposit layer was found over the surface of the sample but no alumina was detected. The EDX maps presented in Figure 90 show that the deposit contains large amounts of chlorine, mainly concentrated in the outer part, while the inner part is mainly composed by sulphur and potassium. Some silicon was also detected close to the surface of the sample.

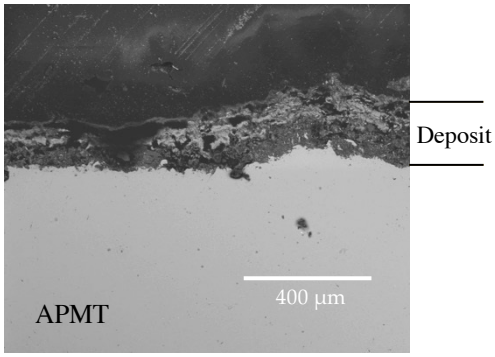

Figure 89. Backscattered SEM image of the APMT sample after 144 hours in the reference exposure

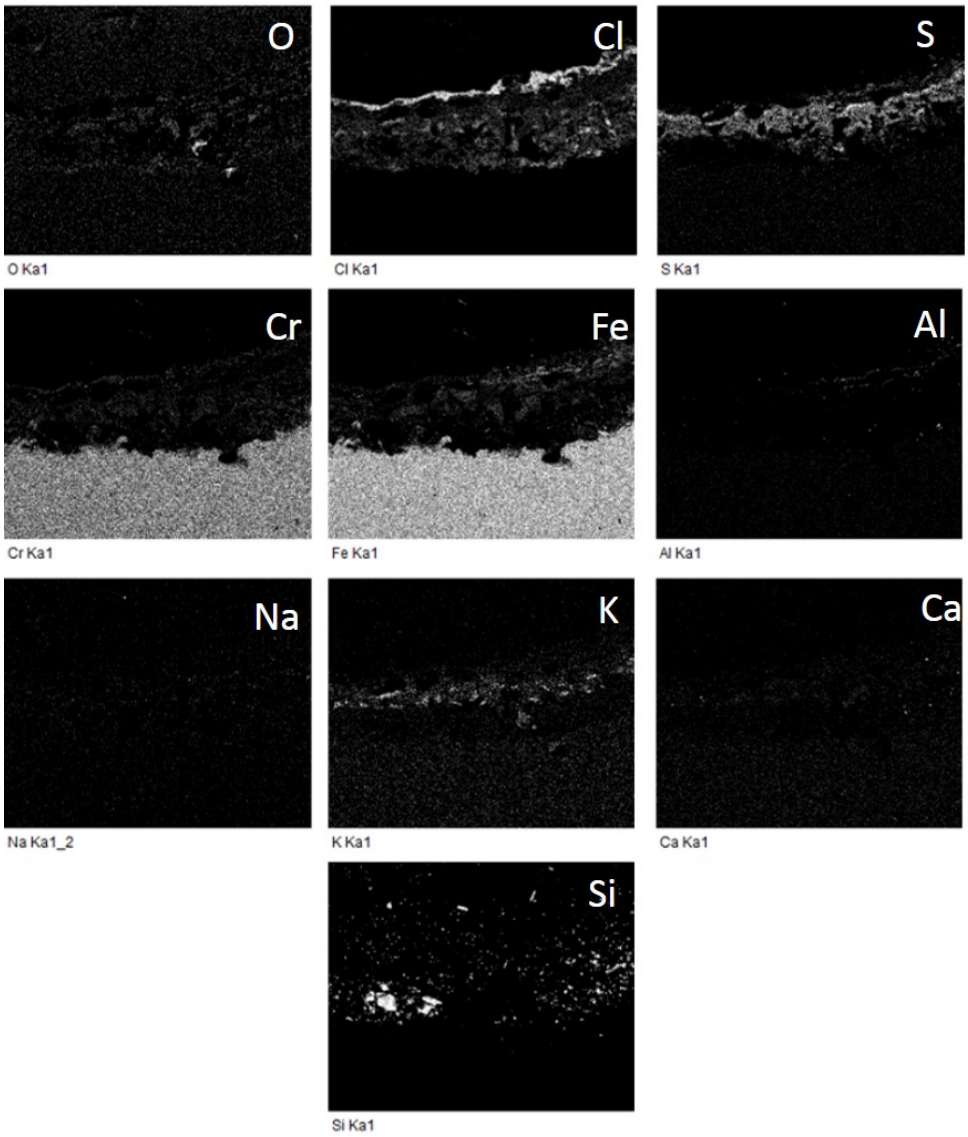

Figure 90. EDX mapping analysis of the APMT sample after 144 hours in the reference exposure

- FeCrAl model alloy, Fe10Cr3Al2Si

Figure 91 shows the FeCrAl model alloy sample (Fe10Cr3Al2Si) after 144 hours in the reference exposure. Unfortunately, the deposit and corrosion product layer spalled off after exposure and the SEM analysis was performed without the corresponding EDX analysis.

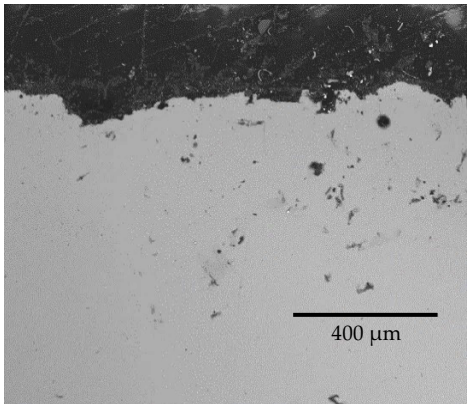

Figure 91. Backscattered SEM image of the model alloy sample after 144 hours exposure in the reference exposure

The thickness of the sample was measured before and after the exposure. The results are presented in Figure 92. The sample presents a maximum material loss of 0.30 mm in the flue gas side. The material loss is close to zero on the lee side of the sample.

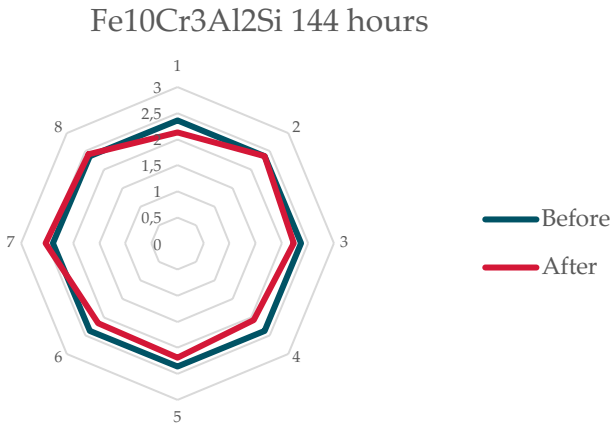

Figure 92. Thickness of the model alloy sample before (blue) and after (red) 144 hours in the reference exposure

SEM/EDX analysis on samples exposed in the ammonium sulphate exposure for 24 hours

Figure 93 shows the probe (a) before and (b) after the 24 hours exposure with ammonium sulphate addition. Both zones of the probe were set at 600 °C. The new material samples were placed in the zone closest to the tip.

(a)

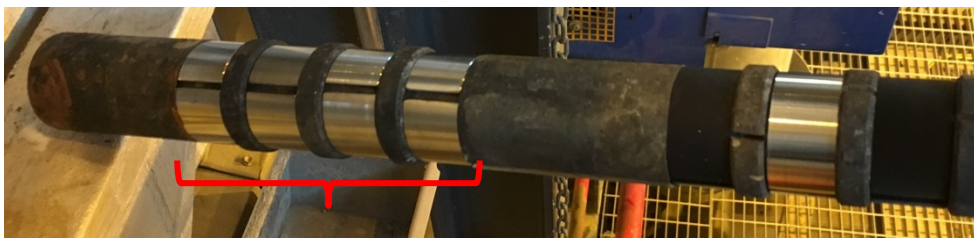

New materials

(b)

Figure 93. Probe with the samples (a) before and (b) after 144 hours exposure with ammonium sulphate addition

Due to lack of KanthalAPMT samples, the 24 hours exposure with Ammonium sulphate addition was exposed with duplicate FeCrAl model alloy samples and none KanthalAPMT sample.

After the 24 hours exposure all the samples were removed and stored in desiccators in order to preserve them until the performance of the analyses. Figure 94 shows optical images of the samples after removal from the probe.

Figure 94. Optical image of the samples after 144 hours exposure with ammonium sulphate addition

In order to study the corrosion attack of the different materials, cross-sections of the samples were prepared to SEM/EDX analysis.

- 347H

The SEM image of the cross section of the sample shows that no deposit is left but a corrosion products layer of about 90 μm thickness was still present on the sample surface, see Figure 95. The EDX analysis presented in Figure 96 shows that the corrosion products are composed by non-homogeneous chromium, nickel and iron oxides. A large amount of chlorine was also found close to the surface of the sample.

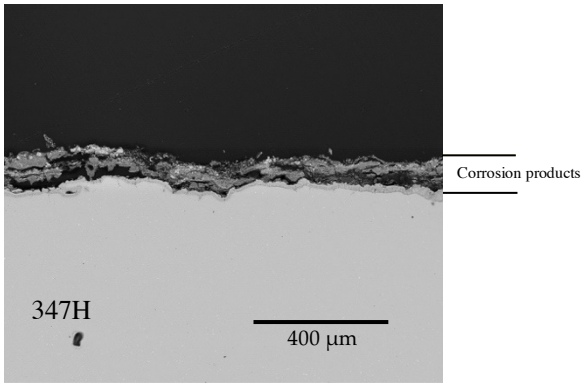

Figure 95. Backscattered SEM image of the 347H sample after 144 hours exposure with ammonium sulphate addition

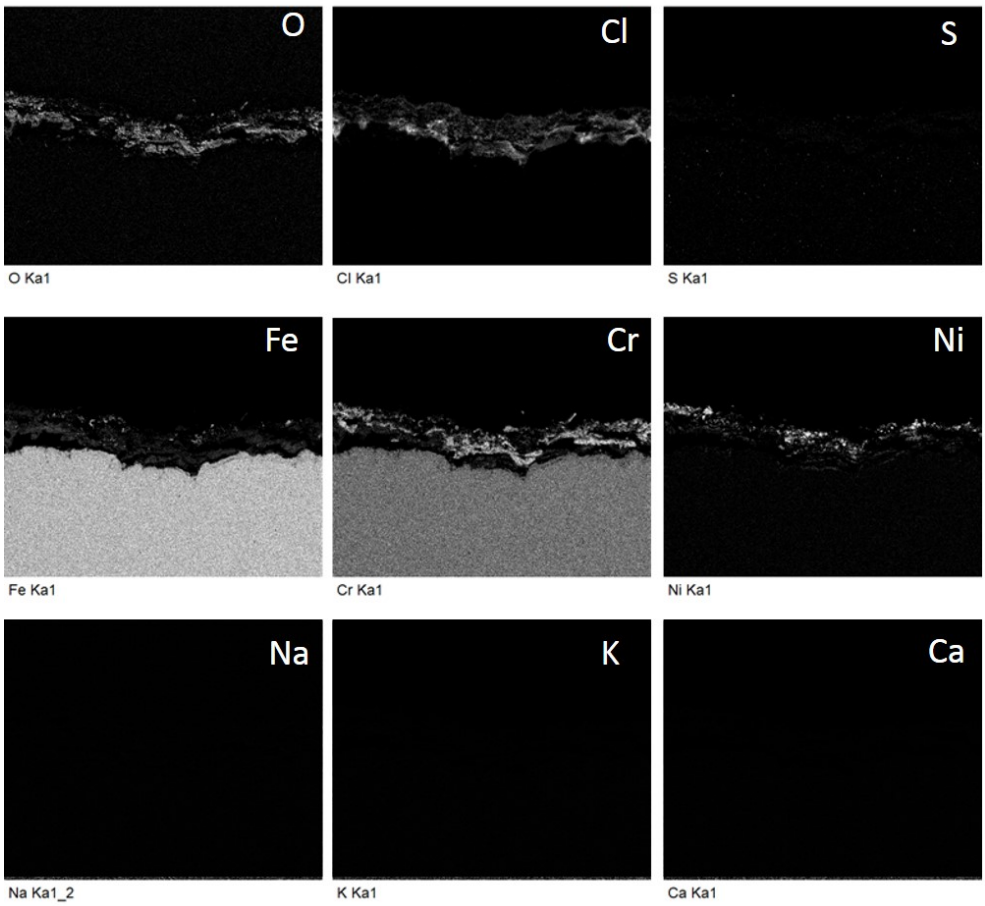

Figure 96. EDX mapping analysis of the 347H sample after 144 hours exposure with ammonium sulphate addition

- Sanicro 33

Figure 97 shows an SEM cross section of the Sanicro 33 sample after 24 hours exposure with ammonium sulphate addition. The oxide scale is composed by a non-

homogeneous inward growing chromium oxide followed by an outward growing iron-chromium oxide.

Some of the deposit formed during the exposure is present over the oxide. The EDX analysis presented in Figure 98 shows that it is composed mainly by calcium and potassium sulphates.

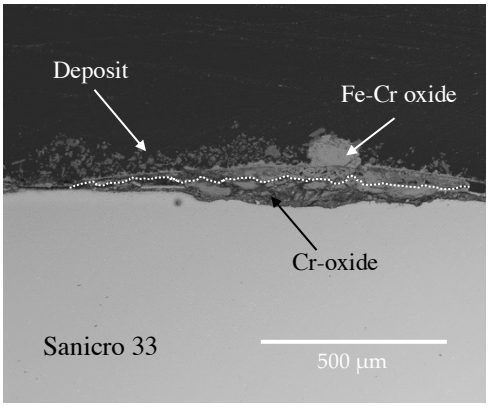

Figure 97. Backscattered SEM image of the Sanicro 33 sample after 24 hours exposure with ammonium sulphate

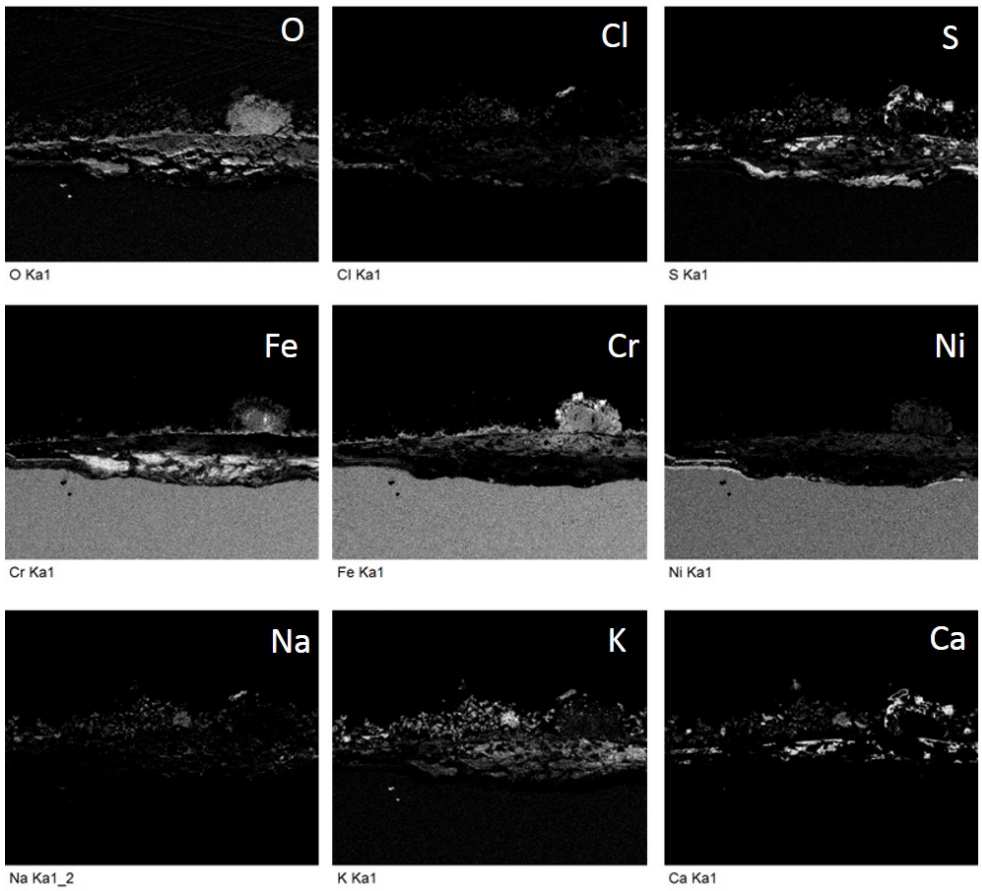

Figure 98. EDX mapping analysis of the Sanicro 33 sample after 24 hours exposure with ammonium sulphate addition

- Fe10Cr3Al2Si

Figure 99 shows the FeCrAl model alloy sample after 24 hours exposure with ammonium sulphate addition. A chromium rich oxide layer was detected all over the surface followed by an iron oxide layer on the top. As an effect of sample preparation, a gap was found between the Cr-oxide and the surface of the alloy.

The EDX maps presented in Figure 100 shows that no deposit was left after the preparation of the samples. A big amount of chlorine was detected and it penetrates all the way through the formed oxides to the surface of the sample. No sulphur was detected.

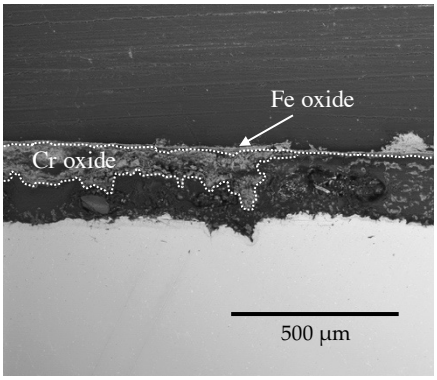

Figure 99. Backscattered SEM image of the Fe10Cr3Al2Si sample after 24 hours exposure with ammonium sulphate addition

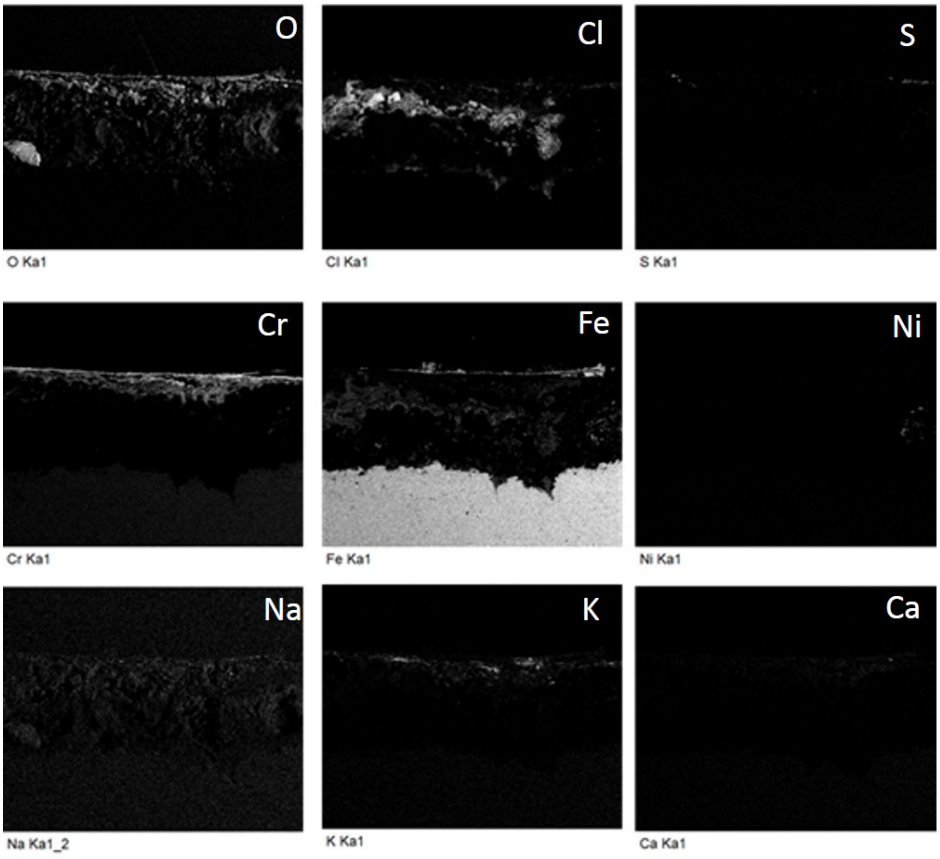

Figure 100. EDX mapping analysis of the model alloy sample after 24 hours with ammonium sulphate addition

SEM/EDX analysis on samples exposed in the ammonium sulphate exposure for 144 hours

Figure 101 shows the probe (a) before and (b) after the 144 hours exposure with ammonium sulphate addition. Both zones of the probe were set at 600 °C. The new material samples were placed in the zone closest to the tip.

(a)

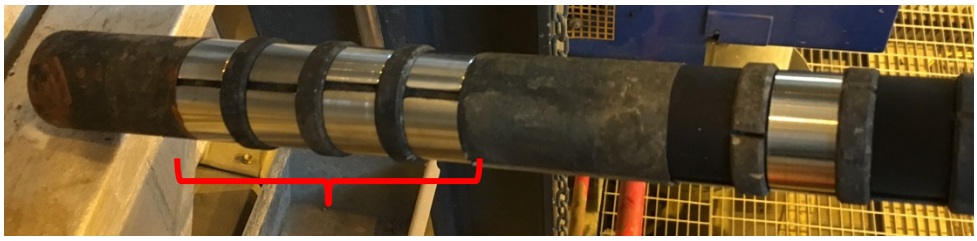

(b)

Figure 101. Probe with the samples (a) before and (b) after 144 hours with ammonium sulphate addition

The materials exposed were the same as for the reference exposures. After the 144 hours exposure all the samples were removed and stored in desiccators in order to preserve them until the performance of the analyses. Figure 102 shows an optical image of the rings after removing them from the probes.

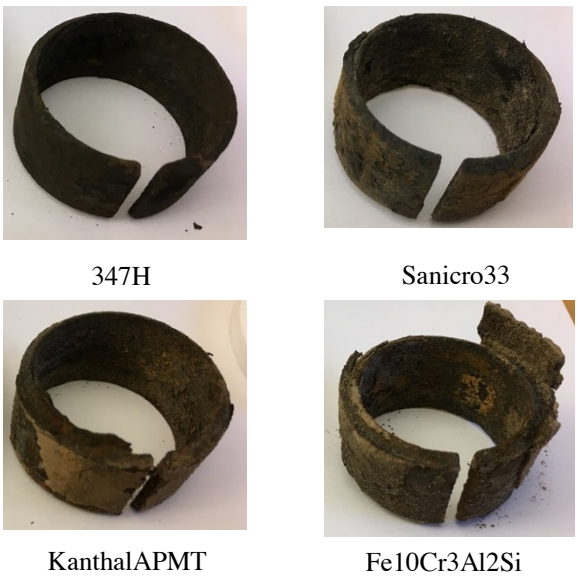

Figure 102. Optical image of the samples after 144 hours exposure with ammonium sulphate addition

In order to study the corrosion attack of the different materials, cross-sections of the samples were prepared to SEM/EDX analysis.

- 347H

The cross-section of the sample shows that no deposit is left but some of the corrosion products were still over the surface, see Figure 103. An approximately 140 μm thick iron oxide was found covering the whole surface of the sample. On the top of it, with brighter contrast, a nickel oxide can be seen followed by a chromium oxide on the very out part.

The EDX analysis presented in Figure 104 shows a very big amount of chlorine in the corrosion products, and, as it happened after the 24 hours exposure, it goes all the way through the formed oxides to the surface of the metal. No sulphur was detected.

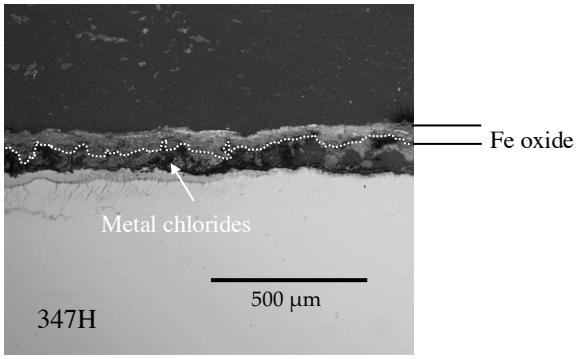

Figure 103. Backscattered SEM image of the 347H sample after 144 hours exposure with ammonium sulphate addition

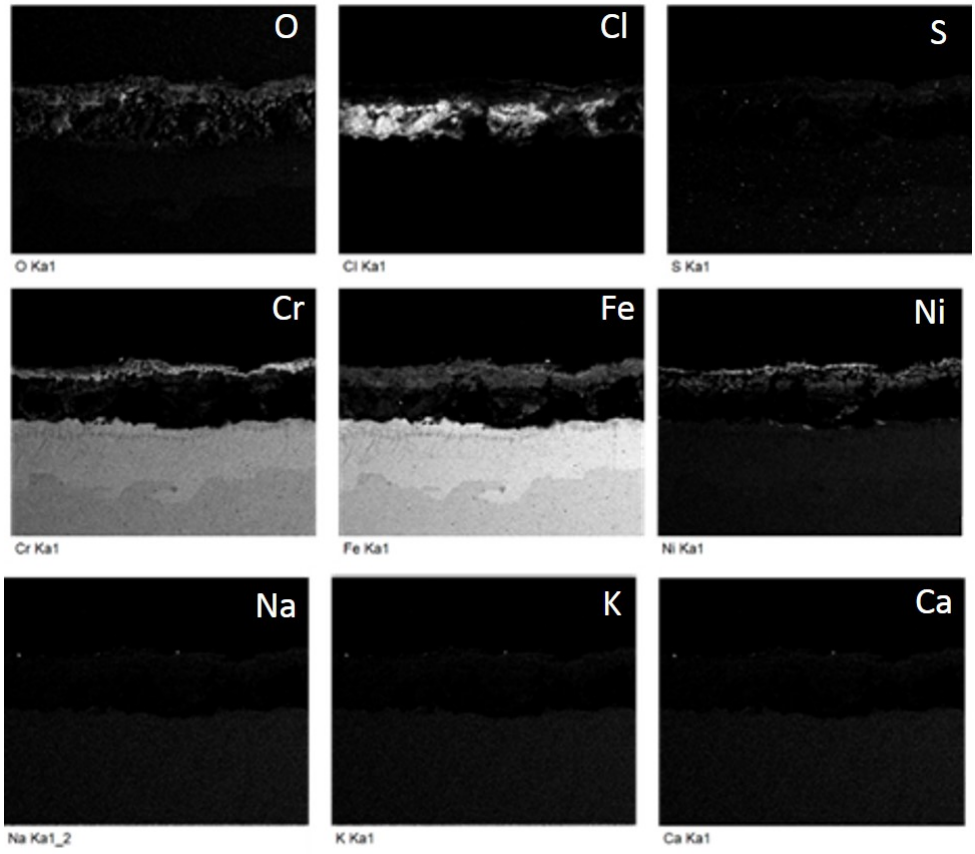

Figure 104. EDX mapping analysis of the 347H sample after 144 hours exposure with ammonium sulphate addition

The thickness of the sample was measured before and after the exposure. The results are presented in Figure 105. The sample presents a maximum material loss of 0.19 mm on the flue gas side. The material loss is close to zero on the lee side of the sample.

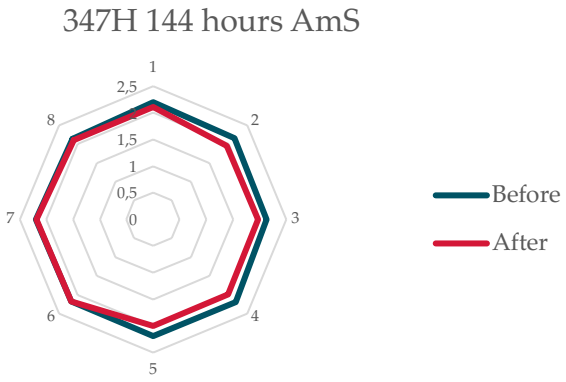

Figure 105. Thickness of the 347H sample before (blue) and after (red) 144 hours exposure with ammonium sulphate addition

- Sanicro 33

The Figure 106 shows an SEM cross section of the Sanicro 33 sample after 144 hours exposure with ammonium sulphate addition. The EDX analysis presented in Figure 107 shows that there is deposit left on the sample after the preparation which is mainly composed of sodium and potassium sulphates. An inward growing chromium oxide and an outward growing iron-rich oxide is detected covering the surface. After the 144 hours exposure, small chromium chlorides start to appear and grow under the surface of the sample.

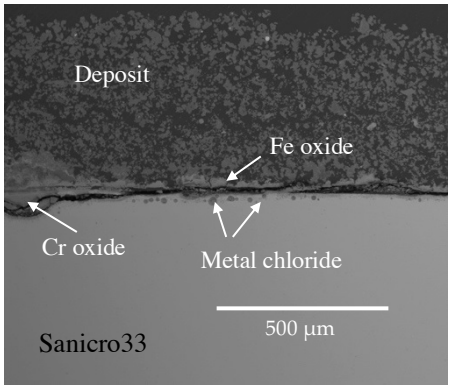

Figure 106. Backscattered SEM image of the Sanicro 33 sample after 144 hours exposure with ammonium sulphate addition

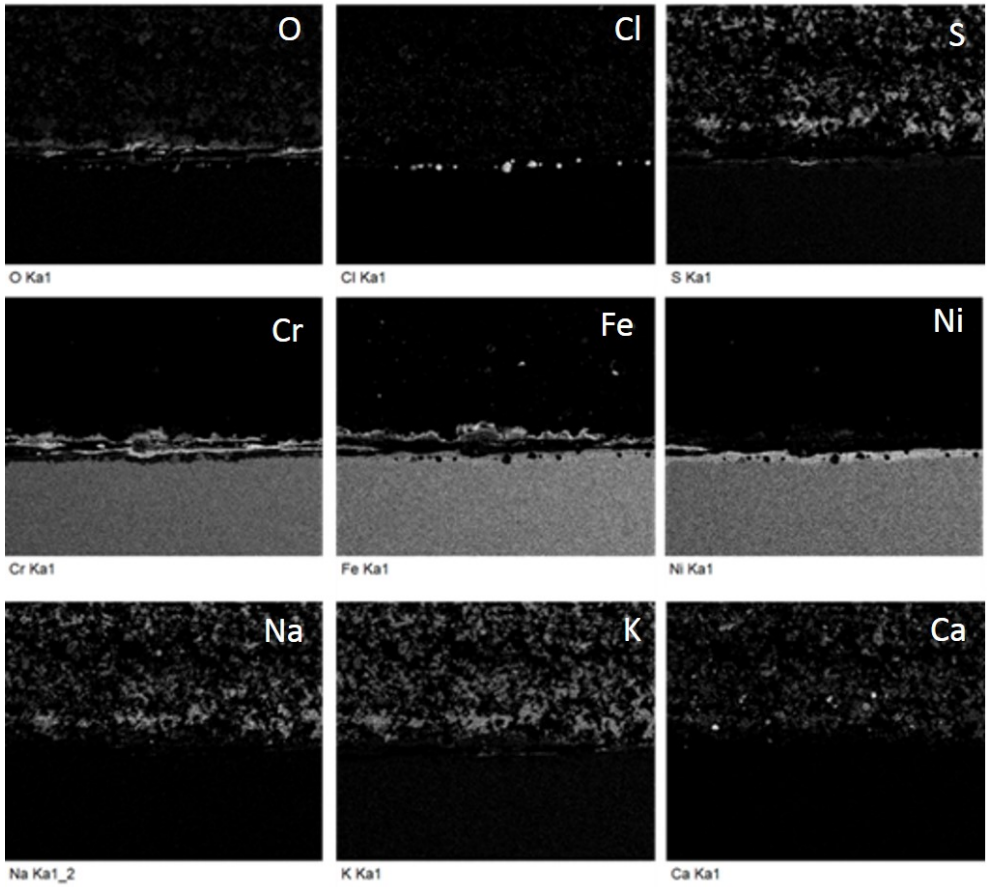

Figure 107. EDX mapping analysis of the Sanicro 33 sample after 144 hours exposure with ammonium sulphate addition

The thickness of the sample was measured before and after the exposure. The results are presented in Figure 108. The sample presents a maximum material loss of 0.31 mm in the flue gas side. The material loss is close to zero on the lee side of the sample.

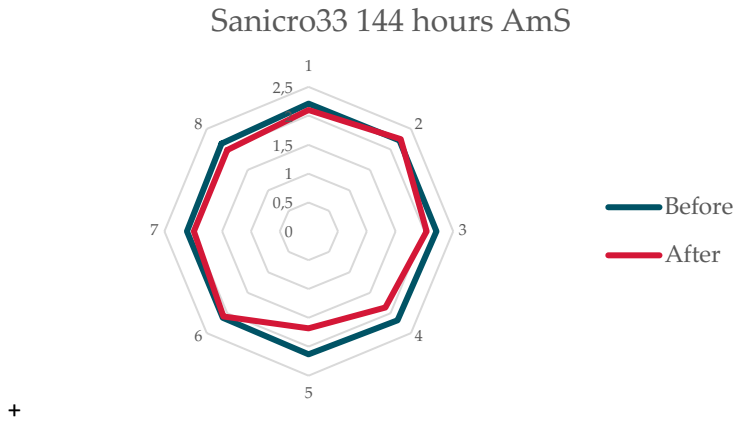

Figure 108. Thickness of the Sanicro 33 sample before (blue) and after (red) 144 hours exposure with ammonium sulphate addition

- KanthalAPMT

Figure 109 shows the KanthalAPMT sample after 144 hours exposure with ammonium sulphate addition. The EDX maps presented in Figure 110 show that nearly no deposit was present on the sample. The sample does not show any signs of corrosion. Despite this, no aluminium oxide was detected on the top of the sample. This result is in good agreement with the material loss measurements presented in Figure 111. One large alumina particle was however detected. It is suggested that this alumina containing particle originates from the deposit rather than have being formed from the alloys.

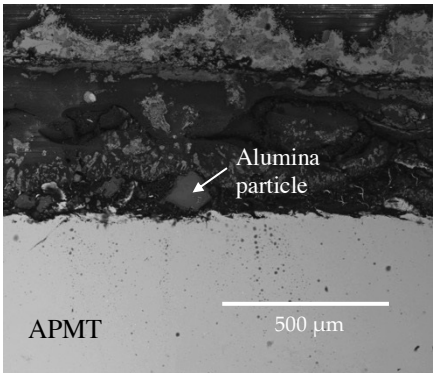

Figure 109. Backscattered SEM image of the KanthalAPMT sample after 144 hours exposure with ammonium sulphate addition

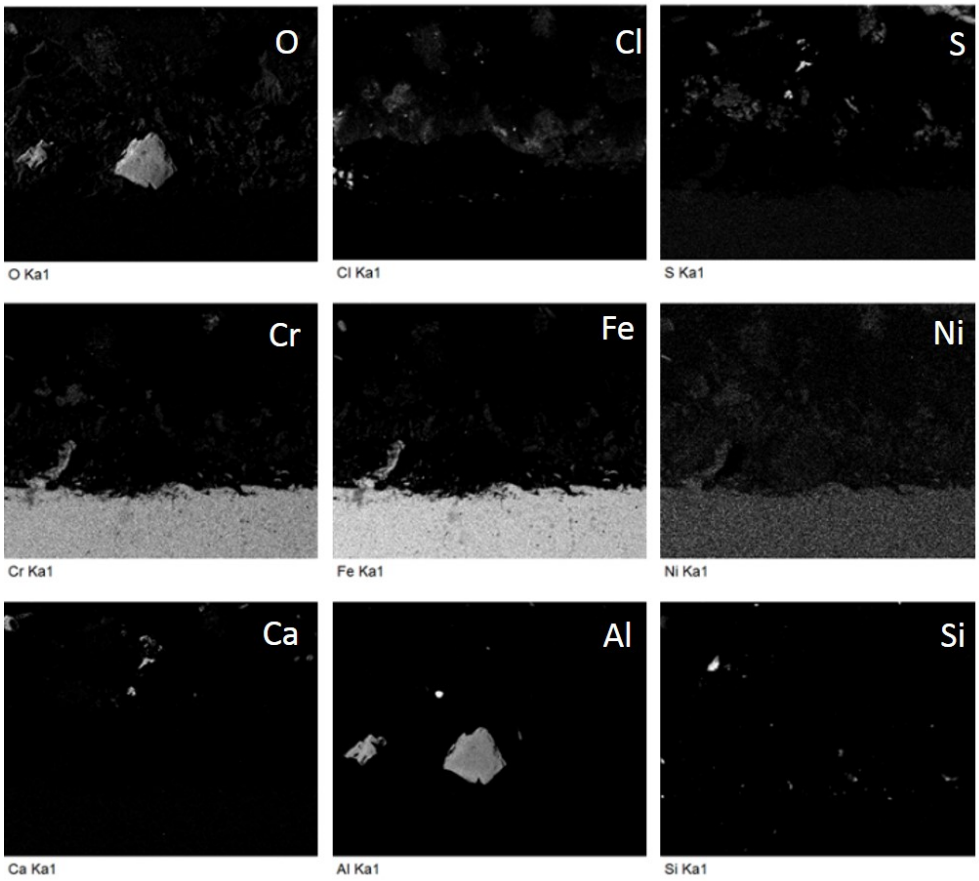

Figure 110. EDX mapping analysis of the APMT sample after 144 exposure with ammonium sulphate addition

The thickness of the sample was measured before and after the exposure. The results are presented in Figure 111. No or very little material loss was observed.

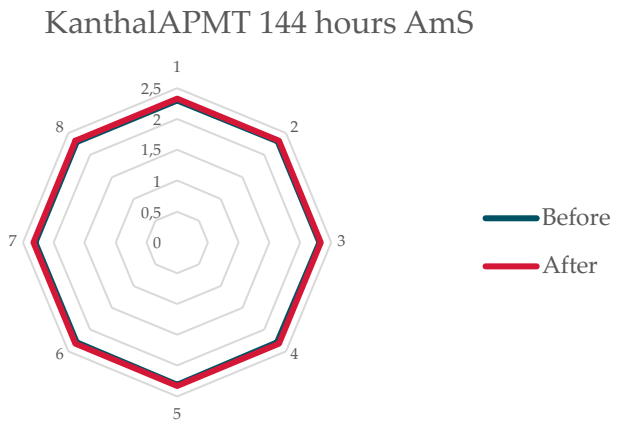

Figure 111. Thickness of the APMT sample before (blue) and after (red) 144 hours exposure with ammonium sulphate addition

- FeCrAl model alloy (Fe10Cr3Al2Si)

The Figure 112 shows the FeCrAl model alloy sample after 144 hours exposure with ammonium sulphate addition. A thick layer of more than 500 μm of corrosion products is covering the surface of the sample. The EDX maps are presented in Figure 113. The layer of corrosion products is mainly composed of chromium and chlorine with some iron oxide on the top. A heterogenous sulphur-rich layer is covering the whole sample. No deposit is present on the sample.

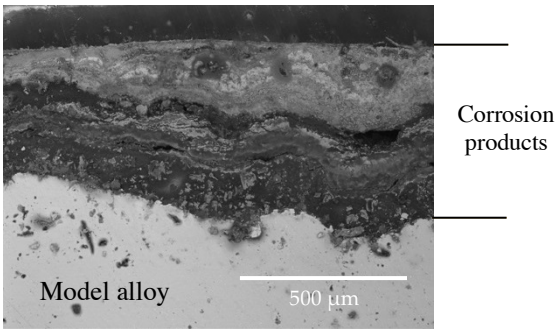

Figure 112. Backscattered SEM image of the cross section of the Fe10Cr3Al2Si sample after 144 hours exposure with ammonium sulphate addition

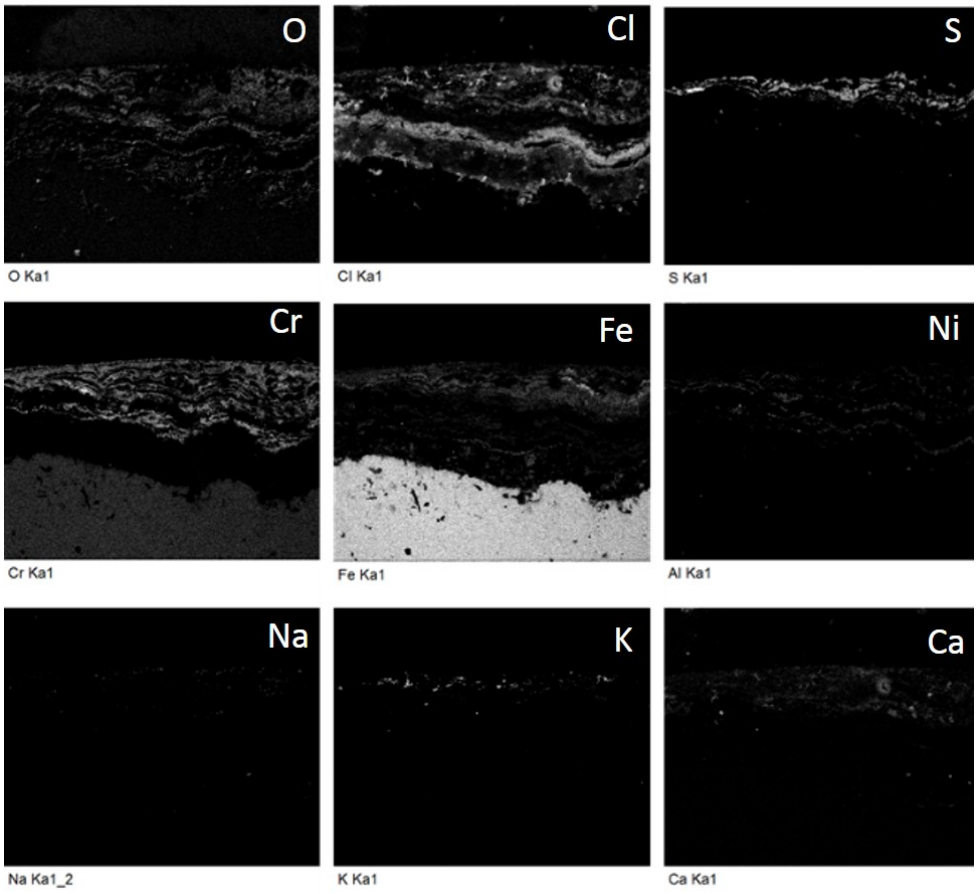

Figure 113. EDX mapping analysis of the Fe10Cr3Al2Si sample after 144 hours with ammonium sulphate addition

The thickness of the sample was measured before and after the exposure. The results are presented in Figure 114. The sample presents a maximum material loss of 0.53 mm in the flue gas side. The material loss is 0.05 mm on the lee side of the sample.

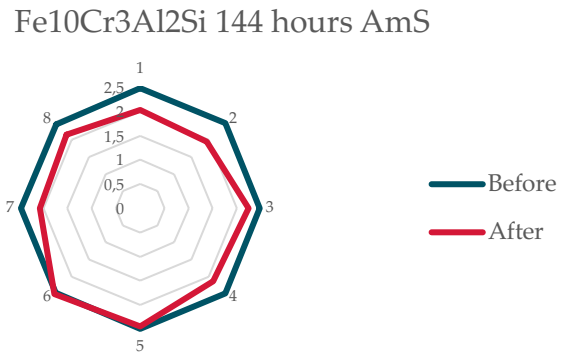

Figure 114. Thickness of the Fe10Cr3Al2Si sample before (blue) and after (red) 144 hours exposure with ammonium sulphate addition

4.4 CORROSION/CORROSIVE ENVIRONMENT PREDICTION

4.4.1 Online corrosion probe

Three test campaigns were conducted with the online corrosion probe. The probe was installed once in the horizontal pass and twice in the empty pass of Händelö P15 CFB boiler, Figure 115.

Figure 115. Online corrosion probe installed in Händelö P15 boiler empty pass during the campaign 3.

Campaign 1.

During the test period, the probe was installed in the horizontal pass of the boiler. Test was conducted in November 2013 - March 2014 and the test materials were austenitic stainless steels 347HFG and 310H. Set temperature of the probe was 360 °C (initially 350 °C). During the whole test period corrosion rates were very low (Figure 116).

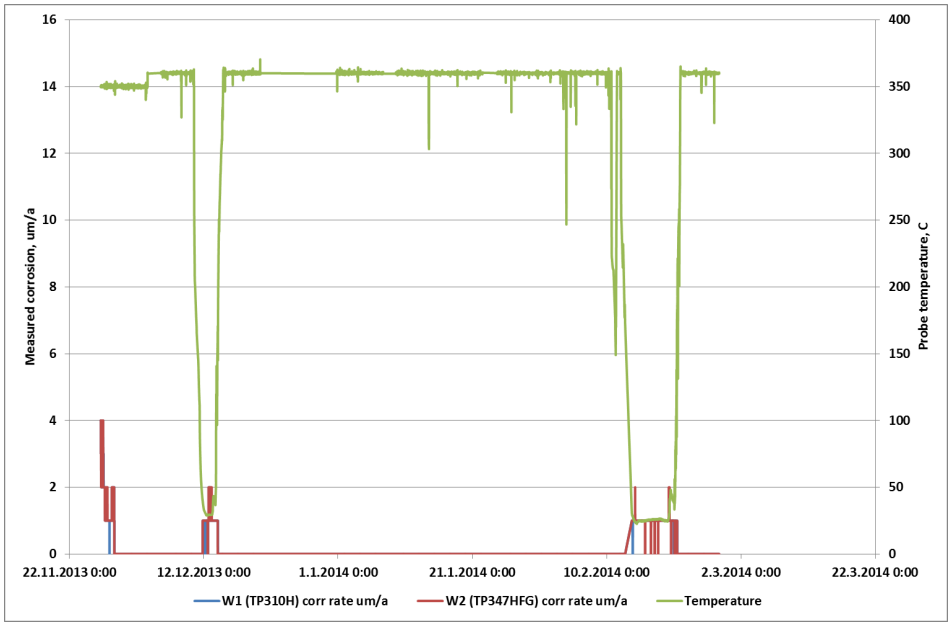

Figure 116. Measured corrosion rates were very low during the whole test campaign 1 in the horizontal pass of Händelö P15.

Also, the optical inspection of the samples did not show any signs of accelerated corrosion attack (Figure 117). The weight loss samples (Figure 118) mass change also indicated very low corrosion rates (310H, 0.003 mm/year; 347HFG, 0.008 mm/year). However, based on XRF analysis deposits that formed are corrosive - they are rich in heavy metals (Pb, Zn and Cu), alkali (Na, K) and chlorine (Table 11).

Figure 117 Online corrosion probe after the test campaign 1.

Figure 118 Exposed weight loss samples before cleaning.

wt%	Metal/deposit 310H	Metal/deposit 347HFG
Na	**1.7**	**5.8**
Mg	1.3	0.1
Al	5.4	0.2
Si	6.1	0.8
S	**7.3**	**1.7**
Cl	**8.2**	**1.8**
K	**2.3**	**0.5**
Ca	**29.9**	**1.0**
Ti	2.6	0.1
Cr	1.2	15.6
Mn	0.5	1.5
Fe	9.2	52.8
Ni	1.6	10.6
Cu	**3.8**	**1.1**
Zn	**5.5**	**3.1**
Nb	0.0	0.8
Mo	0.2	0.2
Pb	**13.2**	**2.1**
SUM	100.0	100.0

Table 11. Deposit composition analyzed with XRF.

Campaign 2.

During the test period probe was installed in the empty pass of the boiler. Test was conducted in November 2014 - September 2015 and the test materials were ferritic steel 13CrMo4-5 and austenitic stainless steel 310H. Set temperature of the probe was initially 420 °C and measured corrosion rates were very high, by reducing the probe temperature to 380 °C measured corrosion rate values became low gradually, and increased only slightly by increasing the probe temperature to 400 °C (Figure 119).

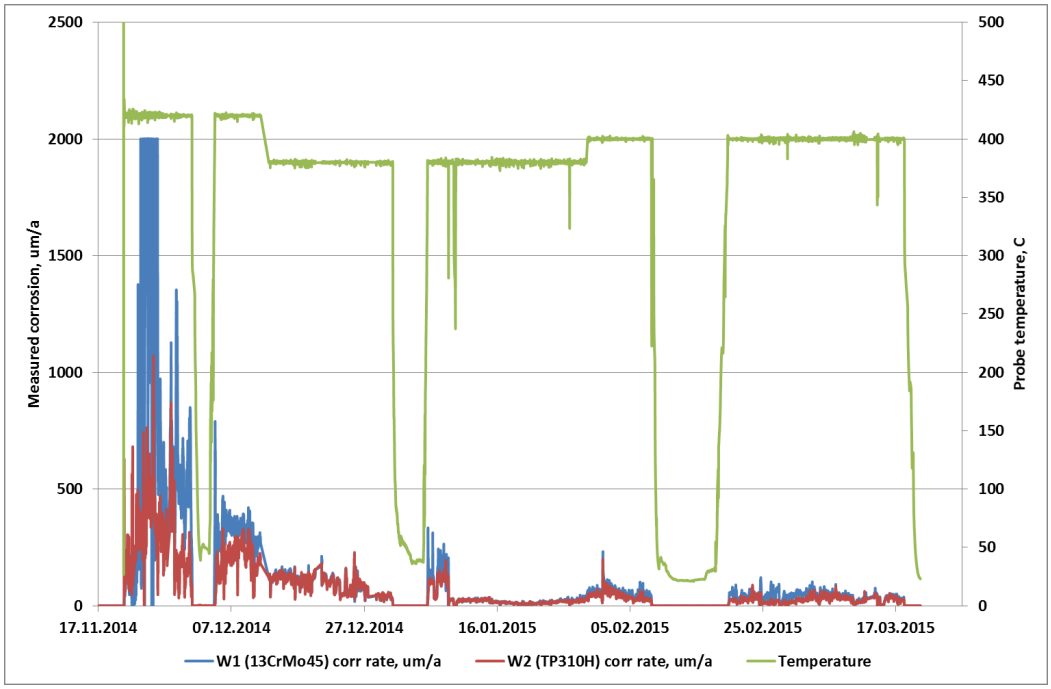

Figure 119. Very high corrosion rate values were measured in the beginning of the test campaign 2 in the empty pass of Händelö P15 - gaps in the data are due to malfunctions in remote connection.

Appearance of the probe samples after exposure is shown in Figure 120. Due to heavy corrosion, samples were partly destroyed while removed from the probe (Figure 121). Thereby, mass change was not determined. Also samples had corroded from the inside surface, therefore it was not possible to do thickness loss measurements from cross section of samples. Based on XRF analysis deposits that formed are corrosive - they are rich in heavy metals (Pb, Zn and Cu), alkali (Na, K) and chlorine (Table 12).

Figure 120. Online corrosion probe after the test campaign 2.

Figure 121. Exposed weight loss samples.

wt%	Metal/deposit 13CrMo4-5	Metal/deposit 310H	Deposit Outter surface
Na	**0.0**	**1.9**	**1.4**
Mg	0.0	0.2	2.0
Al	0.7	1.7	8.3
Si	1.2	2.4	8.7
S	**0.6**	**1.8**	**7.3**
Cl	**9.6**	**9.1**	**10.2**
K	**0.3**	**2.4**	**5.1**
Ca	**0.1**	**2.5**	**31.8**
Ti	0.0	0.2	2.5
Cr	1.1	4.0	0.5
Mn	0.5	0.4	0.6
Fe	84.4	36.0	7.8
Ni	0.1	25.2	0.8
Cu	**0.5**	**8.6**	**6.7**
Zn	**0.1**	**1.4**	**3.9**
Nb	0.0	0.0	0.0
Mo	0.5	0.4	0.0
Pb	**0.3**	**1.8**	**2.2**
SUM	100.00	100.00	100.00

Table 12. Deposit composition analyzed with XRF.

Campaign 3.

During the test period probe was installed in the empty pass of the boiler. Test was conducted in November 2016 - April 2017 and the test materials were ferritic steel 10CrMo9-10 and austenitic stainless steel 347HFG. Set temperature of the probe was 400 °C during the whole test period. Measured corrosion rates were very high in the beginning of the test campaign and gradually reduced to low level (Figure 122).

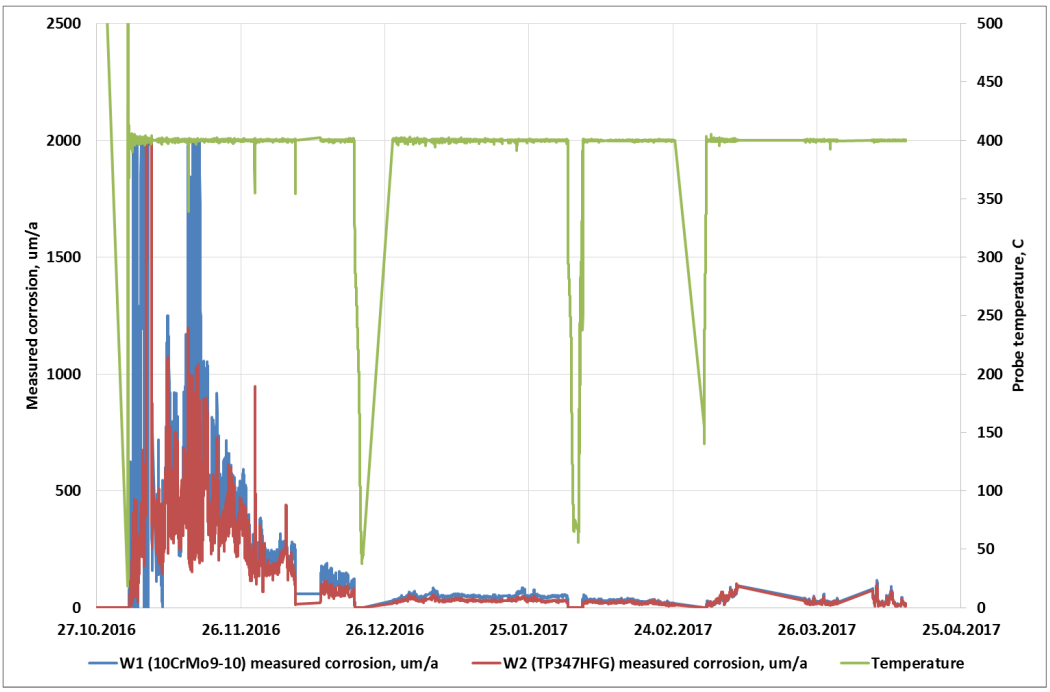

Figure 122. Very high corrosion rate values were measured in the beginning of the test campaign 3 in the empty pass of Händelö P15 - gaps in the data are due to malfunctions in remote connection.

Appearance of the probe samples after exposure is shown in Figure 123. Removed weight loss samples were partly destroyed (Figure 124) – corrosion rate based on mass loss couldn't be determined. Based on thickness measurements from cross section of samples corrosion rates were very high (10CrMo9-10, 1.34 mm/year; 347HFG, 1.02 mm/year). Deposit on the samples were XRF analyzed. Formed deposits are corrosive - they are rich in heavy metals (Pb, Zn and Cu), alkali (Na, K) and chlorine (Table 13).

Figure 123. Online corrosion probe after the test campaign 3.

Figure 124. Exposed weight loss samples.

Wt%	Metal/deposit 10CrMo9-10	Metal/deposit 347HFG	Deposit outer surface
Na	**0.0**	**0.3**	**0.4**
Mg	0.0	0.0	0.7
Al	0.6	0.8	5.3
Si	2.0	1.8	6.7
S	**0.2**	**0.4**	**4.8**
Cl	**10.2**	**10.1**	**17.4**
K	**0.1**	**4.6**	**6.3**
Ca	**0.1**	**1.0**	**40.7**
Ti	0.0	0.1	2.3
Cr	2.0	16.8	0.2
Mn	0.6	1.5	0.3
Fe	83.2	50.2	8.0
Ni	0.1	9.9	0.1
Cu	**0.2**	**0.3**	**3.9**
Zn	**0.0**	**0.1**	**2.6**
Nb	0.0	0.7	0.0
Mo	0.8	0.2	0.0
Pb	**0.0**	**1.1**	**0.3**
SUM	100.00	100.00	100.00

Table 13. Deposit composition analyzed with XRF.

4.4.2 Thermodynamical modelling and IACM measurments

Figure 125 shows the calculated concentration of the alkali chlorides (ACl) in the hot flue gas for the combustion of SWA, SWB, and AS (SWA+ Ammonium Sulphate), based on different combustion temperatures in the CFB boiler. In the case of AS, the ammonium sulphate was used as an additive for the conversion of alkali chlorides in the flue gas to sulphates. For the simulation of the AS combustion case, the amount of the ammonium sulphate injected into the flue gas of the CFB boiler was recalculated (5.547 g/Kg solid waste) and subsequently used as input data together with the SWA. According to the logged data, the average combustion temperature in the furnace of the CFB boiler is approximately 860 °C. Figure 126 shows the calculated ACl in the hot flue gas leaving the furnace for the different combustion cases of SWA, SWB, and AS at 860 °C.

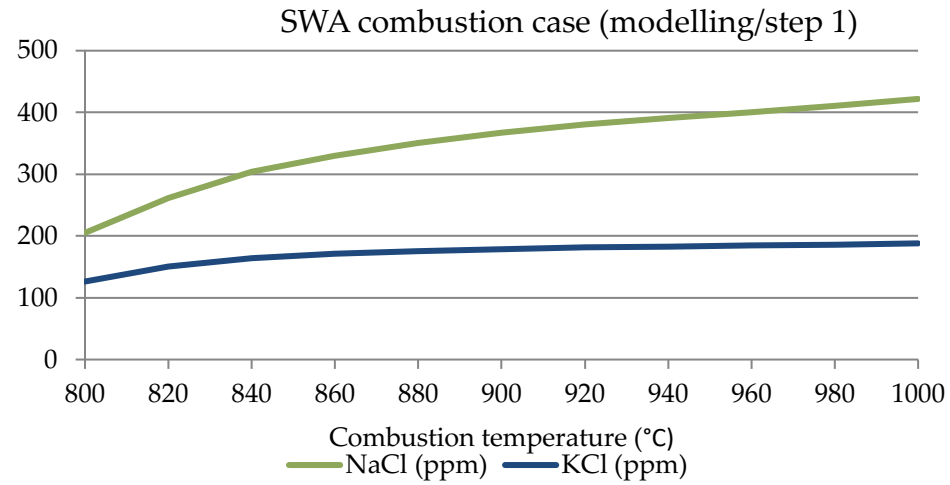

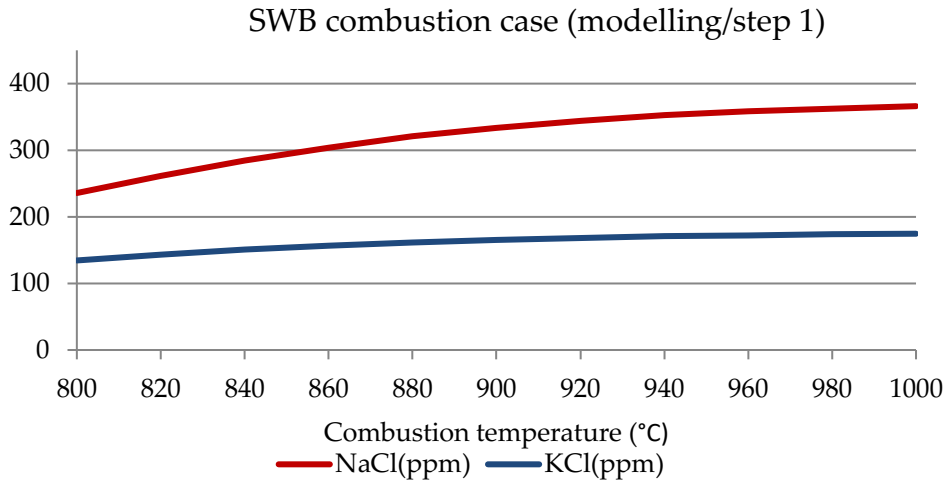

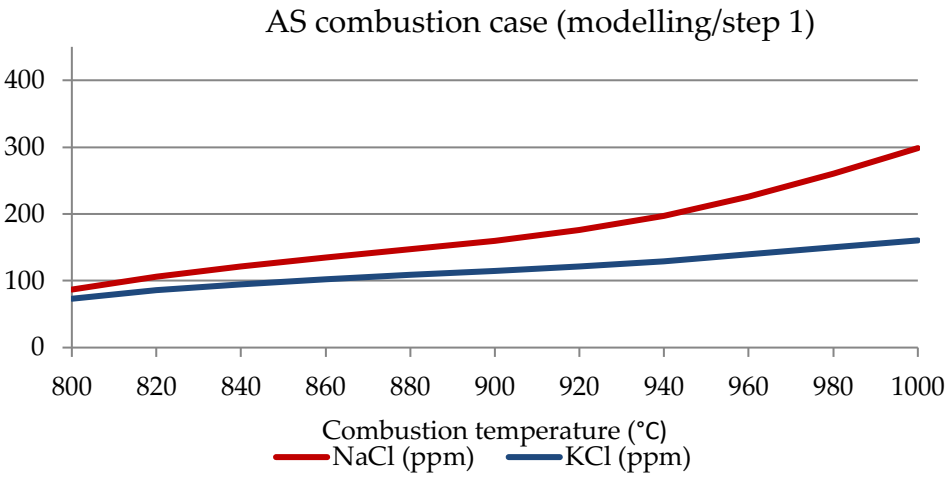

Figure 125. The calculated concentration of the alkali chlorides in the hot flue gas for the SWA, SWB, and AS (SWA+ Ammonium Sulphate) combustion cases, based on different combustion temperatures in the CFB boiler

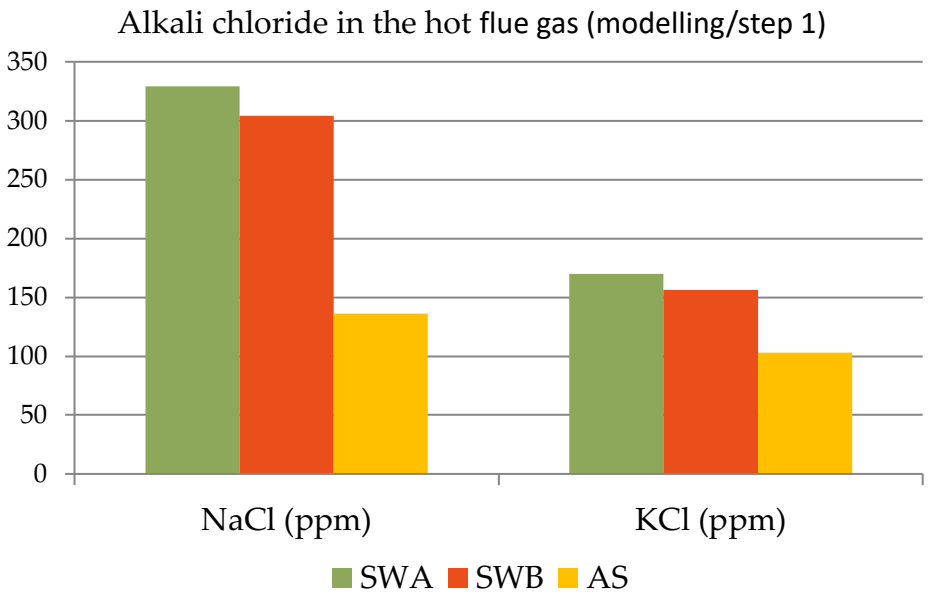

Figure 126. The calculated concentration of the alkali chlorides in the hot flue gas leaving the furnace for the SWA, SWB, and AS (SWA+ Ammonium Sulphate) at 860 °C combustion temperature

The modelling results for the combustion of the SWA and SWB, see Figure 127 indicate that the concentration of the ACl in the flue gas could be affected to some extent as a result of variations in the chemical composition of the solid waste. The most significant change, however, could be seen for the AS case, where the addition of the ammonium sulphate to the flue gas decreased the NaCl(g) concentration from 329 ppm to 136 ppm, and the KCl(g) from 170 ppm to 103 ppm. Furthermore, the modelling results in Figure 125 indicate that the combustion temperature is an important factor which determines the concentration of the ACl, particularly NaCl(g).

Step 2 of the equilibrium calculations (see Figure 18) evaluates the condensation behavior of the generated hot flue gas and calculates the concentration of ACl at lower temperatures prior to the superheater. The calculated flue gas composition (step 1) was used as input for the step 2 of the equilibrium calculations. Little is known about the condensation in the NaCl-KCl system and interaction between the two salts. A study conducted by Broström et al. [14] indicated that the gaseous KCl and NaCl at low concentrations condensed homogeneously with little interaction (i.e. not much solid solution was found in the deposit), and that solid solution was probably formed in a secondary process by sintering of solid NaCl and KCl. Therefore, the same approach was considered for the modelling of the condensation of the ACl in the flue gas, and it was assumed that the NaCl(g) and KCl(g) condense as separate phases (e.g. NaCl(s) and KCl(s)) rather than formation of alkali salt solutions. Figure 127 shows the concentration of alkali chlorides in the flue gas as the hot flue gas was cooled down from 900 °C to 700 °C.

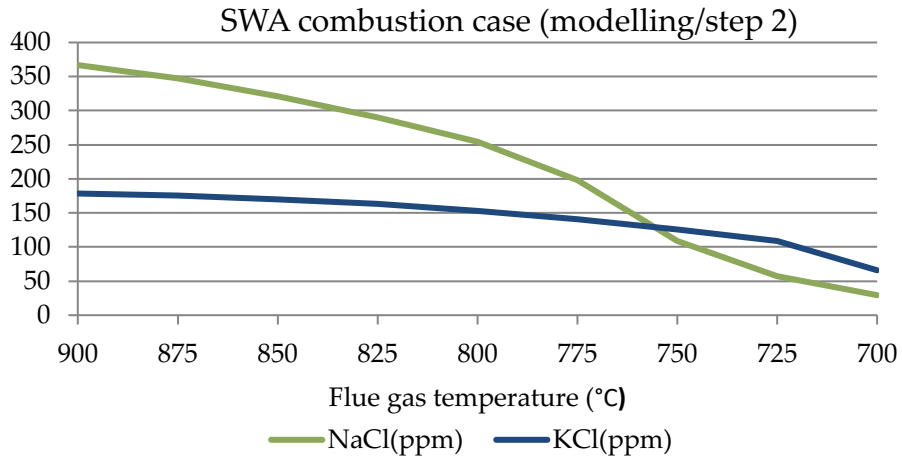

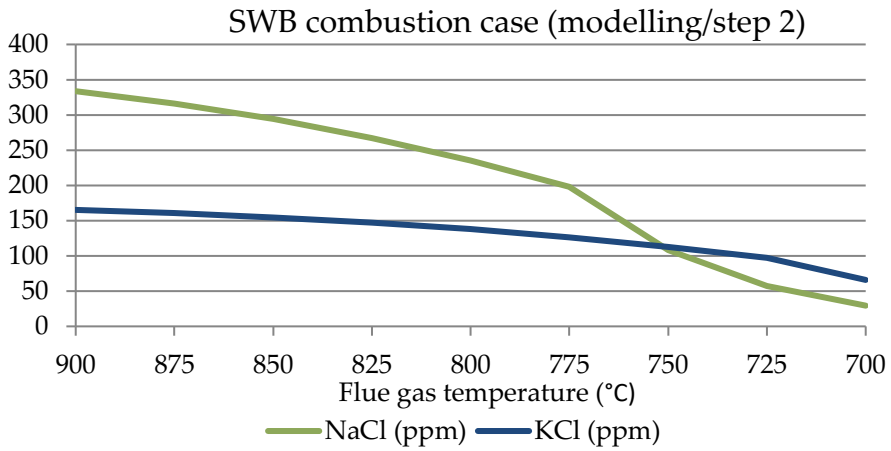

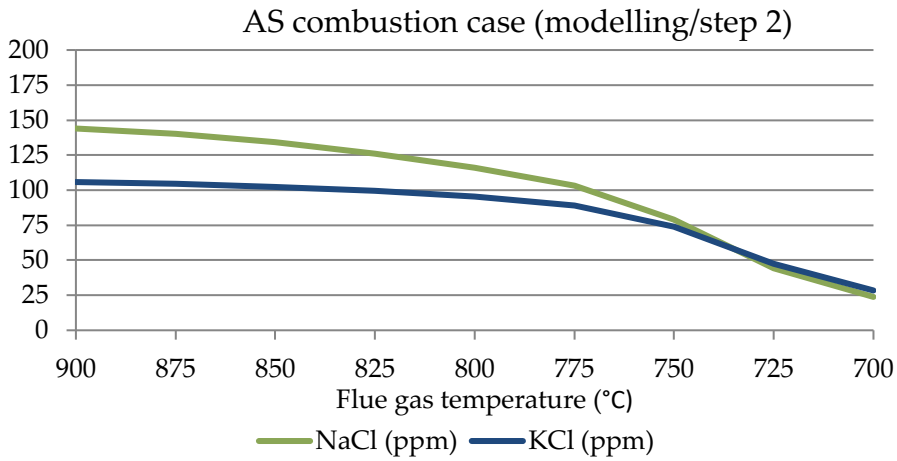

Figure 127. The calculated concentration of alkali chlorides in the flue gas cooled down from 900 °C to 700 °C for the SWA, SWB, and AS (SWA+ Ammonium Sulphate) combustion cases

The online alkali chloride monitoring (IACM) data obtained during the full-scale measurements were used to estimate the reliability of the modelling results. Figure 128 shows the concentration of the ACl in the flue gas at 750 °C which were measured by the IACM (the average amount) and also calculated by the predictive

model. Comparing the IACM data with the modelling results, a fairly good agreement is found between the similar combustion cases. For example, there is a reasonable correlation between the IACM data for the combustion of the solid waste without the additive (SW) and the modelling results for the SWA and SWB. The same is true when comparing the IACM data for the case of ammonium sulphate added into the flue gas (AS) and the modelling results for the AS case. Note that the IACM data presented in Figure 128 are the average data from a relatively long period of measurements, while the modelling results show the ACl in the flue gas for a specified combustion condition including stable fuel composition and combustion temperature. Therefore, the variations in the fuel composition and the operating parameters, as well as certain limitations of the thermodynamic equilibrium models such as the kinetics of the reactions, physical processes, and solid-gas reactions should be taken into account when comparing the IACM data with the modelling results.

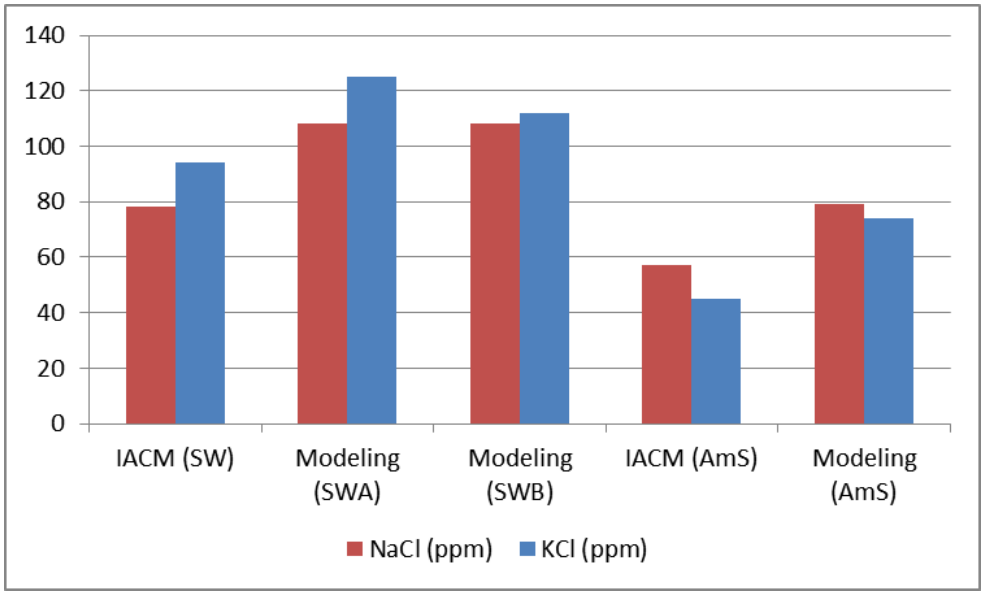

Figure 128. Concentration of the alkali chlorides in the flue gas at 750 °C, measured by the IACM and calculated by the predictive model for the combustion of the solid waste without the additive (SW, SWA, SWB) and also when ammonium sulphate (AS) used as additive

5 Analysis of the results

The background and aim to these two projects have been to perform a wide material testing matrix in two boilers designed with a horizontal pass superheater region. These two boilers have been burning biomass (including waste wood) and waste, respectively. The material matrix has included conventional steels used today as well as newly developed stainless steels, FeCrAl model alloys as well as two different types of thermally sprayed coatings, namely HVOF and HVAF sprayed coatings. Furthermore, the effect of increased fractions of waste wood has been studied, going from 40% to 45%.

These have also been evaluating different corrosion testing and prediction techniques. This has included both short term and long term testing. The short term testing has been focussing on comparing IACM (Online Alkali Chloride Monitor) results with a thermodynamical model as well as an online corrosion probe. The results of these techniques have been compared to air-cooled probe samples exposed for up to 144 hours. The long term testing has been conducted by the novel clamp technique. The corrosion data of these clamps has been evaluated against simultaneously exposed test tubes.

The different tasks presented above have all been targeting superheater corrosion. However, one of the aims was also to investigate how the increased fraction of waste wood in the fuel mix was affecting the corrosion attack of the water walls. Due to safety issues during the startup of the water wall probe exposure, the project have not been able to fulfil this aim.

Below, the different aspects/tasks included in these two projects will be analyzed in a more comprehensive and detailed way:

- Long term corrosion testing
    - Corrosion performance of several materials
    - Comparison between the two boilers
    - Comparison between clamps and tubes
- Short term corrosion testing
    - Corrosion testing and prediction techniques
        - IACM
        - Thermodynamical modelling
        - Online corrosion probe
    - Corrosion performance of new materials
    - The effect of chlorine penetration through oxide scales

5.1 LONG TERM CORROSION TESTING

5.1.1 Corrosion performance of several materials in two boilers

The material matrix within these two projects spans from commercial low alloyed steels and stainless steels to FeCrAl model alloys. The long term testing of the materials have been performed primarily by clamp exposures. However, exposures of test tubes have also been performed in the P15 Händelö boiler. The main aim with the test tube exposures was to evaluate them against the clamp exposures in order verify that the novel clamp technique showed relevant material loss data.

The two boilers utilized within these projects have been the waste fired boiler P15 Händelö operated by E.ON, Norrköping and the biomass fired boiler Örtoftaverket operated by Kraftringen, Lund. Both these boilers are equipped by a horizontal pass superheater region. A major difference between the boilers, apart from the fuel mix, is the lack of an empty pass in the Örtofta boiler. The fuel mix in the waste fired P15 Händelöboiler has been 50% household waste and 50% industrial waste. In the biomass fired Örtoftaboiler the fuel mix consisted of forest residues (25-28%), waste wood (40-45%), Peat (8%), sawdust (11-17%) and Bark (8-11%). The long term corrosion was evaluated by the novel technique denoted clamp corrosion testing. The name refers to the samples being "clamped" on top of the permanently installed superheater tube.

The material temperatures of the clamp samples are designed to be following the underlying superheater tube upon of which the sample is clamped on. Thus, the material temperature of the clamp samples has primarily been dictated by which position in the superheater bundle the clamp has been mounted on. As far as possible, the clamps mounted in the Örtofta boiler has been positioned in such way that a similar temperature has been achieved as in the P15 Händelö boiler. However, also other aspects, such as e.g. accessibility, are needed to be taken into account.

According to the material loss data presented in the 4.2.1 section, the superheater region in the waste fired boiler (P15 Händelö) is slightly less corrosive compared to the similar position in the biomass fired Örtofta boiler. After about one year of exposure in the waste fired boiler, the material loss was 0.03 – 0.15 mm/year (depending on the position) for 16Mo3 compared to the corresponding sample in the biomass fired boiler where the material loss was 0.32 – 0.45 mm/year (depending on the position). However, the material temperature of the samples has differed somewhat, being 360 - 380 °C for the waste fired P15 boiler and 450 – 505 °C for the biomass fired Örtoftaverket boiler. The higher material loss for the Örtoftaverket boiler was also true for several other materials, primarily low alloyed steels. The stainless steels (including thermally sprayed coatings) in the biomass fired boiler with 40% waste wood exhibited similar low corrosion rate as in the waste fired boiler. When the waste wood fraction increased to 45% there were some increase in corrosion rate also for some of the more high alloyed steels.

The reason(s) for the higher material wastage in the biomass fired Örtoftaverket boiler compared to the waste fired P15 Händelöboiler is suggested to primarily be an effect of higher material temperature and the lack of an empty pass, which exposes the samples towards a more corrosive environment.

5.1.2 Comparison between clamps and tubes

In order to evaluate the long term behaviour of superheater tubes, sections of test tubes were welded into the permanently installed superheater bundle. The aim was also to evaluate the corrosion of these tubes with the corresponding clamp exposures so that this novel corrosion evaluating technique could be assessed. The benefit of performing clamp testing, instead of installation of test tubes, is primarily driven from a cost and risk perspective. By avoiding any changes to the pressure bearing superheater tubes, and instead clamping on the test samples on top of the tubes, the risk of a superheater tube failure is actually decreased. The clamp sample may be regarded as tube shield. However, as the test is not risking tube failure, also lower graded materials can be tested and evaluated. Thereby, this novel clamp testing technique can also be used to evaluate cheaper materials. This could also be done performing probe exposures. However, the advantage by clamp exposures is that long term exposures are more feasible. Compared to probe exposures, the exposure time can easily be extended for several years, given that the material is lost due to corrosion. The drawback with clamp exposures is obviously the opposite, if the aim is to study the initiation of the corrosion attack and fast results are needed, probe exposures are the best choice.

The material loss determination of the test tubes compared to the corresponding clamp samples showed similar corrosion rates. For both testing techniques, the SH1b tube section exhibited the highest corrosion rates. The corrosion rates were, however, generally low. Even though there were (small) individual differences between clamp samples and corresponding tube samples it is safe to conclude that the clamp testing technique shows relevant corrosion rates. Thus, this technique can be used for evaluating potential superheater corrosion, without the need of making invasive changes to the pressure-bearing tubes.

5.2 SHORT TERM CORROSION TESTING

In complement to the long term testing also short term corrosion testing have been performed within these two projects. The overall purpose of probe exposures is the same as for long term testing (e.g. by clamp exposures) to evaluate the extent of the corrosion and thereafter optimize material selection and/or mitigate the corrosive environment. It should be noted that the corrosion rates obtained through short term exposures are usually not optimal in predicting the corrosion rate over time. However, short term exposures possesses often more options in testing out a wider range of exposures conditions and/or material matrix. Furthermore, the results from the short term testing are, by definition, faster compared to long term testing.

5.2.1 Corrosion testing and prediction techniques

Thermodynamical modelling and IACM

Both these techniques aim at revealing the amount of gaseous alkali chlorides in the flue gas. Knowing the fraction of alkali chlorides in the flue gas may provide important information about the expected corrosion rate. The use of IACM to measure gasoues alkali chlorides in connection to corrosion has been presented earlier [15, 16]. The developed model proved to be a reliable calculation tool to estimate the concentration of the alkali chlorides in the flue gas of the CFB boiler, based on the chemical composition of the fuel mix and additives, as well as combustion temperature in the boiler. According to the modelling results, the chemical composition of the fuel mix, addition of the ammonium sulphate to the flue gas, as well as combustion temperature are important factors, determining the concentration of alkali chlorides in the flue gas. The model can be implemented as a first indication to assess the concentration of alkali chlorides in the CFB boiler.

Online corrosion probe

The online corrosion probe was installed in the waste fired P15 Händelö boiler for three different campaigns. The first campaign was performed in the superheater region with a material temperature of 360 °C. In similarity to the clamp exposures, the corrosion rate measured on the online corrosion probe was negligible (310H and 347HFG were exposed). The two other campaigns were performed in the empty pass, similar to the short term corrosion probes. In this position, the corrosion rate was higher, especially in the beginning of the exposure. This was in line with the results from the traditional corrosion probes, which also revealed an accelerated corrosion attack started directly when the probe was inserted to the boiler. The deposit analysis did also comply well, the deposit was rich in e.g. alkali chlorides.

The last online corrosion probe campaign was ongoing during the period of time when ammonium sulphate was added to the boiler environment. According to the corrosion results, there were a decrease in corrosion rate after which the ammonium sulphate was added to the boiler. However, it is hard to conclude that this decrease is directly related to the sulphate addition since the corrosion data from the second campaign, where no ammonium sulphate was added, show similar behaviour. The online corrosion probe shows promising results in order to be able to monitor the corrosion online. However, more work is needed to better correlate the momentary corrosion rate to the actual corrosion or remaining material thickness of heat exchangers that the online probe is aimed at monitoring.

5.2.2 Corrosion performance of new materials

The short term corrosion testing included also the evaluation of two materials that has recently been developed or only as model alloys. These two alloys were the stainless steel Sanicro33, which were compared with the more conventional 347H, and the FeCrAl model alloy Fe10Cr3Al2Si, which were compared with the alumina forming Kanthal APMT. The Sanicro33 is a newly developed high alloyed austenitic heat resistant stainless steel. It is designed for having both high creep strength and high corrosion resistance. The grade is targeted for use in superheaters/reheaters in boilers in which more corrosive fuels are used. The FeCrAl model alloy has a composition of Fe (bal), Cr (10%), Al (3%), Si (2%) with the addition of reactive elements (RE's). This alloy has also been exposed in the KME709 project. The aim is to design a FeCrAl alloy for a lower temperature regime compared to e.g. Kanthal APMT.

According to the material loss measurements, the newly developed Sanicro33 exhibited a similar corrosion rate as 347H in the reference exposure whereas the corrosion was slightly higher for Sanicro 33 in the Ammonium Sulphate exposure. However, both materials suffered in this corrosive environment (in the empty pass) and high material temperature (600 °C), which were shown by cross sectional SEM/EDX analysis.

5.2.3 The effect of chlorine penetration through oxide scales

This part of this study has been conducted in such way that the results can be compared to results obtained in laboratory exposure in an HTC funded project. By this combinatory setup we aim to test if the observed results and stipulated conclusions in the laboratory setting are relevant towards the corrosive environment in a waste fired commercial boiler. The main aim of this part is to increase our knowledge about the diffusion/penetration of chlorine through different oxide layers on steels. The formation of metal chlorides in the steel/oxide scale interface is often seen for both field and laboratory exposed samples. However, it is still unclear how this chlorine is able to diffuse through the corrosion product layer. The long term aim is to be able to mitigate this type of corrosion attack by improving the materials so that the diffusion of chlorine species is hindered. In the adjacent HTC project, we have obtained results indicating that the properties of the formed corrosion product layer play an important role of the further chlorine induced corrosion attack. For instance, it has been shown, that the resulting corrosion product layer of stainless steels exposed to alkali rich environments may initially act as a barrier for alkali chloride induced corrosion [17]. However, in the laboratory setting, the corrosive load (i.e. amount of alkali chlorides, gas velocities, other deposit components, etc.) has been rather low. With this study, we have aimed to investigate how this preformed corrosion product layer is able to withstand the corrosion attack when the corrosive environment is much more harsh, i.e. in a waste fired boiler.

To summarize the results, there seems to be an initial effect of the preformed oxide in decreasing the inward diffusion of chlorine, even though the corrosion load is much higher. The samples without pre-oxidation exhibited a slightly more accelerated corrosion attack and a thicker chlorine enriched corrosion product layer compared to the samples that had a corrosion product layer on top of the surface prior to the boiler exposure. However, the corrosion attack was in general very fast, regardless of how the samples were pre-treated. Steel grain boundary attacks could be noted for both types of samples.

5.2.4 The effect of startup sequence of probe exposures

The main scope of this part of the project was to investigate how the startup sequence of probe exposures was affecting the initial stages of deposit formation and corrosion during exposure. In order to address this, probe samples with different startup sequences, were exposed simultaneously in the waste fired boiler P15, Händelö. The probe samples were started from cold/room temperature probe, preheated probe and preheated probe using pre-oxidized samples, respectively. By this matrix setup, the transient period, i.e. the time until the probe reaches its intended material temperature, was addressed. By preheating the probe above 100 °C, the aim was to avoid condensation of a thin water film on the probe sample surface and thereby also dissolving HCl (g) and other gaseous species in the water film. The HCl level in the boiler was about 200 ppm with the fuel mix used during the exposure. The pre-heating to 100 °C is not expected to form a protective oxide scale, which usually is the intention when pre-heating at higher temperatures.

There are, however, only minor differences between the cold samples and the preheated samples. In both cases, the Sanicro 28 samples exhibits accelerated corrosion attack and already after 2 hours the corrosion product layer is up to 100 µm in thickness. The corrosion attack is also attributed by the formation of metal chlorides and poor adherence of corrosion product layer and deposit layer. The composition of the deposit layer was dominated by CaSO4, KCl and NaCl, regardless if the samples were preheated or not.

The results imply that the initial stages of exposure in a waste fired boiler can be rather aggressive. Regardless of preheating or preoxidizing the sample probe the corrosion attack is still very fast leading to thick oxide scales and formation of metal chlorides resulting in poor scale adhesion. By preheating and preoxidizing, the attack as well as the amount of metal chlorides was decreased slightly. Thus, the startup sequence seems to have a minor effect on the initial stages of exposure.

6 Conclusions

These two projects presented in this report have successfully conducted a number of corrosion tests in two commercially operated boilers; the biomass and waste wood fired boiler at Örtoftaverket and the waste fired P15 boiler at Händelö. The following conclusions can be made:

- A wide range of materials, ranging from low alloyed steels to stainless steels and FeCrAl model alloys, has been investigated for up to three years in two different boilers with a horizontally designed superheater pass at several positions. This large matrix of corrosion results can be used for boiler manufactures and boiler owners in order to optimize material selection. For example, in the waste fired Händelö boiler the results show that all tested materials (from low alloyed steels to more highly alloyed steels) can be used, whereas the biomass/waste wood fired Örtofta boiler there is a lower corrosion rate for the stainless steels (including coatings) compared to low alloyed steels. These data in combination with costs of investment and replacement can be used to decrease the overall costs of the boiler operation.
- In general, the corrosion load of the superheater region in the waste fired boiler was rather low (for many samples below 0.1 mm/year and for some samples about 0.2 mm/year), including both low alloyed and stainless steels. This is suggested to primarily be an effect of a rather low material temperature and the presence of an empty pass, which decreases the temperature and corrosive particle load of the flue gas before entering the horizontally designed superheater pass.
- In the biomass fired boiler, the material wastages were higher for the low alloyed steels showing corrosion rates of about 0.3-0.5 mm/year with 40% waste wood and 0.4-0.7 mm/year with 45% waste wood. The reason(s) for the higher material wastage in the Örtoftaverket boiler compared to the waste fired P15 Händelöboiler is suggested to be caused by the higher material temperature and lack of an empty pass.
- The newly developed FeCrAl model alloy showed promising results, i.e. no corrosion, of the one year test performed in the SH region of the waste fired Händelö boiler.
- Both HVAF and HVOF CorEr coatings perform better compared to low alloyed steels and comparably or better results compared to stainless steels. Especially the HVAF CorEr coating showed very little corrosion attack and a good adherence to the substrate.
- The clamp testing technique is suitable for investigating the corrosion rate of large sample matrixes in multiple positions in the superheater bundles and for long periods of time with the possibility to investigate the corrosion rate in a time resolved manner. According to the results, the clamp samples exhibited similar corrosion rate as the corresponding tube samples. Thus, clamp samples are expected to be a low cost and non-invasive alternative to tube samples, still showing relevant corrosion rates.

- The online corrosion probe followed the same trends with respect towards the corrosion attack as the clamps samples and as the "traditional" corrosion probes. The online corrosion detected no or very little corrosion attack in the superheater pass, consisted with the clamps samples. When compared to the corrosion observed on the corrosion probes, exposed in the empty pass, the general trend was also the same; the initiation of the corrosion was very fast and aggressive and levelled off after some time. This was in agreement with the corrosion probes exposed for 24 and 144 hours respectively. This corrosion testing method possesses rather low risk of affecting the plant availability. The complexity and cost associated performing online corrosion probe measurements are to be considered as low to medium. The probe mounting/dismantling and analysis of the data is performed by educated personnel.

- The thermodynamical model and the IACM both aim at revealing the amount of gaseous alkali chlorides in the flue gas. Knowing the fraction of alkali chlorides in the flue gas may provide important information about the expected corrosion rate. The developed model proved to be a reliable calculation tool to estimate the concentration of the alkali chlorides in the flue gas of the CFB boiler, based on the chemical composition of the fuel mix and additives, as well as combustion temperature in the boiler. The model can be implemented as a first indication to assess the concentration of alkali chlorides in the CFB boiler. From a complexity, cost and plant availability point of view, both these methods show potential, e.g. the risk of operation by deploying these two methods is low (for the IACM) or non-existing (for the modelling method). However, there is still work to be performed in order to couple this to corrosion prediction models.

- The effect of the startup sequence of probe exposures proved to be minor, i.e. regardless of preheating the probe the corrosion attack and chlorine load was high. Thus, the normal probe procedure, starting the corrosion exposures with a corrosion probe holding room temperature, can continuously be used.

- The effect of chlorine penetration through oxide scales was investigated in the waste fired boiler and coupled to laboratory exposures. As for the laboratory exposed samples, there seems also to be an initial effect of the preformed oxide in decreasing the inward diffusion of chlorine, even though the corrosion load is much higher in the boiler compared to the laboratory. Thus, the effect is less pronounced. However, the non-pre-oxidized samples exhibited a slightly more accelerated corrosion attack and a thicker chlorine enriched corrosion product layer compared to the samples that had a corrosion product layer on top of the surface prior to the boiler exposure.

7 Goal fulfilment

The overall goal of this study was to improve plant economy by enabling an increased green electricity production and optimum material selection. Below the different goals are specified in detail and if the goal has been reached or not.

- *To correlate the corrosivity of the flue gas with the flue gas temperature in respect to the material temperature.*
- *To verify and quantify the corrosion rates for different superheater materials in superheaters with a horizontal design.*
- *Verify and compare the corrosion properties of a biomass fired boiler (Örtoftaverket) and waste fired boiler (Händelöverket)*
  We have in the project performed a great number of long term corrosion measurement campaigns including a wide palette of materials for several positions. The corrosion tests have primarily been performed with the clamp testing technique. The corrosion rates in the superheater position measured in the waste fired Händelö boiler have been low, regardless of material and position in the superheater bundle. The main reason for this low corrosion rate is suggested to be the low material temperature. At the biomass fired Örtoftaboiler the corrosion rates were higher for the low alloyed steels in the superheater region. For the stainless steels and coated materials, the corrosion rate was still low. The material temperature was however much higher (450-505 °C compared to 360-380 °C) at the Örtofta boiler, which explains the higher corrosion rate.

  With this large exposure matrix, at several positions in two different boilers, coupled also to probe exposures which widens the temperature and material matrix even further, these three goals are considered as fulfilled.

- *Verify and compare the corrosion properties of commercial superheater materials as well as state-of-the-art stainless steels and FeCrAl alloys.*
  As above, the material matrix executed in the exposures has been wide covering both material that are used today and newly developed steels, FeCrAls and coatings. The corrosion analysis has primarily been performed by means of material loss determination and cross-sectional SEM/EDX analysis. This study has brought new insights to the corrosion performance of newly developed alloys as well as compared the corrosion properties in these two boilers of commercial superheater materials that are available today.

  This goal is considered as fulfilled.

- *Verify and compare the corrosion properties of coatings performed with the new generation coating technology HVAF (High Velocity Air Fuel).*
  Samples coated with CorER (a nickel base coating), both with the HVOF and the HVAF technique, have been evaluated and performed overall well. The HVAF coated samples were however always showing lower corrosion rates compared to the HVOF samples and other stainless steels, even though the corrosion rates were low in general. The HVAF coatings were denser compared to the HVOF coatings, which is suggested to be part of the explanation why this coating performed better.

  This goal is considered as fulfilled.

- *Compare different corrosion testing methods (i.e. probes, coils/tubes and clamping) with respect towards their complexity, cost and plant availability risk.*
  Within this study six different methods in order to estimate the potential corrosion/ corrosion risk of superheaters have been tested, namely tube samples, clamp samples, corrosion probe samples, online corrosion probe samples, IACM and a thermodynamical model. The latter two methods are used in order to measure or calculate the amount of gaseous alkali chlorides in the flue gas, which can be used for corrosion prognosis. As described in the section above, the different methods have both advantages and disadvantages. As such, in many cases the different methods are complementary to each other. Hence, there is no overall "best-practise", instead different methods should be used to address different aspects or having different time spans.

  This goal is considered as fulfilled.

- *Investigate how the corrosion performance of water walls is affected by a stepwise increase of the waste wood fraction in the fuel mix.*
  Due to technical difficulties and safety issues this goal has not been met fully and as intended. The construction of a new measurement hole in the water wall led to leakage of hot sand during the startup of the probe tests. These tests were therefore stopped due to a violation of safety environment at the boiler. Consequently, the corrosion performance of the water walls has not been investigated in detail with probes. However, there has been an stepwise increase of the waste wood fraction and according to Kraftringens investigations during revision the permanently installed water walls have not been showing any alarming signs of an accelerated corrosion rate.

  This goal is considered as only partially fulfilled. However, due to safety issues not all planned activities could be performed.

These two projects have also contributed to the following KME goals:

- Verify novel solutions in boiler design with respect towards corrosivity.
- Increase steam parameters and thereby higher electrical efficiency.
- Test improved material solutions – including alumina forming alloys and coatings.

These two projects has also fulfilled the following academic achievements:

- **One licentiate degree:** Mercedes Andrea Olivas Ogaz "High temperature chlorine-induced corrosion of low-alloyed and stainless steels" 2017
- **Contribution to one Ph. D. thesis:** Mercedes Andrea Olivas Ogaz – to be presented in 2018
- **Publication/acceptance of three conference papers.**

8 Literature references

1. Zevenhoven, M., et al., Characterization of Ash-Forming Matter in Various Solid Fuels by Selective Leaching and Its Implications for Fluidized-Bed Combustion. Energy & Fuels, 2012. 26(10): p. 6366-6386.
2. Moradian F, P.A., Richards T., Thermodynamic Equilibrium Model Applied To Predict the Fouling Tendency in a Commercial Fluidized-Bed Boiler, Combusting Solid Waste. Energy & Fuels 2015. 29(5): p. 12.
3. Chevalier, S., et al., High temperature alloy chloridation at 850 degrees C Part II: Influence of pre-oxidation on the chloridation behaviour. Materials and Corrosion-Werkstoffe Und Korrosion, 2007. 58(5): p. 353-361.
4. Grabke, H.J., E. Reese, and M. Spiegel, THE EFFECTS OF CHLORIDES, HYDROGEN-CHLORIDE, AND SULFUR-DIOXIDE IN THE OXIDATION OF STEELS BELOW DEPOSITS. Corrosion Science, 1995. 37(7): p. 1023-1043.
5. Israelsson, N., et al., KCl-Induced Corrosion of an FeCrAl Alloy at 600 A degrees C in O-2 + H2O Environment: The Effect of Pre-oxidation. Oxidation of Metals, 2015. 83(1-2): p. 29-53.
6. Reese, E., & Grabke, H. J. , Einfluß von Chloriden auf die Oxidation des 2¼ Cr-1 Mo-Stahls. Materials and Corrosion-Werkstoffe Und Korrosion, 1992. 43(12): p. 11.
7. Pettersson, J., et al., KCl induced corrosion of a 304-type austenitic stainless steel at 600 degrees C; The role of potassium. Oxidation of Metals, 2005. 64(1-2): p. 23-41.
8. Jonsson, T., et al., Oxidation After Breakdown of the Chromium-Rich Scale on Stainless Steels at High Temperature: Internal Oxidation. Oxidation of Metals, 2016. 85(5): p. 509-536.
9. Lehmusto, J., et al., Comparison of potassium chloride and potassium carbonate with respect to their tendency to cause high temperature corrosion of stainless 304L steel. Fuel Processing Technology, 2013. 105: p. 98-105.
10. Jonsson, T., et al., The influence of KCl on the corrosion of an Austenitic stainless steel (304L) in oxidizing humid conditions at 600°C: A microstructural study. Oxidation of Metals, 2009. 72(3-4): p. 213-239.
11. Israelsson, N., et al., KCl-Induced Corrosion of an FeCrAl Alloy at 600 °C in O2 + H2O Environment: The Effect of Pre-oxidation. Oxidation of Metals, 2015. 83(1): p. 29-53.
12. Pettersson, C., et al., KCl-induced high temperature corrosion of the austenitic Fe-Cr-Ni alloys 304L and Sanicro 28 at 600 degrees C. Corrosion Science, 2006. 48(6): p. 1368-1378.
13. Pettersson, C., L.G. Johansson, and J.E. Svensson, The Influence of Small Amounts of KCl(s) on the Initial Stages of the Corrosion of Alloy Sanicro 28 at 600 degrees C. Oxidation of Metals, 2008. 70(5-6): p. 241-256.
14. Broström M, E.S., Backman R, Mäkelä K., Condensation in the KCl–NaCl system. . Fuel Processing Technology 2013. 105(0): p. 7.
15. H, Kassman, Strategies to reduce gaseous KCl and chlorine in deposits during combustion of biomass in fluidised bed boilers, Ph. Thesis in Dep Energy & Environment 2012, Chalmers University of Technology.
16. T, Leffler, Development and application of optical diagnostics of alkali vapours for solid fuel combustion, Ph. Thesis in Dep Physics 2016, Lund University.

17. M. A. Olivas-Ogaz, J.E., A. Persdotter, M. Sattari, J. Liske, J-E. Svensson, T. Jonsson. Effect of oxide scale microstructure on the influence of KCl(s) on a low-alloyed steel at 400 °C. in EFC Workshop. 2015. Dechema - Germany.

9 Publications

- "The effect of startup procedure of probe exposures on deposit and corrosion formation in a waste fired CFB boiler."
  M.A. Olivas-Ogaz, M.D. Paz, T. Jonsson and J. Liske,
  Proceedings paper, 22 FBC conference, Turku, Finland, 2015.
- "High temperature chlorine-induced corrosion of low-alloyed and stainless steels"
  Mercedes Andrea Olivas Ogaz
  Lic thesis. 2017
- "Correlation between field and laboratory exposures for boiler corrosion test – mechanistic study of chlorine induced corrosion",
  M.A. Olivas-Ogaz, M.D. Paz, T. Jonsson and J. Liske
  Accepted to the 23rd FBC conference in South Korea
- "Testing of new materials to combat superheather corrosion in a waste fired CFB boiler"
  M.D.Paz, T.Jonsson and J.Liske

Combating high temperature corrosion by new materials and testing procedures

This study has been investigating several factors that is expected to have an influence on the overall plant economy for biomass and waste fired boilers. This has been performed in two CFB boilers built by Sumitomo SHI FW and in two parallel projects. The data obtained within this study may be used by the industry in order to optimize material selection and corrosion testing methods. The main scientific aim of this study is to generate new knowledge about various corrosion exposures within boilers with a wide range of materials, both commercially available and newly developed, in a horizontally designed superheater region. Some of the results in short:

- In general, the corrosion load of the superheater region in the waste fired boiler was rather low (for many samples below 0.1 mm/year and for some samples about 0.2 mm/year), including both low alloyed and stainless steels.
- In the biomass fired boiler, the material wastages were higher for the low alloyed steels showing corrosion rates of about 0.3-0.5 mm/year with 40% waste wood and 0.4-0.7 mm/year with 45% waste wood.
- The newly developed FeCrAl model alloy showed promising results, i.e. no corrosion, of the one year test performed in the SH region of the waste fired Händelö boiler.
- Both HVAF and HVOF CorEr coatings perform better compared to low alloyed steels and comparably or better results compared to stainless steels. Especially the HVAF CorEr coating showed very little corrosion attack and a good adherence to the substrate.
- The clamp testing technique is suitable for investigating the corrosion rate of large sample matrixes in multiple positions in the superheater bundles and for long periods of time with the possibility to investigate the corrosion rate in a time resolved manner.